FACULTY OF MEDICINE AND HEALTH SCIENCES

TARGETING THE NORADRENALINE RECEPTORS IN A SEIZURE-INDUCED ZEBRAFISH MODEL

Gryllionaki Markella, Verstraeten Maïté
Student number: 01808922, 01909960

Promotor: Prof. Dr. Raedt Robrecht
Co-promotor: Dr. Syx Delfien

A dissertation submitted to Ghent University in partial fulfilment of the requirements for the degree of Master of Science in Biomedical Sciences

Academic year: 2023 – 2024

GHENT UNIVERSITY

1. Preface

I dedicate this master's dissertation to myself for the five years of studying, crying, sweating, swearing, and celebrating. Honestly, it's been a wild ride with ups and downs. The most important thing to do now is not to panic – I'm (hopefully) graduated.

All jokes aside, in the first place, I want to thank my promotor, professor doctor Robrecht Raedt, and my co-promotor, doctor Delfien Syx for their superb guidance through this master's thesis, for their helpful insights in the topics of epilepsy and zebrafish, for their useful feedback and motivational words when needed. I also want to express my thanks to Zoë Malfait for guiding us through the practical lab work; we would still be trying to figure out how to start the PCR machine without your help.

A very special 'thank you' goes to my thesis partner, Markella Gryllionaki, for doing this master's dissertation by each other's sides, for being there every day inside and outside the lab with a warm smile and a listening ear.

Writing this master's dissertation was quite intense and I therefore would like to express my gratitude to the – for me – two most important women in the world, my mom and my grandmother. I want to thank them for loving me regardless, for showing warmth, encouragement and faith, and for supporting me through every step in this process, not only speaking about this master's dissertation, but also about my Biomedical Science studies, and most importantly, about life. You both are truly my role models that I strive to be in the future.

Maïté Verstraeten
Ghent, May 2024

2. Table of contents

3. Scientific summary

Background. Epilepsy is a common neurological disorder (>70 million people worldwide), characterized by recurrent epileptic seizures. One-third of all patients do not reach seizure freedom by current antiepileptic drugs. Recent interest has emerged for the noradrenergic neurotransmission system and its role in regulating seizures in epilepsy.
Methods. *Behavior analysis.* Valproic acid (antiepileptic drug), clonidine and atipamezole (α_2-noradrenergic agonist and antagonist) are evaluated for their effects on swimming behavior (maximum distance moved, maximum velocity and movement frequency) of 5 dpf zebrafish with pentylenetetrazole (PTZ)-induced seizures. *Expression analysis.* RNA extraction, cDNA synthesis and RT-qPCR analysis are performed on different pools (1-2-3-6-12 bodies/heads) of 5 dpf zebrafish bodies/heads, targeting the noradrenaline receptors (*adra1aa*, *adra1ab*, *adra1ba*, *adra1bb*, *adra2a*, *adra2b*, *adrb1*, *adrb2a* and *adrb2b*).
Results. *Behavior analysis.* Valproic acid acts as an anticonvulsant agent by reducing seizure behavior in PTZ-treated zebrafish. Clonidine has a depressant effect on control zebrafish, however, shows no proconvulsant, nor anticonvulsant effect. Atipamezole exerts anticonvulsant effects. *Expression analysis.* Stable expressed reference genes are different for 5 dpf zebrafish heads (*gapdh* and *rnf7*) and bodies (*rps18* and *rnf7*). At least pools of 6 or 12 zebrafish heads/bodies are needed to obtain reproducible results to see the expression levels of the noradrenergic receptors in 5 dpf zebrafish.
Conclusions. This project proves that the noradrenergic neurotransmission system plays a key role in regulating seizures in zebrafish. However, future research is needed to explore and investigate the involvement of the noradrenergic system in epilepsy in further detail.

4. Societal impact

Epilepsy encompasses a diverse range of neurological conditions, affecting more than 70 million people worldwide. It is characterized by a persistent tendency to generate spontaneous, recurrent epileptic seizures resulting in several neurobiological, cognitive and psychosocial consequences. The cornerstone of epilepsy treatment is the use of antiepileptic drugs, however, approximately one-third of all epilepsy patients remains unable to reach seizure freedom despite using a variety of antiepileptic drugs [1]. Given the significance of this condition, numerous research groups have investigated its pathophysiology using diverse experimental models, with rodents being commonly used. However, only a few researchers have used a zebrafish model for examining different aspects of epilepsy. Zebrafish have several advantages, rendering it a valuable model for various central nervous system diseases, including epilepsy [2]. Moreover, recent evidence from several studies highlights a role for noradrenaline in having antiepileptic functions. However, the exact working mechanisms of noradrenaline in epilepsy are not yet fully elucidated. This project aims to investigate the involvement and the role of the noradrenergic neurotransmission system in seizures, on the one hand via examining the expression levels of multiple noradrenaline receptors in larval wild-type zebrafish, and on the other hand by analysing the effects of noradrenergic agonists and antagonists, besides antiepileptic drugs used in the clinic, on the swimming behavior of seizure-induced zebrafish. Thereby, we hope to advance novel treatment options for epilepsy patients that are not helped with current antiepileptic drugs.

5. Introduction

5.1 Epilepsy

5.1.1 Definition and central hypothesis of epilepsy

Epilepsy is a heterogeneous group of neurological disorders characterized by the sudden and spontaneous occurrence of epileptic seizures. An epileptic seizure is defined as a transient manifestation of signs and symptoms arising from an aberrant hypersynchronous neuronal brain activity. This neurological disease is the most common severe brain condition, affecting approximately over 70 million people worldwide. Its occurrence exhibits a bimodal distribution, with the highest risks observed in infants, mostly having genetic forms of epilepsy due to genetic, metabolic or obstetrical causes, and elderly age groups, mostly having acquired forms of epilepsy due to stroke and neurodegenerative diseases [3]. Epilepsy management varies across the world due to discrepancies in the availability of antiepileptic drugs (AEDs) and diagnostic tools. Nonetheless, antiepileptic medication remains the cornerstone of treatment globally. However, one-third of all patients fails to achieve seizure control even after using multiple antiepileptic drugs [1]. Furthermore, this pathology significantly affects patients provoking pronounced neurobiological, psychosocial and cognitive consequences attributable to seizures, medication side effects and social stigma. Research can help improve the overall quality of life of patients by providing novel treatment options where the adverse effects of pharmacological treatments are reduced and the efficacy is improved. A deeper understanding of the molecular mechanisms of epilepsy is needed to develop new antiepileptic drugs [1].

The central hypothesis of seizure genesis postulates an imbalance in excitation and inhibition mechanisms in neurons, in favor of the abnormal excitation of neurons. Epilepsy is characterized by a variety of symptoms influenced by various risk factors, such as brain traumas and genetic predispositions, emphasizing the complexity of the disorder as opposed to being exclusively characterized by a single expression or cause. Advancements in genomic technology are unravelling the complexity of the genetic architecture of the most prevalent epilepsy types, which has led to a new classification of epileptic seizures and syndromes. It is important to note that a single epileptic seizure occurs in up to 5% of the general population attributable to an unbalanced brain caused by systemic problems, medication intake, hypoglycemia or drug abuse. Epilepsy can be considered as an illness defined by any of the following criteria: (1) experiencing at least two unprovoked seizures with an interval of more than 24 hours, (2) having one unprovoked seizure and a likelihood of future seizures similar to the general recurrence of risk (at least 60%) after two unprovoked seizures within the following ten years, and (3) being diagnosed with an epilepsy syndrome. For a proper clinical diagnosis, a detailed (hetero)anamnesis of the patients' medical history and a reliable eyewitness of an epileptic seizure are of utmost significance. Additional examinations, such as long-term video-EEG monitoring and MRI, will lead to a more accurate diagnosis [1].

5.1.2 Classification of epilepsy and epileptic seizures

To unravel the structural and functional causes of this group of disorders, it is important to identify the paroxysmal events as epileptic or non-epileptic. The clinical manifestation of an epileptic seizure is diverse and depends on the affected region(s) in the brain. Semiological features encompass both motor and non-motor phenomena, such as sensory experiences, autonomic responses, behavioral changes, cognitive alterations and emotional manifestations, which may occur with or without impairment of awareness. However, those symptoms may also occur in other diseases which may mimic seizures and pose a clinical challenge. In adults, the primary imitators of epilepsy are syncopes, psychogenic non-epileptic seizures (PNES), migraine, parasomnias, cerebrovascular disease (e.g., transitory ischemic attack (TIA)) and movement disorders including paroxysmal dystonia and non-epileptic myoclonus. In paediatric cases, epilepsy syndromes encompass a broad array of conditions and behavioral states [4].

Frequently, individuals are indiscriminately labelled as having epilepsy, whereas diagnostic precision and specificity are significant. Adequate classification schemes are needed to provide the best medical care considering that the most suitable medication for one syndrome/type of epilepsy could be detrimental for another. Classification is based upon three levels: seizure type, epilepsy type and epilepsy syndrome. At each level, it is essential to identify causative factors and comorbidities as these may pronouncedly affect therapeutic decisions [1].

The causes exist out of six categories: genetic, structural, metabolic, infectious, immune and unknown [1]. Comorbidities refer to the simultaneous occurrence of two conditions at a higher frequency than typically observed in the general population. In this pathology, those comorbid conditions encompass medical, psychiatric and cognitive disorders, occurring either individually or in combination with one another. A few examples of these additional medical problems are dementia, migraines, anxiety, somatic autoimmune diseases, heart diseases, type 1 diabetes and arthritis [5]. Their prevalence in individuals with epilepsy can be up to eight times higher compared to the general population. Epilepsy rarely stands alone, and the presence of comorbidity affects the quality of life of the patients. Therefore, screening for these additional disorders should be integrated into the management of the disorder as effectiveness and tolerability of antiepileptic drugs are heavily influenced by them [1].

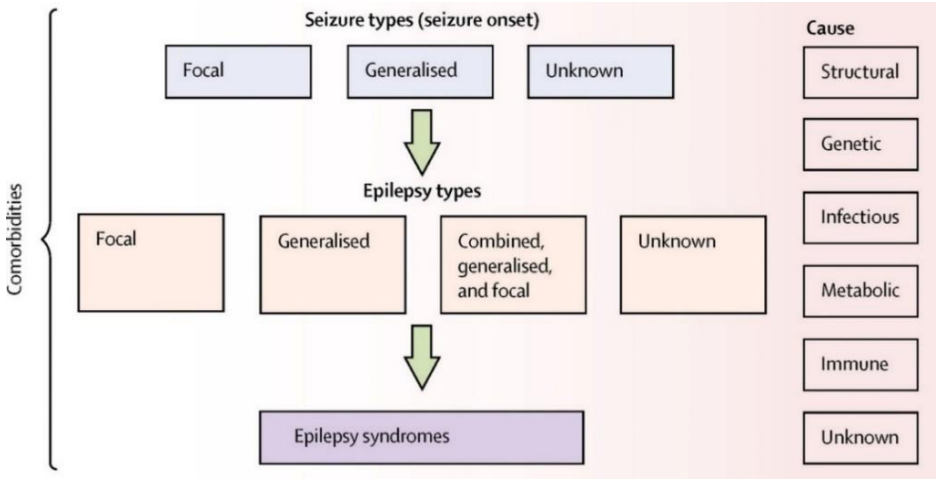

Figure 1: The classification of epilepsies according to the framework set forth by the International League Against Epilepsy. Different seizure types based on the seizure onset zone (focal, generalized and unknown), different epilepsy types (focal, generalized, combined generalized and focal, and unknown) and different causes for epilepsy (structural, genetic, infectious, metabolic, immune and unknown) can be seen on the figure [1].

Moreover, seizure types are initially classified by their onset as either focal, generalized or of unknown origin. Focal seizures are firstly subdivided by the level of consciousness of the patient in retained or impaired awareness, and additionally further categorized in motor or non-motor based on the primary and predominant manifestation. Generalized seizures are classified into motor and non-motor (absence) seizures. Unknown onset seizures may still possess identifiable features for classification. Furthermore, unknown onset tonic-clonic seizures are categorized when a patient has convulsions without clear clinical evidence that the origin of onset is focal or generalized. For individuals presenting with convulsions presumed to have a focal onset, the categorization focal to bilateral tonic-clonic is made, while the group generalized tonic-clonic seizures is reserved for those with generalized epilepsy. Epilepsy types are arranged in four groups: focal, generalized, combined generalized and focal, and unknown. The most precise classification can be obtained by diagnosing the epilepsy syndrome, which physicians can only identify from a cluster of clinical features such

as comorbidities, EEG, imaging features, seizure types and age of onset. Examples of syndromes are Dravet and Lennox-Gastaut. Figures 1 and 2 give a more structured scheme of all the types mentioned above [1].

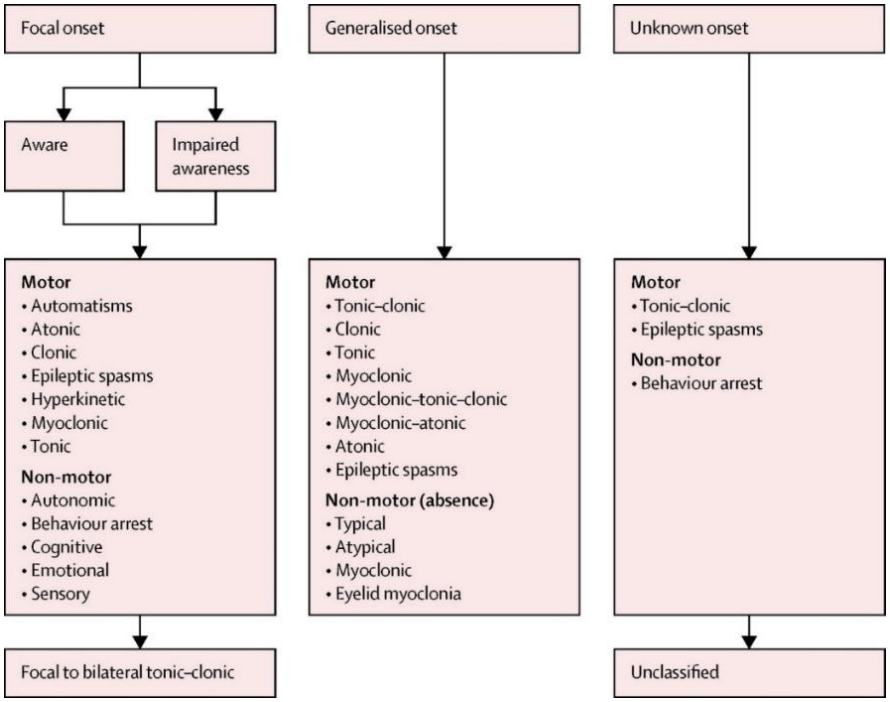

Figure 2: Classification of epileptic seizures within the framework established by the International League Against Epilepsy. Epileptic seizures can be classified on their seizure onset zones (focal, generalized or unknown onset), on their (impaired) awareness and on their (non-)motor symptoms [1].

5.1.3 Consequences and mortality

A significant public health problem among people suffering from epilepsy is premature mortality [1]. Recent studies have shown a two to three times more elevated mortality rate than the general population, which is measured using the standardized mortality ratio (SMR). Additionally, it is stated that comorbidities emerge as the leading cause of death, especially short after a patient is diagnosed with the pathology. In epidemiological contexts, it is observed that mortality rates exhibit a higher prevalence in low-income countries when contrasted with their counterparts in high-income settings. The causes are divided into two groups. The first category is the direct premature deaths where status epilepticus and sudden unexpected death in epilepsy (SUDEP) are classified. Secondly, the indirect group includes aspiration pneumonia, suicide, drowning, and neoplastic disorders [6].

5.1.4 Drug-resistant epilepsy

There are currently millions of people suffering from epilepsy, where the cornerstone of treatment is therapy with antiepileptic drugs with the ultimate goal to achieve seizure freedom for the patient. Despite the various pharmacological treatments, one-third of all epilepsy patients still suffers from drug-resistant epilepsy (DRE). In 2010, the International League Against Epilepsy (ILAE) formulated a definition for DRE as following: *“Failure of adequate trials of two tolerated, appropriately chosen and used antiepileptic drug schedules (whether as monotherapies or in combination) to achieve sustained seizure freedom.”*. Several mechanisms could conceivably influence both the pharmacological response to seizures and the pathogenesis of DRE [7].

Since the burden of this disorder is explained in the section above such as comorbidities, mortality and decreased quality of life, the unmet needs for the patients will be further discussed in this part. Over the past two decades, despite the emergence of advanced AEDs with comparable or enhanced efficacy and improved tolerability compared to older medication, there has been a noticeable absence of substantial advancement in the management of epilepsy. This stagnation is reflected in the lack of significant improvements in epilepsy-treatment related outcomes and no notable diminishment of the frequency of DRE. It would be expected that the adaptation of newer AEDs should have translated into overall improved success in treatment and better individual outcomes. However, this expectation stays unmet, with additionally a reduction of the probability of achieving seizure freedom after each additional AED attempted [3].

5.1.5 Treatment

Despite the wide array of drugs available globally for various medical conditions, only a few are considered first-line treatments. A lot of medications are generally used for focal and generalized epilepsies, but there are also specific types of drugs which are used for particular forms of this disease, such as sodium channel modulators given for focal epilepsy [1]. The selection of the exact therapy is influenced by the seizure type and epileptic syndrome, as well as individual circumstances, such as age, sex, child-bearing potential, comorbidities and tolerability issues. It is also very crucial to avoid drug-to-drug interactions, especially in elderly people, who are often taking multiple concomitant medications for comorbidities. Determining the optimal stage or the number of seizures at which treatment initiation should begin is important, as starting AEDs after a first seizure typically does not alter prognosis. Patients who have a higher risk of recurrence should start treatment as soon as possible. Ideally, antiseizure medication should be introduced gradually, with doses incrementally adjusted based on symptoms. If there is no benefit at the maximum tolerated dose, another first-line drug should be considered. Additionally, if events persist despite administrating an optimal dose of first-line antiseizure medication, a critical re-evaluation of the epilepsy diagnosis is necessary [1]. Some antiepileptic drugs are listed in Table 1.

Table 1: Non-exhaustive table of antiepileptic drugs used in the clinic [1].

List of antiepileptic drugs (AEDs)			
Focal and most generalized seizures		**Focal seizures only**	
Benzodiazepines	Lamotrigine	Carbamazepine	Gabapentin
Levetiracetam	Phenobarbital	Phenytoin	Pregabalin
Topimarate	Sodium valproate	Tiagabine	Vigabatrin

In more detail, valproic acid (VA), or sodium valproate, is a compound used in this project to evaluate the antiepileptic effects through which the drug exerts its therapeutic benefit in epilepsy patients. VA is a widely utilized medication in the clinic known for its diverse therapeutic applications in both neurological and psychiatric disorders: it is used for the treatment of epilepsy (various seizure types), for the management of bipolar disorder and migraines. It is a medication with diverse mechanisms-of-action which are not yet fully understood. Studies have shown that this drug exhibits its antiepileptic effects by reducing high-frequency neuronal firing, accomplished through the inhibition of voltage-gated sodium, potassium and calcium channels. Additionally, it modulates GABA- or glutamate-mediated neurotransmission, influencing the excitation/inhibition-balance in neurons. It is administered to patients orally or via intravenous route and can be used as monotherapy for simple or adjunctive therapy for complex seizures. The use of VA is contraindicated in pregnancy, as it has the capability to cross the placental barrier, entering the foetal circulation and having teratogenic effects [8].

Furthermore, besides the negative consequences of the disorder, such as SUDEP, learning and development problems in children, epilepsy-related injuries and an increased risk in mental and behavioral problems, the therapies given against this disease still have a big amount of side effects. Memory issues, fatigue, tremors, gastrointestinal symptoms, nausea, fluctuation in weight, dizziness, osteoporosis, depression, and drowsiness are among the range of commonly occurring adverse effects of AEDs. Side effects escalate the burden of the disorder from an economic and humanistic standpoint. Treating patients with new AEDs that have an improved tolerability and efficacy, whilst enhancing their quality of life and decreasing comorbidities, remains the greatest unmet medical need. New therapies and better understanding of the underlying mechanisms of epilepsy are needed to address this urgent public health concern [3].

5.2 Animal models in epilepsy research

5.2.1 The need for an adequate animal model

It is crucial to acknowledge the complex nature of epilepsy by realizing that there is no single animal model that fully replicates the manifestations of the disorder. An animal model of this disease commonly denotes a specific species with either an induced or a genetically engineered predisposition to develop seizures. It is fundamental to mention that, ideally, the validity of an animal model for epilepsy requires three main criteria: (1) face validity, which is achieved when phenotypical symptoms and behavioral manifestations caused by the epilepsy model are similar to the symptoms experienced by epilepsy patients, (2) construct validity, which is achieved when animals mimic the underlying mechanisms that are inherent to the human pathophysiological condition, and (3) predictive validity, which is achieved when animals show specific and selective responsiveness to treatments in a manner consistent with clinical outcomes. Although the concept of an ideal model encompasses all these above-mentioned criteria, achieving such a standard in practice remains a significant challenge [9].

Furthermore, it is essential to consider that all animal studies are fundamentally comparative and thus can unveil aspects of epileptogenesis that are widely observed across various animal species, thereby offering insights into clinically significant features in humans. Moreover, animal experiments provide a means to explore specific processes accessible only in certain species, leading to a deeper understanding of the disease. Additionally, epilepsy has a wide range of comparative anatomical and physiological studies across a variety of primarily mammalian species, but rodent models (mice (*Mus musculus*) and rats (*Rattus norvegicus*)) have emerged as the predominant choice in epilepsy research. Frequently, those choices are made for reasons of convenience, although ideally, decisions should be factored by experimental rationale [9].

Lastly, recent advances in genetic research have unraveled a wide array of genes associated with numerous types of epilepsy, highlighting the diverse nature of this condition. Adequate animal models play a crucial role in investigating the underlying pathological mechanisms triggered by genetic mutations linked to epilepsy, and in developing novel therapeutic approaches. Thus, zebrafish have emerged as a valuable vertebrate model for investigating innovative antiepileptic treatments through genetic manipulation and chemical exposure to anticonvulsant drugs, such as pentylenetetrazole (PTZ). PTZ is an antagonist of the $GABA_A$-receptors, which are chloride-channel complexes, and therefore, are critical components of seizure activity modulation. Chemical exposure to PTZ leads to increased excitation signals in multiple neural networks and can therefore be used to induce (epileptic) seizures in different rodent models. It can be concluded that rodent models have notably contributed to our understanding of this condition, however, the fundamental underlying mechanisms of this complex array of diseases remain unclear, thus novel innovative models are required [10].

5.2.2 Zebrafish model

5.2.2.1 The advantages of this model

In the past few decades, there has been a notable increase in the utilization of animals for research, underlying the urgent need for the advancement of alternative methods and animal models. Before executing experiments involving animal models, it is crucial to carefully assess the 3R-principle (replace, reduce, refine), which has been implemented in the legislative framework of this thesis. Currently, the European Commission Directive 2010/63/EU authorizes experiments in zebrafish embryos and early larvae up to the stage of free-swimming and independent feeding (typically occurring at 5 days post fertilization (dpf)) without being regulated as animal experiments. This gives the big advantage of using 5 dpf zebrafish as an alternative model to animal testing in other vertebrates [11].

Zebrafish have gathered significance as a valuable vertebrate organism for modelling various human diseases, ranging from cardiovascular issues to cancer and neurological disorders. Its small size, oviparous nature, very rapid growth, transparency and permeability during early developmental stages make this model particularly advantageous. *Danio rerio* has the advantages of a vertebrate, such as highly conserved organ architecture and genetic code, their minor size and ease of genetic manipulation. Their suitability for high-throughput automatic screening of behavior (e.g., video-tracking tools) and high-throughput drug screening, their permeable membranes to various medication and various fluorescent markers of cellular processes has made them an excellent model in epilepsy research [10].

In addition to all the previously mentioned advantages, it is crucial to mention that the brain morphology of both adult and larval zebrafish exhibits striking similarities with rodent models and humans. It is a vertebrate species with both physiological and genetic homology to mammals and humans (70%), together with high conservation of all major neuromediator systems, such as neurotransmitters, receptors, transporters and enzymes. Moreover, duplicated genes, also referred to as orthologs, commonly encode proteins with similar or substantially overlapping functions and properties [12]. Lastly, despite already yielding significant contributions, zebrafish research continues to hold promise in advancing our understanding of the intricate roles of specific genes in human diseases, ranging from rare to common conditions [13]. While zebrafish are valuable in studying acute evoked seizure events, their true strength lies in their capacity to model genetic epilepsies. In this thesis, 5 dpf zebrafish are used to study acute evoked seizure events [9].

5.2.2.2 The disadvantages of this model

While the zebrafish model is a valuable non-mammalian model, it also has a few drawbacks. Firstly, *Danio rerio* is a poikilothermic vertebrate, meaning that their internal temperature varies with a preferable temperature around 28°C. This variability could pose a significant challenge in studies where the homeostatic temperature is crucial. Secondly, it is important to consider the genome duplication in zebrafish, which occurred during teleost evolution, resulting in the presence of two copies of several genes. It can be hypothesized that certain genes may have redundant functions, or that functions are diverging from their hereditary genes' function, potentially complicating molecular and genetic studies. Lastly, the availability of commercially available antibodies against zebrafish tissues is limited, but this is partially compensated by reporter transgenic zebrafish lines [14].

5.3 Zebrafish behavioral assays

Studying zebrafish behavior holds much potential towards evaluation of behavioral and developmental research questions. Some examples of these zebrafish behavioral assays include locomotor assays to assess the swimming behavior, Y-maze tests to test for working memory and executive function [15], light/dark-preference tests for testing anxiety-like behavior [16] and tests for screening novel neuropharmacological agents [17]. Locomotor assays are widely used for screening and evaluating the effects of different chemical compounds on the zebrafish swimming behavior and movements. In this master's thesis, the DanioVision Observation Chamber (Noldus, The Netherlands), associated with the EthoVision

XT Software (Noldus, The Netherlands), is used to analyse the swimming behavior of 5 dpf zebrafish. The EthoVision XT Software is the most widely applied high-throughput tracking and video-recording system that tracks and analyses the behavior, movement and activity of larval zebrafish. Larval activity and movement patterns are basic research measurements that can reveal valuable information on epileptic and stereotypic behavior patterns, motor control, circadian rhythms and neural development in studies related to drug development, toxicity, behavioral genetics and circadian rhythmicity.

5.4 Noradrenergic neurotransmission system

5.4.1 The LC-NE neurotransmission system in the mammalian body and brain

Noradrenaline (or norepinephrine) (NE) exerts a dual function by both acting as one of the most important monoamine neurotransmitters in the sympathetic nervous system, besides serotonin, histamine, dopamine and adrenaline (or epinephrine), as well as acting as a hormone of the adrenal glands, the small glands on top of both kidneys. As a hormone, noradrenaline is released in the bloodstream from the adrenal glands in reaction to low blood pressure and (acute) stress, to prepare to combat ('fight') or escape ('flight') dangerous situations – the so-called fight-or-flight response. Physiological symptoms of this acute stress response are vasoconstriction resulting in an increased blood pressure, an increased heart rate and an increased breathing. When the danger situation is over and this fight-or-flight state of the body is thus no longer required, the parasympathetic nervous system takes over to return the body to pre-arousal levels. Other functions of noradrenaline are maintaining metabolism and biorhythm (including the circadian rhythm), ensuring proper organ functioning and providing the necessary energy [18]. As a neurotransmitter, noradrenaline acts as a neuromodulator by facilitating signal transmission between nerve cells. The release of noradrenaline in the brain is mostly supplied by noradrenergic neurons. In the brain cortex and hippocampus, the noradrenaline release is mainly produced by the locus coeruleus (LC), a small bilateral nucleus deeply located in the pons and consisting of ~24.000 neurons in humans. The locus coeruleus-noradrenaline system (LC-NE) knowns noradrenergic projections to nearly all brain regions, thus highlighting its role as one of the most important neurotransmitters in the sympathetic nervous system [19] (Figure 3).

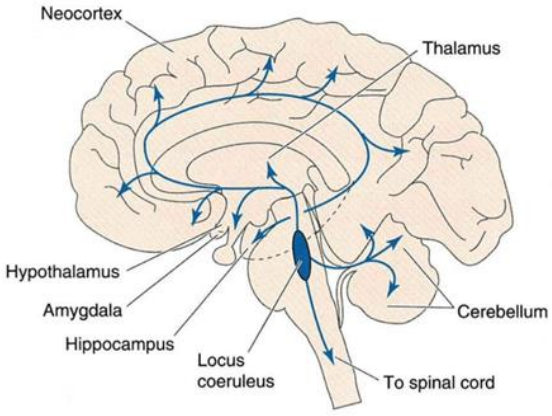

Figure 3: Noradrenergic projections of the locus coeruleus. The locus coeruleus (LC) is known as the noradrenergic nucleus, since most of the noradrenergic neurons are located in this small bilateral nucleus located in the pons. This figure shows multiple noradrenergic projections of the locus coeruleus-noradrenaline (LC-NE) system to almost every brain region [19].

The noradrenergic system and the release of noradrenaline in the brain is important for multiple functions, including modulating attention, vigilance, arousal, sleep-wake cycle, reward, motivation, motor behavior, cognition, learning and memory [20]. Disturbances in the LC-NE network and signaling can be linked to several disorders, emphasizing the clinical importance of this noradrenergic neurotransmitter system. As an example, decreases in noradrenaline activity are thought to be related to depression, lack of energy and poor memory function, whereas increases in noradrenaline activity are thought to be related to mania, anxiety and sleep disorders. Unravelling the precise mechanisms of the LC-NE transmission system and discovering (new) therapeutic targets will definitely result in more effective treatment options for diseases and disorders linked to disruptive LC-NE transmission.

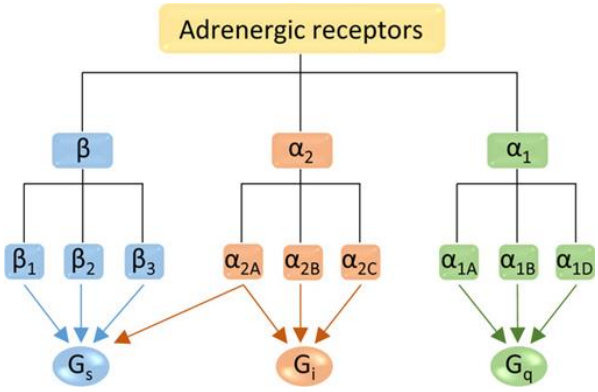

Figure 4: The subtypes of the noradrenergic receptor family and their G-protein downstream pathways. The (nor)adrenergic receptor family consists of three main receptor types, namely the β-, α_2- and α_1-adrenergic receptors, which can be then further subdivided into nine different subtypes: β (β_1, β_2, β_3), α_2 (α_2A, α_2B, α_2C) and α_1 (α_1A, α_1B, α_1D). The β-, α_2- and α_1-adrenergic receptors are G-protein-coupled receptors, mainly coupled with G_s, G_i and G_q, respectively [21].

The noradrenergic neurotransmission system exerts its effects in mammals via three main receptor types, namely the α_1-, α_2- and β-adrenergic receptors. All three of these receptors are classified as G-protein-coupled receptors or metabotropic receptors, referring to a type of membrane receptors that require an intracellular metabolic cascade to modulate cell activity effects. These main receptor types are subclassified into nine adrenergic receptors, namely α_1A, α_1B, α_1D, α_2A, α_2B, α_2C, β_1, β_2 and β_3. These adrenergic receptors are, as mentioned above, G-protein-coupled receptors and couple to different G-proteins, with the α_1-, α_2- and β-adrenergic receptor types primarily coupling to G_q, G_i and G_s, respectively. G_i results in inhibition of multiple intracellular signaling cascades, whereas G_q (activation of the phospholipase C (PLC) pathway) and G_s (activation of cAMP and the protein kinase C (PKC) pathway) are listed as stimulatory receptor types. As can be seen in Figure 4, the α_2A-adrenergic receptor exerts dual pharmacological effects by simultaneously coupling to G_i- and G_s-proteins, in response to respectively low and high agonist concentrations. The exact mechanism-of-action of this dual effect of the α_2A-adrenergic receptor, namely inhibition or activation of intracellular pathways, remains unclear [21].

5.4.2 The LC-NE transmission system in zebrafish

The vertebrate-specific locus coeruleus is an evolutionary conserved noradrenergic nucleus across species, thus also existing in the non-mammalian vertebrate zebrafish. These conserved properties of the LC across species are reflected in the LC consisting out of a small number of cells (~7-10 noradrenergic neurons in adult zebrafish) with extensive projection patterns to multiple brain regions, consisting out of highly homogeneous cell types and having potent influences on the brain. This high level of conservation of LC-NE projections can be seen in Figure 5, where a comparison between the axonal projections of zebrafish' and mammals' LC is made [22].

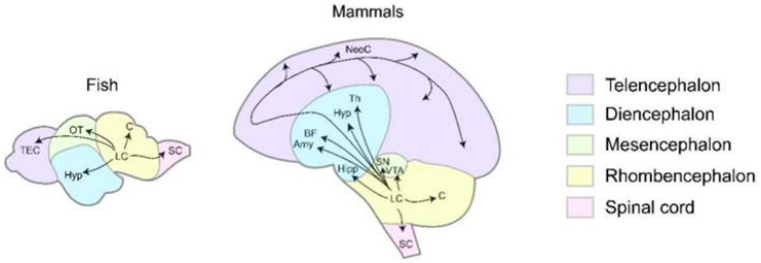

Figure 5: The high level of LC conservation across vertebrate species is reflected in the axonal LC-NE projection patterns. In zebrafish, axons of the LC known projections from the pons (the pons forms, together with the cerebellum and the medulla oblongata, the rhombencephalon (yellow)) to the telencephalon (purple), the diencephalon (blue), the mesencephalon (light green) and the spinal cord (pink). In mammals, the LC axons project roughly to the same regions. TEC, telencephalon; DCm, dorsal medial cortex; W, wulst; NCM, caudomedial nidopallium; NeoC, neocortex; Hyp, hypothalamus; Th, thalamus; BF, basal forebrain; Amy, amygdala; Hipp, hippocampus; OT, optic tectum; SN, substantia nigra; VTA, ventral tegmental area; C, cerebellum; SC, spinal cord [22].

As mentioned above (5.2.2.2), an important key fact to keep in mind is that the zebrafish genome underwent a partial duplication [13]. As a direct result of this duplication, this project will specifically focus on the zebrafish orthologs of the noradrenaline receptor genes, namely *adra1aa*, *adra1ab*, *adra1ba*, *adra1bb*, *adra2a*, *adra2b*, *adrb1*, *adrb2a* and *adrb2b*.

5.4.3 The noradrenergic neurotransmission system as a target in the treatment of epilepsy

5.4.3.1 Noradrenaline as a seizure suppressing neuromodulator

Previously conducted research on the noradrenergic system in zebrafish focused on behavioral studies related to ADHD (attention deficit hyperactivity disorder) [23], wakefulness [24] and depression [25]. Moreover, zebrafish are now widely used and accepted as a valid animal model for studying multiple different central nervous system (CNS) diseases, including epilepsy [2]. However, very little research has been done on the noradrenaline system in relation to epilepsy or seizures in adult and/or larval zebrafish [26]. Therefore, this project investigates the importance of the noradrenergic system in seizures in 5 dpf zebrafish, by both focusing on the expression levels of the noradrenaline receptors in 5 dpf wild-type zebrafish, as well as studying the effects of different noradrenergic agonists and antagonists on the swimming behavior of zebrafish with PTZ-induced seizures.

Based on research in rodent models, the noradrenergic neurotransmission system has emerged as a key factor in the regulation of brain hyperexcitability and seizure susceptibility, both hallmarks in the pathophysiology of epilepsy [27]. It is hypothesized that noradrenaline exerts an antiepileptic role by suppressing seizures. The observation that noradrenaline can act as a seizure suppressing neuromodulator stems from some noteworthy key research observations. First, damage to the LC-NE neurotransmission pathways by lesioning the LC leads to an increase in seizure susceptibility, as well as to an exacerbation of the epileptic seizures in rodent models [28]. Secondly, stimulation of the LC holds protective effects against epileptic seizures. Moreover, knockout of the noradrenaline transporter in rodents results in anticonvulsant effects, by elevating the noradrenaline levels in the synaptic cleft. Thirdly, genetically epilepsy-prone rats show abnormalities in noradrenaline concentrations and decreases in LC-NE neurotransmission [29]. Lastly, a key mechanism associated with the seizure suppressing clinical effects of vagus nerve stimulation (VNS) is the facilitation of LC-NE neurotransmission. In particular, noradrenaline is believed to exert its anticonvulsant effects by preventing seizure development and by inducing long-term plasticity changes, restoring the abnormal brain circuit in epilepsy [30,31].

5.4.3.2 α_1-, α_2- and β-adrenergic receptors as noradrenergic targets in the treatment of seizures

However, recent evidence has presumed a more nuanced role for the LC-NE neurotransmission system in epilepsy. It is suggested that the neuromodulatory effects of noradrenaline are concentration-dependent: for example, increased levels of noradrenaline can have proconvulsant effects under certain conditions rather than anticonvulsant effects. This concentration-dependent hypothesis can probably be related to the various expression levels of the different noradrenergic receptor types: the α_1-, α_2- and β-adrenergic receptors have varying degrees of affinity for noradrenaline, namely an intermediate (~300 nM), a high (~50 nM) and a low (~0.8 µM) affinity, respectively [32]. Consequently, activation of α_1- and α_2-adrenoceptors, both binding low and intermediate concentrations of noradrenaline, leads to anticonvulsant effects, whereas β-adrenoceptor activation is hypothesized to result in proconvulsant effects. When studying the noradrenaline receptors in relation to epilepsy and seizures, it is important to consider these individual effects of the different noradrenergic receptors contributing to the total effect of seizure suppression or elevation.

The role of α_1-adrenoceptors in epilepsy has to be discussed according to their subtypes (α_1A, α_1B and α_1D). On the one hand, activation of α_1A-adrenoceptors results in inhibition of seizures of the limbic system and attenuation of the epileptiform discharges rate by increasing the activity of GABAergic interneurons, which are critical in displaying inhibitory effects [33]. On the other hand, overactivity of α_1B-adrenoceptors leads to spontaneous recurrent epileptic seizures in mice that are genetically modified to show an overexpression of α_1B-adrenoceptors [34].

The role of α_2-adrenoceptors in epilepsy is again highly disputed: different study data report anticonvulsant effects attributable to the released noradrenaline activating postsynaptically located α_2-adrenoceptors, more specifically the α_2A-adrenoceptors (Figure 6). One hypothesis about the mechanism-of-action of the noradrenergic receptors suppressing seizures is that activation of α_2A- and β_2-adrenoceptors leads to an increase in noradrenaline in the hippocampus, resulting in seizure suppression via an increase in the dopamine levels. Another hypothesis states that activation of α_1A-adrenoceptors results in increased GABA levels in inhibitory interneurons, resulting in seizure inhibition [35]. On the contrary, others report proconvulsant effects caused by the effects of α_2-adrenoceptor agonists through presynaptically located α_2-adrenoceptors [36]. Moreover, the effects of α_2A-adrenoceptor agonists (e.g., clonidine) on seizure activity vary depending on the selected dose: high doses of clonidine are linked to anticonvulsant effects, whereas low doses exert a proconvulsant effect [37].

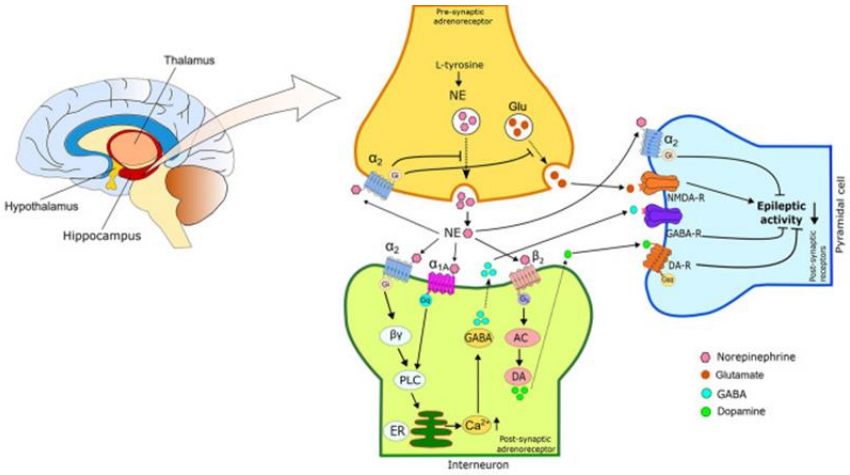

Figure 6: Overview of the mechanism-of-action of the noradrenergic receptors in epilepsy in support of the anticonvulsant hypothesis. It is hypothesized that activation of α_2A- and β_2-adrenergic receptors leads to an increase in hippocampal noradrenaline levels, leading to suppression of epileptic seizures via increasing the hippocampal dopamine (DA) levels. Moreover, activation of α_1A-adrenergic receptors leads to an increase in GABA levels in interneurons, thus resulting in seizure inhibition. AR, adrenoceptor; NE, norepinephrine (noradrenaline); DA, dopamine; GABA, gamma-aminobutyric acid; Glu, glutamate; PLC, phospholipase C; ER, endoplasmic reticulum; AC, adenylate cyclase. [38].

The role of β-adrenoceptors in epileptic seizures remains heavily discussed, since different studies show conflicting findings. There are studies that demonstrate anticonvulsant effects of β-adrenoceptor antagonists (e.g., propranolol) via sodium channel blockage (sodium channel blockage prevents passage of sodium ions, preventing depolarization and (repetitive) firing of the neuron). However, this exact same mechanism is also proposed as the anticonvulsant working mechanism of β-adrenoceptor agonists (e.g., clenbuterol). Although the underlying working mechanisms of these β-adrenoceptor agonists and antagonists remain poorly understood, the majority of the research results support the hypothesis that activation of the β-receptors plays a key role in the anticonvulsant effects of noradrenaline [38].

Concluding, some of the above literature supports the 'noradrenaline as a proconvulsant agent'-hypothesis, whereas other research shows evidence in support of the anticonvulsant hypothesis. However, these two hypotheses are not mutually exclusive and can occur under different circumstances in different species, as was demonstrated in the above-mentioned experiments. It is stated that the noradrenergic system and manipulation of this system by focusing on noradrenergic receptors can hold therapeutic potential, however, the precise mechanisms have not yet been fully elucidated.

5.4.3.3 Studying the effects of noradrenergic compounds on seizures

Different chemical compounds, such as clonidine and atipamezole, exert their effects via targeting the adrenergic receptors. Clonidine is a partial α_2-adrenergic receptor agonist, whereas atipamezole is an α_2-adrenergic receptor antagonist. However, both compounds are thus thought to be binding to *adra2a* and *adra2b*. When looking at Figure 6, some research hypotheses with regard to the effects of these two noradrenergic compounds can be

mentioned. It is hypothesized that, when a noradrenergic antagonist (e.g., atipamezole) binds presynaptically, autoinhibition disappears, leading to more release of noradrenaline in the synaptic cleft, and thus having anticonvulsant effects in the end. On the other hand, a noradrenergic agonist (e.g., clonidine) that binds presynaptically, will exert the same effects as noradrenaline binding: there will be autoinhibition, leading to less release of noradrenaline from the presynaptic terminal, which will have proconvulsant effects in the end. Although these hypotheses are clearly stated, it's important to mention that the working mechanisms of the noradrenergic system are complex and not yet fully elucidated. Moreover, not only the noradrenergic neurotransmission system has an influence in seizures, also other systems (e.g., GABAergic system, glutamatergic system) play an important key role in regulating seizures. Therefore, it's important to keep in mind that there is always a complex interplay and interaction between different regulating brain systems.

5.5 International state-of-the-art of epilepsy research in zebrafish

Regarding the (inter)national state-of-the-art of epilepsy research, it can be said that many different laboratories are investigating the underlying (molecular) mechanisms of epilepsy and seizures, and the effects of different treatment options in *ex vivo* (brain slices) and *in vivo* models (animal models such as rodents and zebrafish), with the common aim of finding a cure for epilepsy. Our thesis project covers the topic of targeting the noradrenaline receptors in a seizure-induced zebrafish model, and is performed in a collaborative effort between the Center for Medical Genetics (CMGG) lab and the 4BRAIN lab (Figure 7). The CMGG lab accommodates a zebrafish core facility that is able to house multiple (genetic) zebrafish lines, including wild-type zebrafish. Research on modelling and elucidating the molecular underpinnings of heritable diseases and disorders (e.g., Ehlers-Danlos syndromes, osteogenesis imperfecta, Marfan syndrome…) is performed in this lab based on various zebrafish models. On the other hand, the 4BRAIN lab has decades of experience with multiple techniques (e.g., electrophysiological techniques) to study (acquired) forms of epilepsy in mice and rats. Thus, combining the epilepsy knowledge and experience of the 4BRAIN lab with the benefits of the zebrafish model and molecular analysis techniques of the CMGG lab definitely forms the optimal research environment for conducting this thesis.

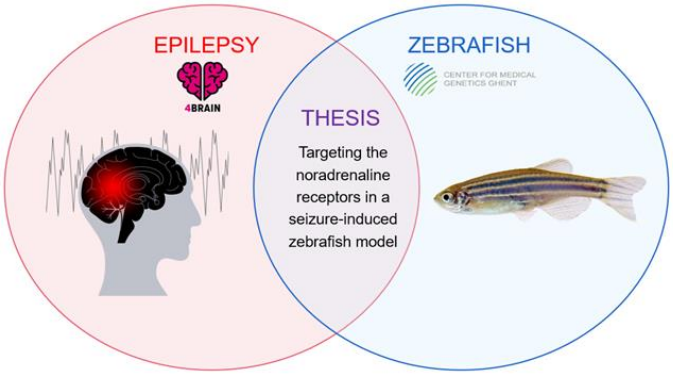

Figure 7: Schematic representation of the collaboration between the 4BRAIN lab on the one hand and the CMGG lab on the other hand. Both labs have decades worth of experience, knowledge and expertise about epilepsy (4BRAIN lab) and zebrafish models (CMGG lab), thus forming a solid foundation and an optimal research environment for conducting this master's thesis project.

5.6 Scientific research objectives and hypotheses

In this thesis, the contribution and role of the noradrenergic system in epilepsy and seizures is investigated by making use of a 5 dpf zebrafish model. This project studies the involvement of the noradrenergic system in regulating seizures in 5 dpf zebrafish in two different ways. A first approach is to study the underlying mechanisms of the noradrenergic system by exploring the expression levels of different noradrenaline receptor subtypes in untreated wild-type 5 dpf zebrafish. Therefore, an expression analysis consisting of an RNA-extraction, cDNA-synthesis and RT-qPCR analysis is performed. It is hypothesized that noradrenergic receptors are expressed in 5 dpf zebrafish and are playing a key role in the anticipated antiseizure effect of noradrenaline. A second approach is to compare the effects of a noradrenergic agonist (clonidine) and antagonist (atipamezole) with an established antiseizure drug (valproic acid) on the PTZ-induced seizure behavior. It is hypothesized that administration of VA (antiepileptic

compound) and clonidine (noradrenaline agonist) will suppress PTZ-induced seizures, whereas atipamezole, acting as a noradrenaline antagonist, is thought to exert opposite effects.

To conclude, 5 dpf zebrafish are used to set up a seizure model for epilepsy in which antiepileptic and noradrenergic compounds are evaluated on their effects on the zebrafish behavior. Moreover, the expression of different noradrenaline receptors is assessed in 5 dpf zebrafish. The aim is to gain more detailed insights into the underlying mechanisms and role of the noradrenergic neurotransmission system in seizures and epilepsy by making use of zebrafish as a valuable preclinical animal model. In this way, it is possible to contribute to innovative research with translational potential for developing new antiepileptic strategies for epilepsy patients that are not helped with current epilepsy treatment options.

6. Material and methods

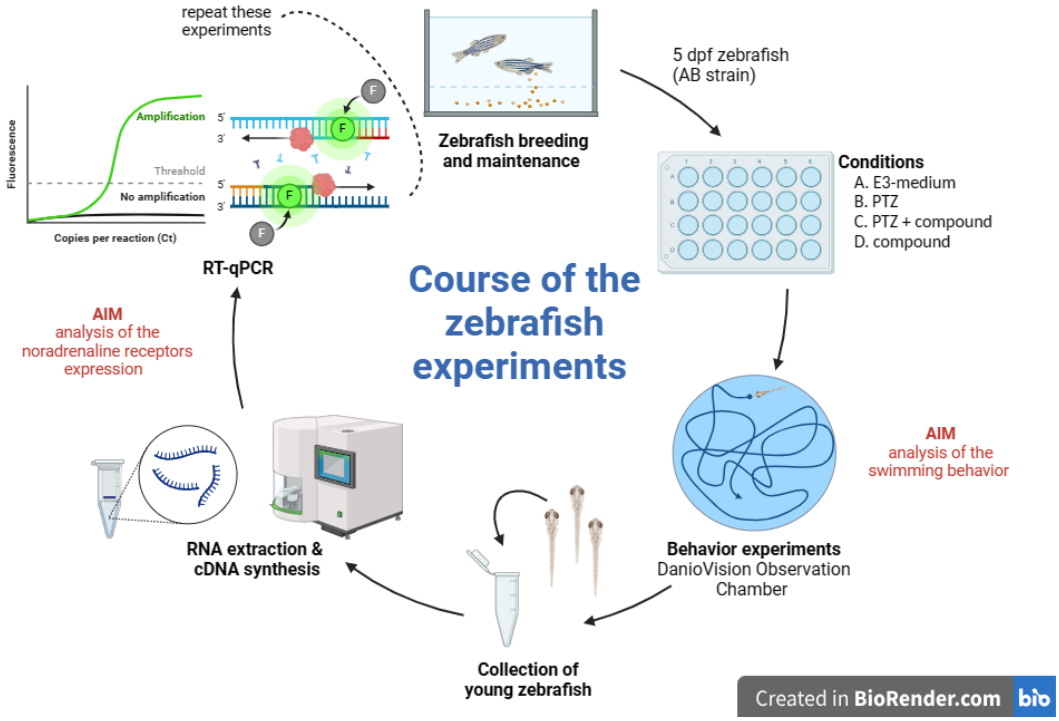

Figure 8: Graphical abstract (created in BioRender.com) of the course of the zebrafish experiments of this thesis. To study the effects of a noradrenaline agonist (e.g., clonidine) and antagonist (e.g., atipamezole), besides an antiepileptic compound (valproic acid) on seizures, the swimming behavior is assessed of 5 dpf zebrafish with PTZ-induced seizures prior and following treatment. To evaluate the expression of noradrenaline receptors in 5 dpf untreated zebrafish, RNA is extracted from 5 dpf zebrafish for cDNA-synthesis and RT-qPCR analysis. This allows us to study the noradrenaline receptors expression levels in 5 dpf zebrafish.

6.1 Behavior analysis

6.1.1 Overview of the behavior experiments

In order to perform the behavior experiments, some preparatory steps need to be taken. First, a zebrafish breeding needs to be set up and young zebrafish need to be maintained to obtain 5 days post fertilization (dpf) zebrafish to use in further behavior experiments (6.1.2). Then, randomized plate layout designs need to be generated to randomly assign the different wells to different conditions (6.1.3.1). Afterwards, stock and working solutions need to be prepared for the compounds that are tested in the behavior analysis, namely VA, PTZ, clonidine and atipamezole (6.1.3.2). In a last step, the behavior analyses can be performed with the

DanioVision Observation Chamber and EthoVision Software (6.1.3.3) (both Noldus, The Netherlands) and the behavior data is analysed (6.1.4).

6.1.2 Breeding and maintenance of young zebrafish (5 dpf)

The following steps are based on the in-house protocol for setting up a zebrafish breeding and maintaining young zebrafish until 5 dpf, used in the CMGG lab and the Zebrafish Core Facility at the University of Ghent. A zebrafish breeding is set up for each behavior experiment by putting two adult female and two adult male wild-type zebrafish (AB strain) into a breeding tank. After this breeding, the eggs are rinsed and collected in a Petri dish filled with E3 medium, which is then placed into an incubator at 28°C. Until 5 dpf, daily inspections are performed to assess fertilization, viability and quality, and to check whether the zebrafish eggs have hatched from their chorion, which occurs mostly around 2-3 dpf. Debris and/or dead zebrafish are also daily removed from the Petri dish. This protocol was set up and documented with pictures by dr. Delfien Syx, and can be found in the Addendum (12.1.1.1).

6.1.3 DanioVision Observation Chamber & EthoVision Software

6.1.3.1 Generating randomized plate layouts

The program PlateDesigner (PlateDesigner (clinicalresearch-apps.com)) is used to generate randomized plate layouts of the 24-well plates used for following zebrafish experiments, to prevent measurement bias. Random plate layouts with the required plate format (24-well plate) and the wanted number of replicates (6 replicates/condition) can be generated (Addendum: 12.1.1.2).

6.1.3.2 Preparing stock solutions and working solutions of the compounds

After generating the randomized plate layouts, the next preparatory step consists of making the stock and working solutions of the compounds that are used in the behavior experiments. For valproic acid (VA) and pentylenetetrazole (PTZ), the working solutions are 2 mM and 5 mM, respectively. Different concentrations of working solutions of clonidine are used: 50 nM, 100 nM, 200 nM, 5 µM, 10 µM, 20 µM and 30 µM. For atipamezole, the working solutions are the following: 5 nM, 10 nM, 20 nM, 50 nM, 100 nM, 300 nM, 1 µM, 10 µM, 30 µM, 50 µM and 200 µM. Working solutions are made with E3 medium as solvent and are kept in the freezer (-20 °C) until further usage or used immediately.

6.1.3.3 DanioVision Observation Chamber and EthoVision software

After setting up a zebrafish breeding, generating the randomized 24-well plate layouts and preparing the stock and working solutions, the behavior experiment is continued at 5 dpf. For the behavior analysis, a 24-well plate (4 conditions, 6 zebrafish/condition, 1 zebrafish (5 dpf) per well) is used to investigate the effects of different conditions on the zebrafish swimming behavior. The well plates are filled with the required compounds according to the earlier generated randomized plate layouts. For the PTZ + VA, PTZ + clonidine and PTZ + atipamezole behavior tests, these conditions consist of: (1) E3 medium (negative control), (2) 5 mM PTZ (seizure-induced zebrafish), (3) 2 mM VA/30 µM clonidine/30 µM atipamezole and (4) 5 mM PTZ + 2 mM VA/30 µM clonidine/30 µM atipamezole. To find the optimal concentrations of clonidine and atipamezole, different concentration levels are tested. The plate layout for these experiments is as following: (1) E3 medium (negative control), (2+3+4) different concentrations of the compound clonidine/atipamezole.

After administration of the different solutions (Addendum 12.1.1.3), an incubation period of 15 minutes is used for the compounds VA, clonidine and atipamezole. The 24-well plate is then placed in the heated water reservoir of the DanioVision Observation Chamber (Noldus, The Netherlands), which consists of distillated water and is at a constant temperature of 28°C. After appropriately enclosing the well plates in the machine and lowering the lens to prevent angular distortion, the settings are checked in the EthoVision XT15 software (Noldus, The Netherlands). This consists of checking the arena settings (i.e., the correct 24-well plate has to be detected by the machine), the trial control settings (i.e., the desired protocol is selected

and adjusted), the detection settings (i.e., every zebrafish needs to be clearly visible and detected by the software program) and the trial list (i.e., assigning every well to the right experimental conditions). The protocol that is used for these behavior analyses consists of a 20-minute light period (5% intensity), followed by a 20-minute dark period, followed by 5 cycles of alternating light-dark periods (5 minutes each), resulting in a total behavior analysis time of 1 hour and 30 minutes. In this thesis, every test of 1 day consists of 3-4 behavior trials (from 9 AM till 4 PM) and every test is independently executed on 3 different testing days. Possible toxicity effects of all compounds (PTZ, VA, clonidine and atipamezole) are monitored by checking the survival of the zebrafish after the experiment. The behavior data will be recorded and subsequently analysed. The EthoVision software generates multiple datasets with various parameters, namely distance moved (mean, maximum, total), velocity (mean, maximum) and movement (mean, frequency, cumulative duration, latency to first), over 1-minute, 5-minutes and 10-minutes intervals.

6.1.4 Data-analysis

The different parameters obtained with the EthoVision software are plotted in GraphPad Prism (version 9.0.0) with bar plots to visualize and compare differences between the control condition and the PTZ condition. Data are checked for normal distribution by plotting residual plots and QQ-plots. Statistics are performed using an unpaired t-test.

Based on these results, three different parameters are chosen to discriminate between the control and the PTZ phenotype. For the PTZ + compound (VA, clonidine or atipamezole) behavior tests, an ANOVA-test (one-way analysis of variance) is chosen to compare the mean of every single column with the mean of every other column. Šidák correction is chosen as post-hoc test in all the behavior tests.

6.2 Expression analysis

6.2.1 Overview of the expression experiments

The main objective of this thesis is to assess the involvement of the noradrenergic system in epilepsy and to understand how the expression of the noradrenaline receptors varies in different zebrafish tissues. Therefore, samples of zebrafish heads and full bodies (containing head and body) are selected and evaluated on their noradrenaline receptor expression levels, to investigate whether there are expression differences in these zebrafish tissues. For these expression experiments, reference genes are selected based on literature (6.2.2.1). These reference genes are tested on their expression stability in samples of pools of 10 5 dpf zebrafish (AB strain) heads and bodies of eight different clutches (6.2.2.2). Therefore, an RNA extraction (6.2.2.3), a cDNA synthesis (6.2.2.4) and an RT-qPCR analysis (6.2.2.5) are performed on these heads and bodies samples. Stable reference genes are used in further experiments with pools of 1, 2, 3, 6 and 12 zebrafish heads and bodies, on which also dissections, an RNA extraction, a cDNA synthesis and an RT-qPCR analysis are performed, to evaluate and normalize the expression levels of different noradrenaline receptors (6.2.3).

6.2.2 Determining stably expressed reference genes in 5 dpf zebrafish on samples of 10 zebrafish heads or bodies

6.2.2.1 Primer design and primer efficiency testing

Prior to performing the RT-qPCR analysis, primers are designed for following reference genes: *b2m*, *cat*, *cyp19a1b*, *eef1a1a*, *eif2s2*, *gapdh*, *hprt1*, *lsm12b*, *mobk13*, *rnf7*, *rpl7*, *rpl13a*, *rplp2*, *rps18*, *sdha*, *slc25a5*, *tbp*, *tuba1a*, *ube2a* and *ywhaz*. The selection of these reference genes is based on previous literature studies [39,40,41]. Additionally, primers are designed and tested, specifically targeting the zebrafish orthologs of noradrenaline receptor genes: *adra1aa* (α_1Aa-adrenoceptor), *adra1ab* (α_1Ab-adrenoceptor), *adra1ba* (α_1Ba-adrenoceptor), *adra1bb* (α_1Bb-adrenoceptor), *adra2a* (α_2A-adrenoceptor), *adra2b* (α_2B-adrenoceptor), *adrb1* (β_1-adrenoceptor), *adrb2a* (β_2A-adrenoceptor) and *adrb2b* (β_2B-adrenoceptor). Using Ensembl, UCSC Genome Browser and NCBI primer-blast, it is possible to ensure that the primers fulfill

stringent criteria: a melting temperature of 60°C, amplification length of maximal 120bp targeting the coding region, and not containing any single nucleotide polymorphisms (SNPs) at the primer annealing sites. Primers are then ordered (Integrated DNA technologies), dissolved with H_2O to make a 100 µM stock solution of each primer and diluted to 5 µM using RNase-free H_2O. To evaluate primer efficiencies, an initial RT-qPCR experiment is conducted, utilizing a cDNA dilution series from 5 dpf zebrafish tissue (fin) as template (the concentrations and dilution can be found below in Table 2). All samples are run in duplicate. The Cq-values are then obtained, and primer efficiency is determined by using the slope of the log Cq-values.

Table 2: cDNA dilution series

	Starting volume	Diluted with
Point 1: 32 ng/µl	100 µl cDNA	6.25 µl 50x carrier + 206.25 µl nuclease-free water
Point 2: 8 ng/µl	78 µl point 1	234 µl 1x carrier
Point 3: 2 ng/µl	78 µl point 2	234 µl 1x carrier
Point 4: 0.5 ng/µl	78 µl point 3	234 µl 1x carrier
Point 5: 0.125 ng/µl	78 µl point 4	234 µl 1x carrier
Point 6: 0.0312 ng/µl	78 µl point 5	234 µl 1x carrier
Negative control	240 µl 1x carrier	

6.2.2.2 Dissections and collections of pools of 10 zebrafish heads or bodies

To reduce variability in the samples to a minimum, dissection and collection experiments are always performed in the afternoon (4PM). Prior to dissection, all instruments (Petri dish, scalpel, forceps and stereoscope) and surfaces are decontaminated with the RNaseZap™ RNase Decontamination solution (Invitrogen by Thermo Fisher Scientific). The 5 dpf zebrafish are euthanized in a tricaine solution (25x) and gently transferred into a Petri dish using forceps. The Petri dish is placed under the stereoscope where the zebrafish head is removed using a scalpel (Figure 9) and collected in an Eppendorf tube which is placed on dry ice. For the collection of bodies, the whole 5 dpf zebrafish is collected using forceps and stored in an Eppendorf tube. Samples consist of 10 zebrafish heads or bodies from 8 different zebrafish clutches, each in triplicate. The samples are stored in the -80°C freezer.

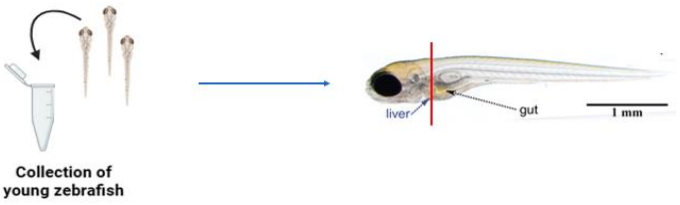

Figure *9: Dissection of the head of 5 dpf zebrafish: ventral view of the incision made by the scalpel (red vertical line).*

6.2.2.3 RNA extraction

RNA is extracted from the previously pooled 5 dpf zebrafish bodies and heads. This is performed by using the miRNeasy mini kit (Qiagen) and the Qiagen RNase-free DNase kit according to the instructions of the manufacturer (Addendum 12.1.2.1). To assess the quality and the concentration of the RNA, the Little Lunatic machine is used. An A260/A280 ratio > 2, which indicates the purity of the RNA sample, results in good quality RNA. Samples are stored in a -80°C freezer or immediately used for cDNA synthesis.

6.2.2.4 cDNA synthesis

cDNA (complementary DNA) is synthesized from 500 ng RNA with the iScript Advanced cDNA synthesis kit (Bio-Rad), following the in-house protocol (Addendum 12.1.2.2). During cDNA synthesis, the enzyme reverse transcriptase converts total RNA into cDNA. Degradation of RNA is prevented by working on ice during the whole experiment. Finally, a 5 ng/µl dilution of the samples is prepared in nuclease-free water and samples are stored in a -20°C freezer or directly used for RT-qPCR analysis.

6.2.2.5 RT-qPCR analysis

Expression levels of the reference genes (*b2m*, *cat*, *cyp19a1b*, *eef1a1a*, *eif2s2*, *gapdh*, *hprt1*, *lsm12b*, *mobk13*, *rnf7*, *rpl7*, *rpl13a*, *rplp2*, *rps18*, *sdha*, *slc25a5*, *tbp*, *tuba1a*, *ube2a* and *ywhaz)* are analysed using reverse transcriptase quantitative polymerase chain reaction (RT-qPCR), since its advantage is that amplification of the PCR products can be monitored in real-time by making use of SYBR Green. To perform the RT-qPCR, a mix is prepared containing 1x SsoAdvanced™ SYBR Green Supermix, 5 µM of the forward and reverse primer (for each gene) and 2 µl cDNA (2.5 ng/µL), extracted from the zebrafish tissue in previous experiments. Samples are always run and analysed in duplicate, and 8 different clutches are used as biological replicates. The plate is analysed with the LightCycler 480, following the SsoAdvanced™ SYBR GREEN cDNA program (Addendum 12.1.2.4).

6.2.2.6 Data analysis

For the data analysis of the expression experiments the qbase+ software (CellCarta) is used. This software can determine the expression stability of reference genes in zebrafish tissues of 10 heads and 10 bodies. Afterwards, a geNorm analysis is performed to determine the most stable reference genes in zebrafish head and body samples separately. Samples are included for the geNorm analysis if the difference between the two Cq-values of both duplicates is not higher than 0.5.

6.2.3 Determining the noradrenaline receptor genes expression levels in zebrafish heads or bodies

Collections and dissections are performed on different pools of 1, 2, 3, 6 and 12 zebrafish heads and bodies. These series of ascending numbers of 5 dpf zebrafish heads and bodies are chosen to determine the number of 5 dpf zebrafish heads and bodies that are needed to be pooled in order to detect expression levels of noradrenergic receptors, and to investigate whether the number of zebrafish heads and bodies also has an influence on the expression of these noradrenaline receptor genes.

For these expression analyses, three biological replicates are used for every sample series, since samples from three different zebrafish clutches are tested. RNA extractions and cDNA syntheses are performed as described above. Lastly, RT-qPCR analysis is performed on the chosen stable reference genes (specifically for head or body samples) and on the noradrenaline receptor genes. For the data analysis, the results from qbase+ are used to make plots in GraphPad Prism (version 9.0.0), with on the x-axis the different samples (1, 2, 3, 6 and 12 heads/bodies) and on the y-axis the relative quantities. However, some samples are excluded from the analyses due to having a Cq-value higher than 35, which indicates a late Cp call in the last five cycles and thus a higher uncertainty.

7. Results

7.1 Behavior analysis

7.1.1 Results during stable light, switch light-dark and stable dark period

The behavior experiments are divided into two separate analyses. In this way, this project investigates firstly the behavior of 5 dpf zebrafish in the stable light and stable dark phases (10:00-20:00 (light) and 30:00-40:00 (dark)) and in the switch phase between light and dark

(20:00-30:00 (dark)), and secondly the effect of a light stimulus on the behavior (and on PTZ-induced seizures) of the 5 dpf zebrafish (alternating phases 40:00-90:00).

For the results of behavior, the selection to define a PTZ-induced seizure is made first (7.1.1.1). Therefore, several parameters are plotted and the ones with the most clear difference between control and PTZ are selected. The first 10 minutes in the light (00:00-10:00) of the behavior experiment are defined as acclimatization period and during the other 30 minutes (10:00-20:00 (light), 20:00-30:00 (dark), 30:00-40:00 (dark)) the different conditions are compared to each other (control, PTZ, VA/clonidine/atipamezole, PTZ+VA/clonidine/atipamezole). Subsequently, the same method is used to examine the alternating light/dark phases, focusing on the difference in maximum distance moved during switching from light to dark and dark to light.

7.1.1.1 Selection of behavior parameters to define a PTZ-induced seizure

In order to use 5 dpf zebrafish to study seizures, it is important to define seizure-like behavior in these 5 dpf zebrafish. Therefore, the start of the behavior experiments in this project consists of an analysis of some of the different parameters that are generated by the EthoVision Software: distance moved (total, mean, maximum), velocity (mean, maximum), movement: moving (mean, maximum, frequency, latency to first, cumulative duration) over different time bins. The choice was made to divide the first 40 minutes into time bins of each 10 minutes. After an acclimatization period of 10 minutes (00:00-10:00), the 10:00-20:00 stable light condition, 20:00-30:00 switch light-dark and 30:00-40:00 stable dark condition are plotted. This way, the 5 dpf are able to adapt to the light condition (10:00-20:00) (Figure 10), then the conditions are switched from light to dark and the influence of that switch can be examined (20:00-30:00) (Figure 11) and then again the 5 dpf zebrafish are able to acclimatize to the new dark conditions (30:00-40:00) (Figure 12).

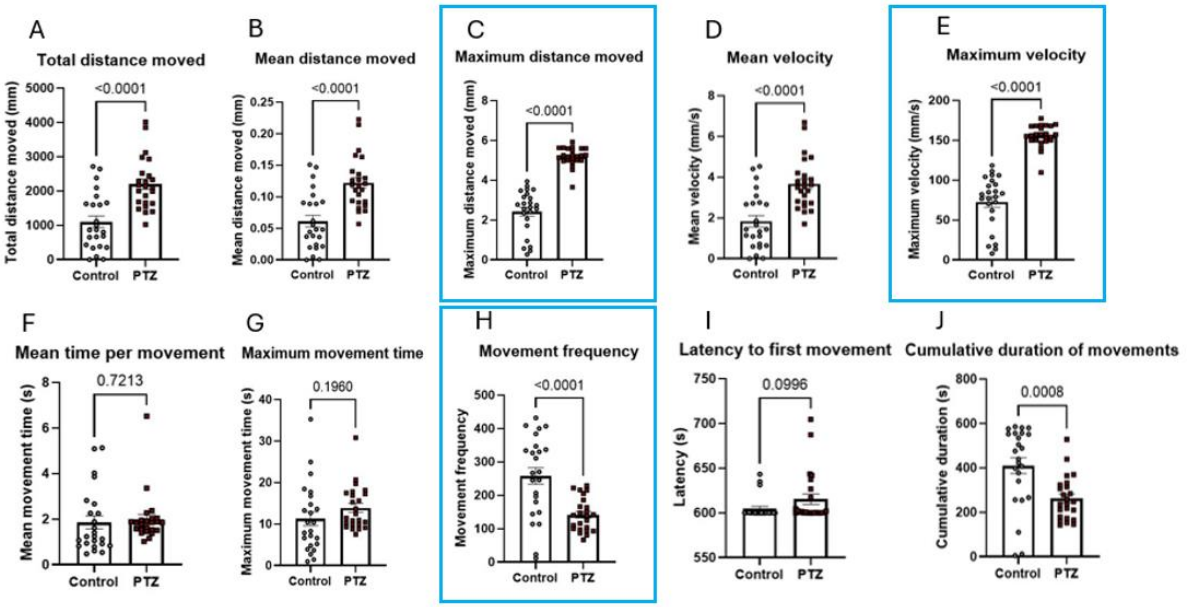

Figure 10: Different parameters ((A) total distance moved (mm), (B) mean distance moved (mm), (C) maximum distance moved (mm), (D) mean velocity (mm/s), (E) maximum velocity (mm/s), (F) mean time per movement (s), (G) maximum movement time (s), (H) movement frequency, (I) latency to first movement (s), (J) cumulative duration of movements (s)) are shown for the time bin of 10:00-20:00. Control (white circles) and 5 mM PTZ (red squares with black border) are plotted on the x-axis, the parameters are plotted on the y-axis. The three selected parameters (maximum distance moved, maximum velocity and movement frequency) are indicated with blue squares. Data (n = 24 zebrafish/condition (3 trials)) are plotted as mean ± SEM, a one-way ANOVA test with Šidák correction for multiple comparisons as post-hoc test is chosen, and p-values are shown above the graph.

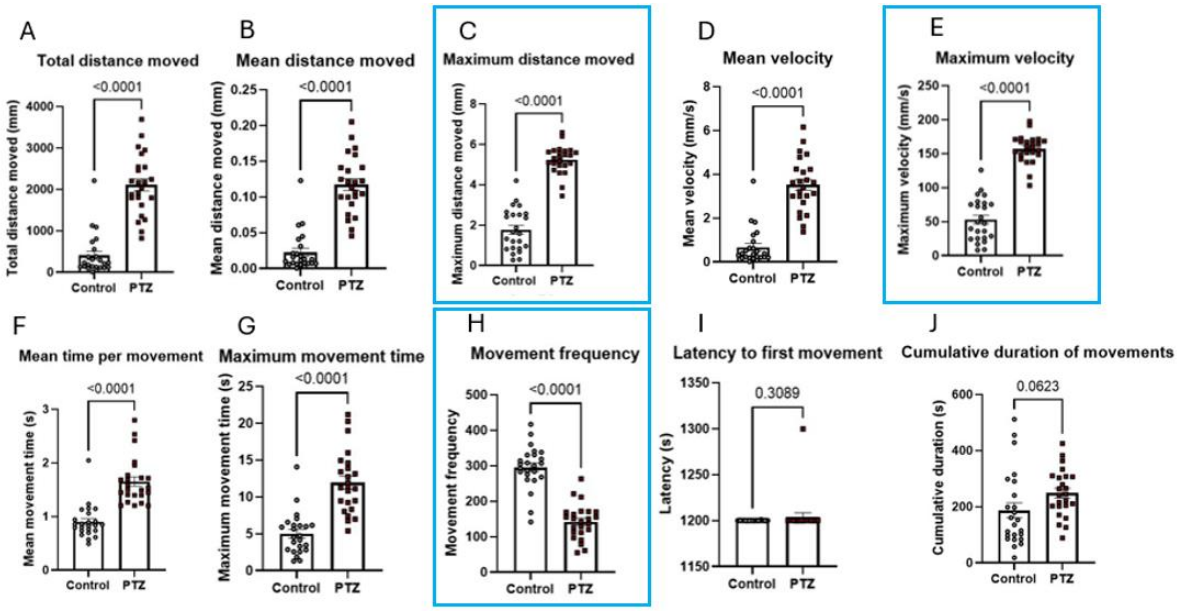

Figure 11: Different parameters ((A) total distance moved (mm), (B) mean distance moved (mm), (C) maximum distance moved (mm), (D) mean velocity (mm/s), (E) maximum velocity (mm/s), (F) mean time per movement (s), (G) maximum movement time (s), (H) movement frequency, (I) latency to first movement (s), (J) cumulative duration of movements (s)) are shown for the time bin of 20:00-30:00. Control (white circles) and 5 mM PTZ (red squares with black border) are plotted on the x-axis, the parameters are plotted on the y-axis. The three selected parameters (maximum distance moved, maximum velocity and movement frequency) are indicated with blue squares. Data (n = 24 zebrafish/condition (3 trials)) are plotted as mean ± SEM, a one-way ANOVA test with Šidák correction for multiple comparisons as post-hoc test is chosen, and p-values are shown above the graph.

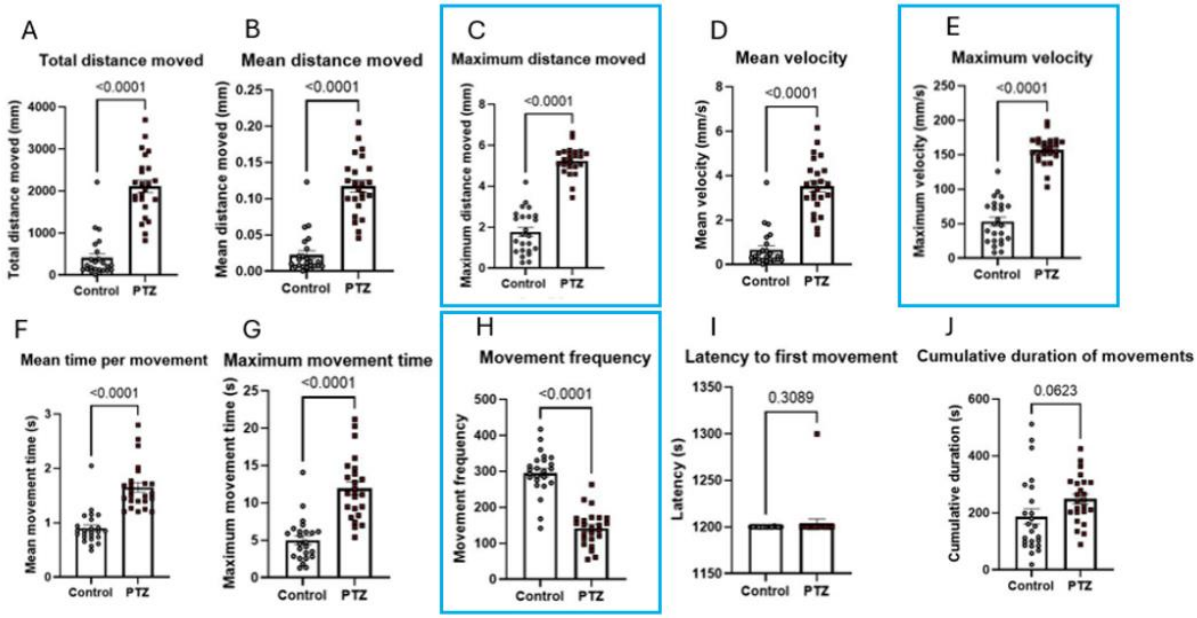

Figure 12: Different parameters ((A) total distance moved (mm), (B) mean distance moved (mm), (C) maximum distance moved (mm), (D) mean velocity (mm/s), (E) maximum velocity (mm/s), (F) mean time per movement (s), (G) maximum movement time (s), (H) movement frequency, (I) latency to first movement (s), (J) cumulative duration of movements (s)) are shown for the time bin of 30:00-40:00. Control (white circles) and 5 mM PTZ (red squares with black border) are plotted

on the x-axis, the parameters are plotted on the y-axis. The three selected parameters (maximum distance moved, maximum velocity and movement frequency) are indicated with blue squares. Data (n = 24 zebrafish/condition (3 trials)) are plotted as mean ± SEM, a one-way ANOVA test with Šidák correction for multiple comparisons as post-hoc test is chosen, and p-values are shown above the graph.

Based on the results of the different parameters in the different times bins, and on their ability to discriminate between the control zebrafish and the phenotype introduced by PTZ (Figures 10, 11 and 12) a selection of three parameters is made: maximum distance moved (Figure 13), maximum velocity (Figure 14) and movement frequency (Figure 15). Those graphs are plotted and discussed below.

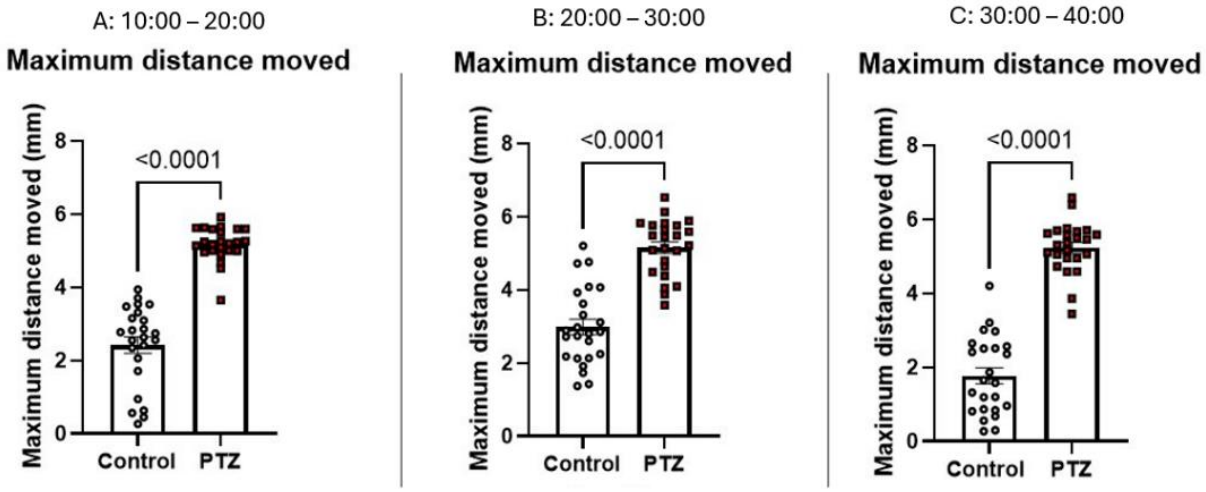

Figure 13: Scatter plot of the maximum distance moved (mm) in the control group and the PTZ-treated group. Control (white circles) and 5 mM PTZ (red squares with black border) are plotted on the x-axis; the maximum distance moved (mm) in a time bin of 10 minutes ((A) min. 10:00-20:00, (B) min. 20:00-30:00 and (C) min. 30:00-40:00) is plotted on the y-axis. Data (n = 24 zebrafish/condition (3 trials)) are plotted as mean ± SEM, a one-way ANOVA test with Šidák correction for multiple comparisons as post-hoc test is chosen, and p-values are shown above the graph.

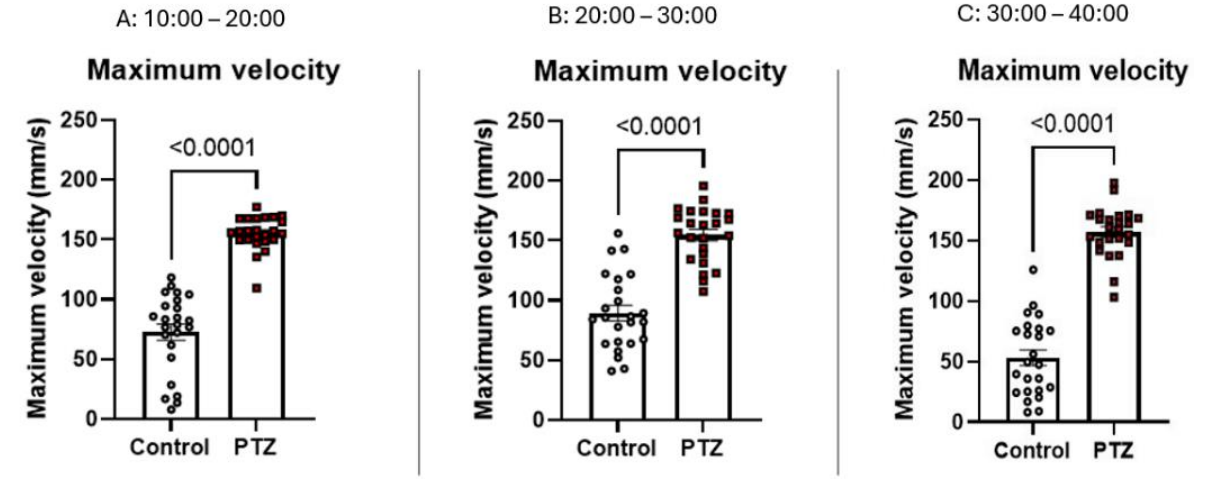

Figure 14: Scatter plot of the maximum velocity (mm/s) in the control group and the PTZ-condition. Control (white circles) and 5 mM PTZ (red squares with black border) are plotted on the x-axis; the parameter maximum velocity (mm/s) in a time bin of 10 minutes ((A) min. 10:00-20:00, (B) min. 20:00-30:00 and (C) min. 30:00-40:00) is plotted on the y-axis. Data (n = 24 zebrafish/condition (3 trials)) are plotted as mean ± SEM, a one-way ANOVA test with Šidák correction for multiple comparisons as post-hoc test is chosen, and p-values are shown above the graph.

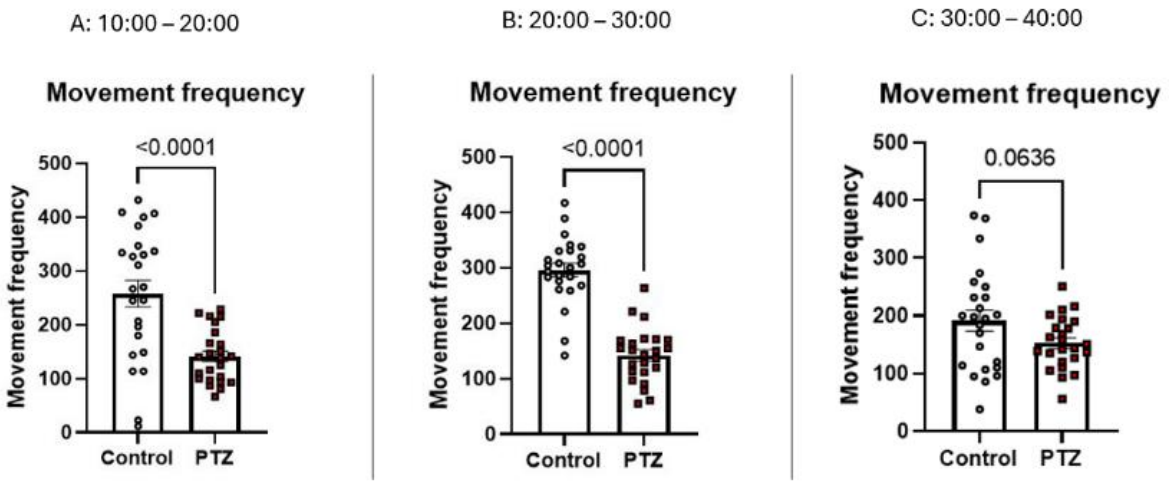

Figure 15: Scatter plot of the movement frequency in the control group and the PTZ-condition. Control (white circles) and 5 mM PTZ (red squares with black border) are plotted on the x-axis; the parameter movement frequency in a time bin of 10 minutes ((A) min. 10:00-20:00, (B) min. 20:00-30:00 and (C) min. 30:00-40:00) is plotted on the y-axis. Data (n = 24 zebrafish/condition (3 trials)) are plotted as mean ± SEM, a one-way ANOVA test with Šidák correction for multiple comparisons as post-hoc test is chosen, and p-values are shown above the graph.

It can be seen on Figures 13, 14 and 15 that there is a significant increase in both maximum distance moved and maximum velocity in the PTZ-treated group, while there is a significant decrease in movement frequency in this group. Zebrafish in the PTZ condition initiate thus fewer times a locomotor response (reflected in their lower movement frequency), but when they move, their movements are of a longer distance (reflected in their higher maximum distance moved) and have a higher velocity (reflected in their higher maximum velocity).

7.1.1.2 Effect of the antiepileptic drug VA on PTZ-induced seizures

Next, this project aims to validate the use of a PTZ-dependent seizure model in a behavior experiment and to provide its relevance for patients. The anticonvulsant effect of a standard AED used in the clinic, namely valproic acid (VA) is explored in a 5 dpf larval zebrafish model of PTZ-evoked seizures.

In general, 5 dpf zebrafish have a specific behavior pattern when exposed to light-dark conditions. In normal conditions, 5 dpf zebrafish move more in the dark compared to the light condition. The convulsant agent PTZ, besides increasing the swimming activity reflecting the seizures, induces a reversal in this behavioral activity in the stable phases. This reversal is characterized by an increasing locomotor activity in the light period and a decreasing activity in the dark. Additionally, in the dark phases, it is observed that the other three groups of 5 dpf zebrafish (control, VA, PTZ+VA) are more active [17].

The graphs with the overview of the parameters maximum distance moved and maximum velocity show the overall data of control, VA-treated, PTZ-treated and VA+PTZ co-treated zebrafish for all the phases (the stable light (10:00-20:00), switch light-dark (20:00-30:00) and dark period (30:00-40:00) and alternating light-dark phases (40:00-90:00)) (Figure 16). The overview graphs (Figure 16) show an overall quasi-opposite light-dependent swimming pattern in the PTZ-treated zebrafish, which is similar with results found in literature [17]. Differences are observed between the light and dark phases during the whole experiment, with the greatest variance occurring within the first minute immediately following a change in light. Both effects do not decrease during the experiment.

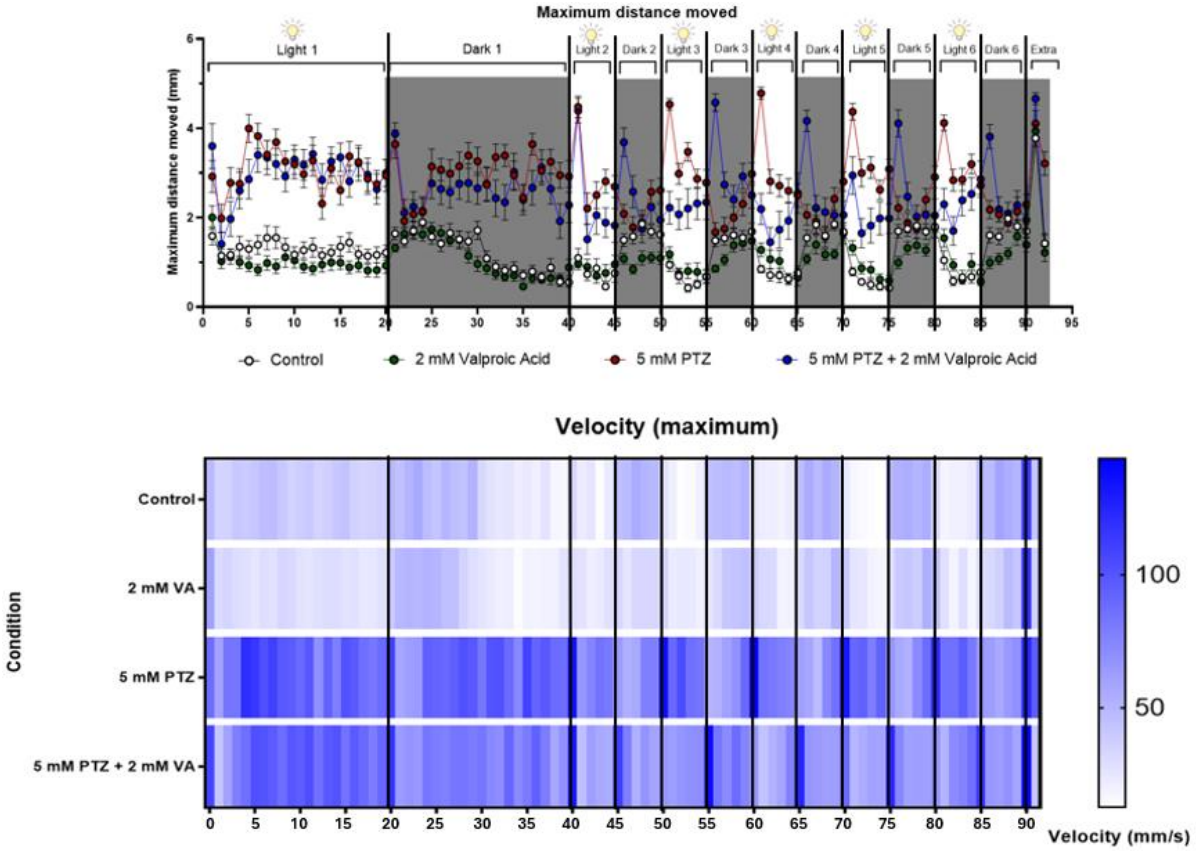

Figure 16: Overview of the maximum distance moved in mm (upper graph) and heatmap of the maximum velocity in mm/s (lower graph) in the following conditions: control (white), 2 mM VA (green), 5 mM PTZ (red) and 5 mM PTZ + 2 mM VA (blue). On the upper graph, the parameter maximum distance moved (mm) (mean ± SEM) is plotted on the y-axis, whereas different time points (minutes) are plotted on the x-axis. White and grey squares indicate light and dark periods, respectively. On the lower graph, the parameter maximum velocity (mm/s) is plotted. On the x-axis, the time (min) can be seen; on the y-axis, the different conditions can be seen. The more intense the color blue is, the higher the maximum velocity. (n = 24 zebrafish/condition (3 trials)).

The behavioral analyses for maximum distance moved and maximum velocity show the effect of VA on the seizure in Figures 17 and 18. For the comparison of the control and VA group, administration of 2 mM VA only significantly decreases the maximum distance moved (Figure 17A and C) and the maximum velocity (Figure 18A and C), however, no significant difference is observed in the light-dark switch period (Figure 17B and Figure 18B). There is also no significant decrease observed between the PTZ and PTZ+VA co-treated group in the min. 10:00-20:00 time bin (Figure 17A and Figure 18A). For all the other comparisons, there is an overall significant difference observed.

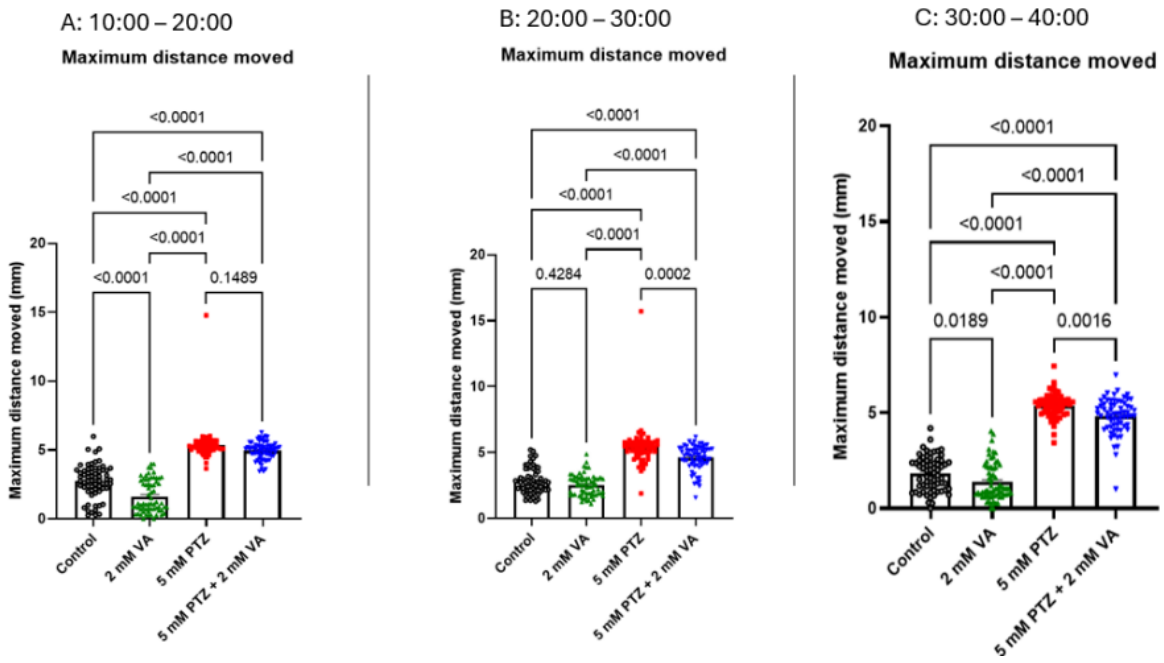

Figure 17: Scatter plot of the maximum distance moved (mm) in the different conditions: control, 2 mM VA, 5 mM PTZ and 5 mM PTZ + 2 mM VA. Control (white), 2 mM VA (green), 5 mM PTZ (red) and 5 mM PTZ + 2 mM VA (blue) are plotted on the x-axis; the parameter maximum distance moved (mm) in a time bin of 10 minutes ((A) min. 10:00-20:00 with F-value = 173.2 and p-value < 0.0001, (B) min. 20:00-30:00 with F-value = 109.2 and p-value < 0.0001 and (C) min. 30:00-40:00 with F-value = 370.4 and p-value < 0.0001) is plotted on the y-axis. All the three PTZ+VA tests are plotted together (n = 66 zebrafish/condition (3 tests, 3-4 trials/test (11 trials in total))). Data are plotted as mean ± SEM, a one-way ANOVA test with Šidák correction for multiple comparisons as post-hoc test is chosen, and p-values are shown above the graph.

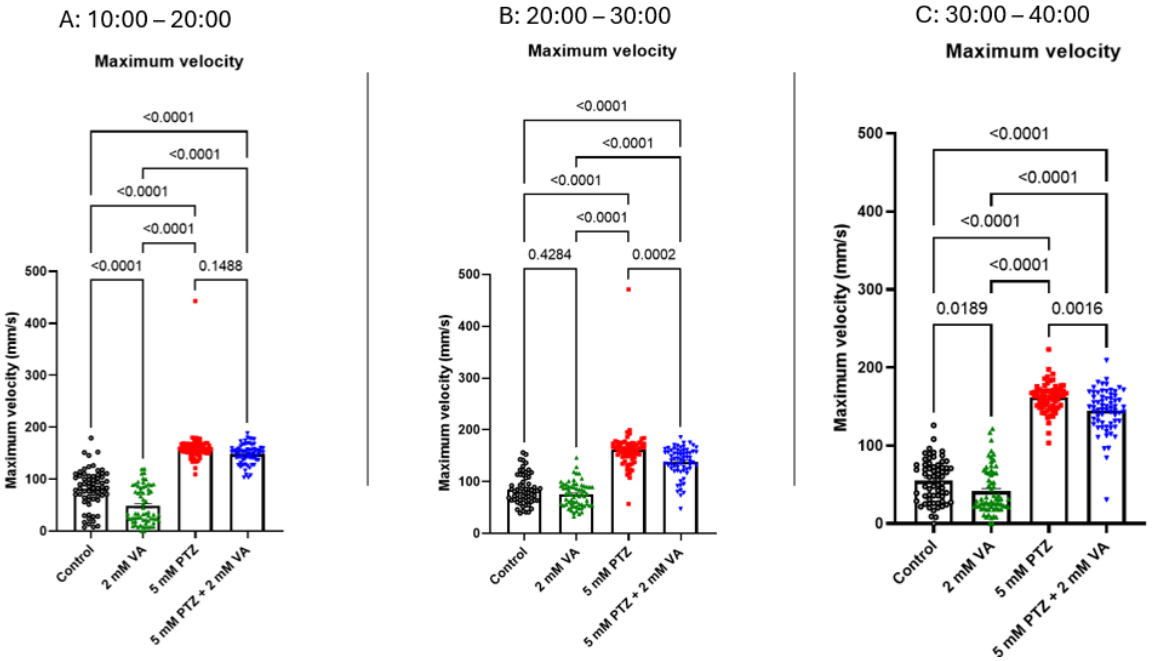

Figure 18: Scatter plot of the maximum velocity (mm/s) in the different conditions: control, 2 mM VA, 5 mM PTZ and 5 mM PTZ + 2 mM VA. Control (white), 2 mM VA (green), 5 mM PTZ (red) and 5 mM PTZ + 2 mM VA (blue) are plotted on the x-axis; the parameter maximum velocity (mm/s) in a time bin of 10 minutes ((A) min. 10:00-20:00 with F-value = 173.2 and p-value < 0.0001, (B) min. 20:00-30:00 with F-value = 109.2 and p-value < 0.0001 and (C) min. 30:00-40:00 with F-value = 370.4 and p-

value < 0.0001) is plotted on the y-axis. All the three PTZ+VA tests are plotted together (n = 66 zebrafish/condition (3 tests, 3-4 trials/test (11 trials in total))). Data are plotted as mean ± SEM, a one-way ANOVA test with Šidák correction for multiple comparisons as post-hoc test is chosen, and p-values are shown above the graph.

No significant differences in movement frequency are observed between the control group and the VA-treated group on the one hand, and between the PTZ-treated group and the PTZ+VA co-treated group on the other hand in all time bins. For all the other comparisons, there are significant differences seen. Nevertheless, it can be concluded that zebrafish in the PTZ-treated and PTZ+VA co-treated groups move less frequently (Figure 19) but cover longer distances (Figure 17) and have a higher maximum velocity (Figure 18) when having a seizure.

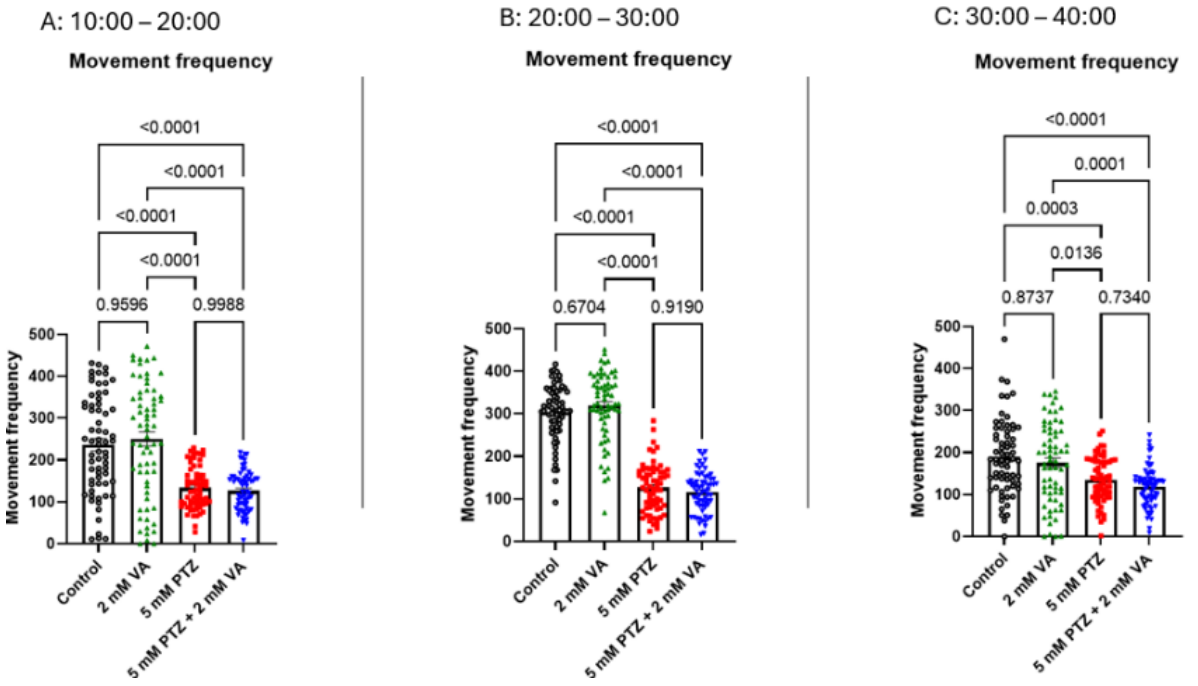

Figure 19: Scatter plot of the movement frequency in the different conditions: control, 2 mM VA, 5 mM PTZ and 5 mM PTZ + 2 mM VA. Control (white), 2 mM VA (green), 5 mM PTZ (red) and 5 mM PTZ + 2 mM VA (blue) are plotted on the x-axis; the parameter movement frequency in a time bin of 10 minutes ((A) min. 10:00-20:00 with F-value = 30.93 and p-value < 0.0001, (B) min. 20:00-30:00 with F-value = 19.8 and p-value < 0.0001 and (C) min. 30:00-40:00 with F-value = 13.00 and p-value < 0.0001) is plotted on the y-axis. All the three PTZ+VA tests are plotted together (n = 66 zebrafish/condition (3 tests, 3-4 trials/test (11 trials in total))). Data are plotted as mean ± SEM, a one-way ANOVA test with Šidák correction for multiple comparisons as post-hoc test is chosen, and p-values are shown above the graph.

It is concluded that the antiepileptic drug VA does have an anticonvulsant effect because 5 dpf zebrafish cover longer distances (Figure 17) and have a higher maximum velocity (Figure 18) when having a seizure, but it doesn't affect the number of times that they initiate a movement, thus the movement frequency (Figure 19). VA has also a decreasing effect on the control group, characterized by a significant decrease in maximum distance moved and maximum velocity without affecting movement frequency.

7.1.1.3 Effect of the α_2-agonist clonidine on PTZ-induced seizures

Due to the limited availability of pharmacokinetic data of the noradrenergic agonist clonidine in 5 dpf zebrafish seizure models, the drug concentrations used in this project are based on the few existing literature studies [24,42] and on own preliminary experiments conducted at various, gradually increasing drug concentrations: 50 nM, 100 nM, 200 nM, 5 µM, 10 µM and 20 µM (Figure 20A and B). A concentration of 30 µM clonidine is selected for further behavior

analyses, since no toxicity is associated with a concentration of 20 µM clonidine, and since the zebrafish are following the normal light-dark pattern of the controls.

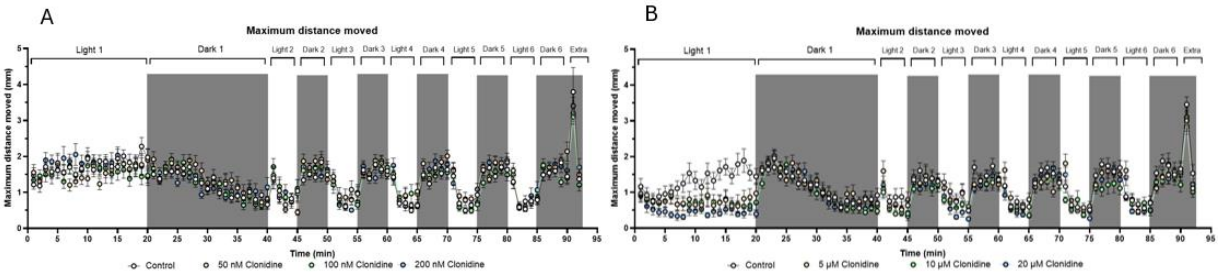

Figure 20: Maximum distance moved (mm) for different clonidine concentrations. The parameter maximum distance moved (mm) (mean ± SEM) is plotted on the y-axis for the different conditions, whereas different time points (minutes) are plotted on the x-axis. White and grey squares indicate light and dark periods, respectively. (A) Control (white), 50 nM clonidine (pink), 100 nM clonidine (light green), 200 nM clonidine (light blue) (n = 18 zebrafish/condition (3 trials)), (B) Control (white), 5 µM clonidine (pink), 10 µM clonidine (light green), 20 µM clonidine (light blue) (n = 18 zebrafish/condition (3 trials)).

The overview graphs (Figure 21) indicate that clonidine elicits a decreasing effect in both maximum distance moved and maximum velocity. However, no differences in seizure behavior are noted between the PTZ-treated and PTZ+clonidine co-treated groups. In the switch light-dark period, maximum distance moved and maximum velocity are similar as observed in the PTZ+VA experiments. Thus, the 5 dpf zebrafish treated with PTZ (both PTZ- and PTZ+clonidine group) have, in addition to seizures, a reversed light/dark-response during the stable light, switch light-dark and stable dark periods (10:00-40:00) but also in the alternating phases (40:00 – 90:00).

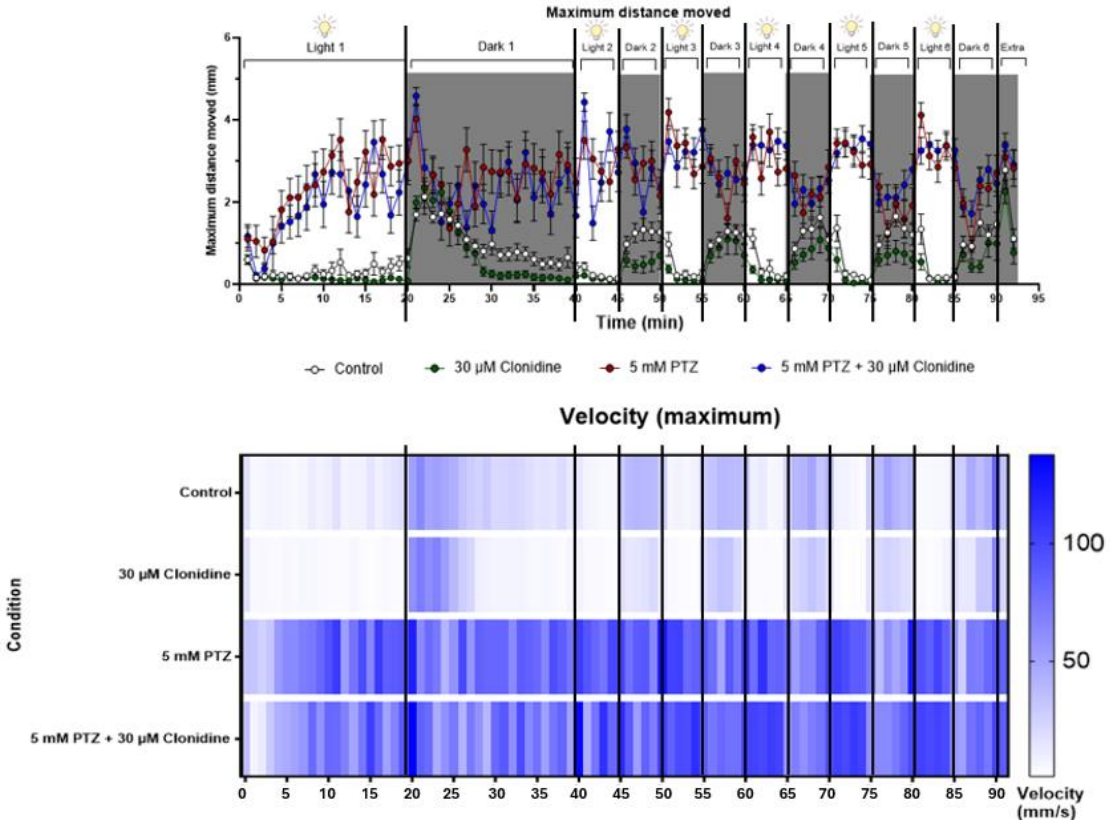

Figure 21: Overview of the maximum distance moved in mm (upper graph) and heatmap of the maximum velocity in mm/s (lower graph) in the following conditions: control (white), 30 µM clonidine (green), 5 mM PTZ (red) and 5 mM PTZ + 30 µM clonidine (blue). On the upper graph, the

parameter maximum distance moved (mm) (mean ± SEM) is plotted on the y-axis, whereas different time points (minutes) are plotted on the x-axis. White and grey squares indicate light and dark periods, respectively. On the lower graph, the parameter maximum velocity (mm/s) is plotted. On the x-axis, the time (min) can be seen; on the y-axis, the different conditions can be seen. The more intense the color blue is, the higher the maximum velocity. (n = 18 zebrafish/condition, except for the control condition: 17 zebrafish/condition (excluded: well A6 in trial 3) (3 trials)).

In all three parameters (maximum distance moved (Figure 22), maximum velocity (Figure 23) and movement frequency (Figure 24)) and across all three time periods ((A) min. 10:00-20:00, (B) min. 20:00-30:00 and (C) min. 30:00-40:00), no significant differences between the PTZ-treated group and the PTZ+clonidine co-treated group can be seen. These results suggest that clonidine does not exert an effect on seizure behavior under these conditions, indicating the need for further investigation with different clonidine concentrations or with other experimental conditions.

In contrast with the above-mentioned results, comparison between the control and the clonidine group shows a significant decrease of maximum distance moved (Figure 22), maximum velocity (Figure 23) and movement frequency (Figure 24) in the group treated only with clonidine. However, in the switch light-dark period (20:00-30:00), no significant reduction is observed for all three parameters (Figure 22B, Figure 23B, Figure 24B). For all the other comparisons, there is an overall significant difference between all the groups for maximum distance moved (Figure 22), maximum velocity (Figure 23) and movement frequency (Figure 24).

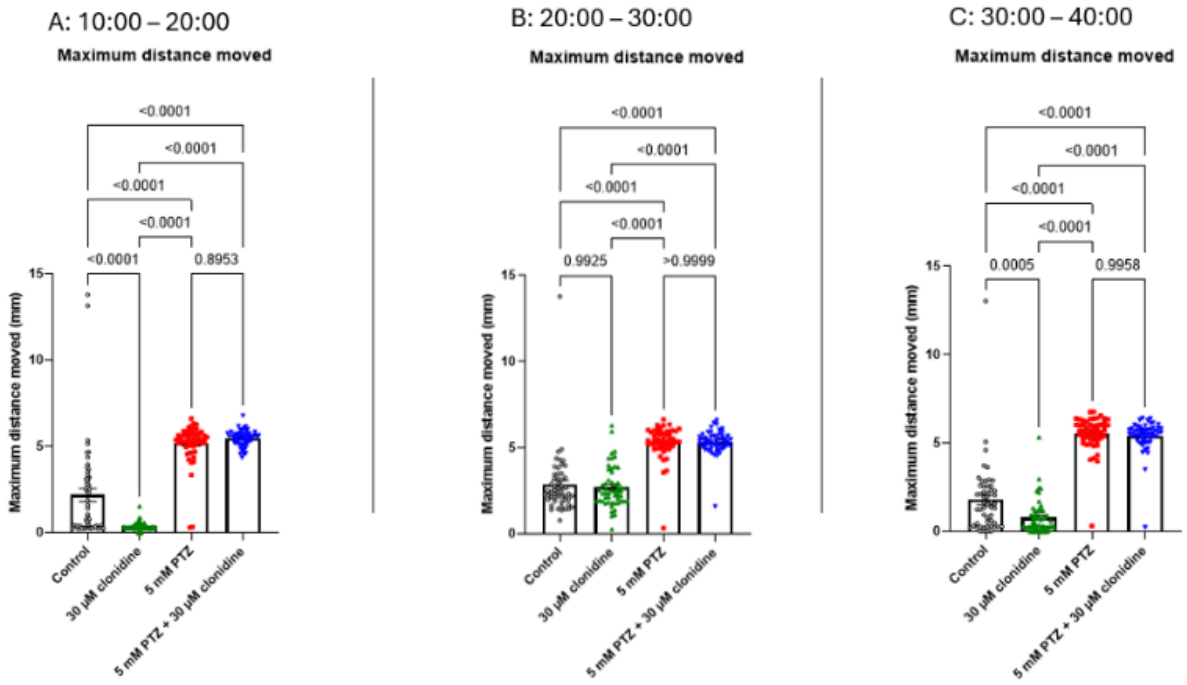

Figure 22: Scatter plot of the maximum distance moved (mm) in the different conditions: control, 30 µM clonidine, 5 mM PTZ and 5 mM PTZ + 30 µM clonidine. Control (white), 30 µM clonidine (green), 5 mM PTZ (red) and 5 mM PTZ + 30 µM clonidine (blue) are plotted on the x-axis; the parameter maximum distance moved (mm) in a time bin of 10 minutes ((A) min. 10:00-20:00 with F-value = 144.1 and p-value < 0.0001, (B) min. 20:00-30:00 with F-value = 78.16 and p-value < 0.0001 and (C) min. 30:00-40:00 with F-value = 196.0 and p-value < 0.0001) is plotted on the y-axis. All the three PTZ+clonidine tests are plotted together (n = 54 zebrafish/condition, except for the control condition: 53 zebrafish/condition (excluded: well A6 in trial 3 in test 1) (3 tests, 3 trials/test (9 trials in total))). Data are plotted as mean ± SEM, a one-way ANOVA test with Šidák correction for multiple comparisons as post-hoc test is chosen, and p-values are shown above the graph.

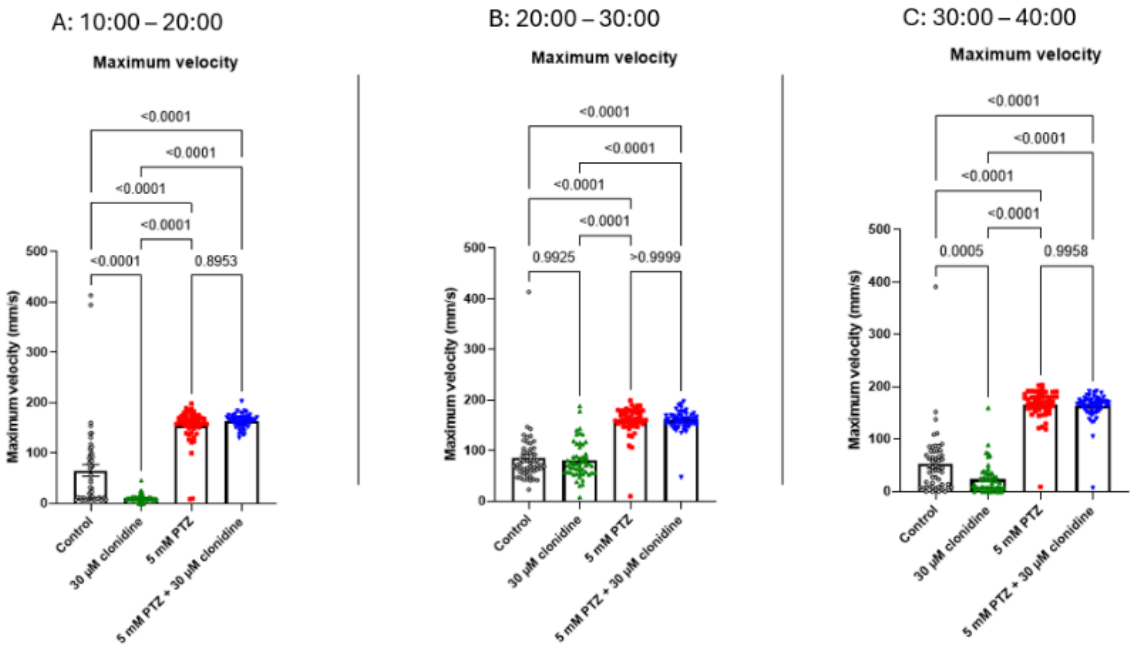

Figure 23: Scatter plot of the maximum velocity (mm/s) in the different conditions: control, 30 µM clonidine, 5 mM PTZ and 5 mM PTZ + 30 µM clonidine. Control (white), 30 µM clonidine (green), 5 mM PTZ (red) and 5 mM PTZ + 30 µM clonidine (blue) are plotted on the x-axis; the parameter maximum velocity (mm/s) in a time bin of 10 minutes ((A) min. 10:00-20:00 with F-value = 144.1 and p-value < 0.0001, (B) min. 20:00-30:00 with F-value = 78.16 and p-value < 0.0001 and (C) min. 30:00-40:00 with F-value = 196.0 and p-value < 0.0001) is plotted on the y-axis. All the three PTZ+clonidine tests are plotted together (n = 54 zebrafish/condition, except for the control condition: 53 zebrafish/condition (excluded: well A6 in trial 3 in test 1) (3 tests, 3 trials/test (9 trials in total))). Data are plotted as mean ± SEM, a one-way ANOVA test with Šidák correction for multiple comparisons as post-hoc test is chosen, and p-values are shown above the graph.

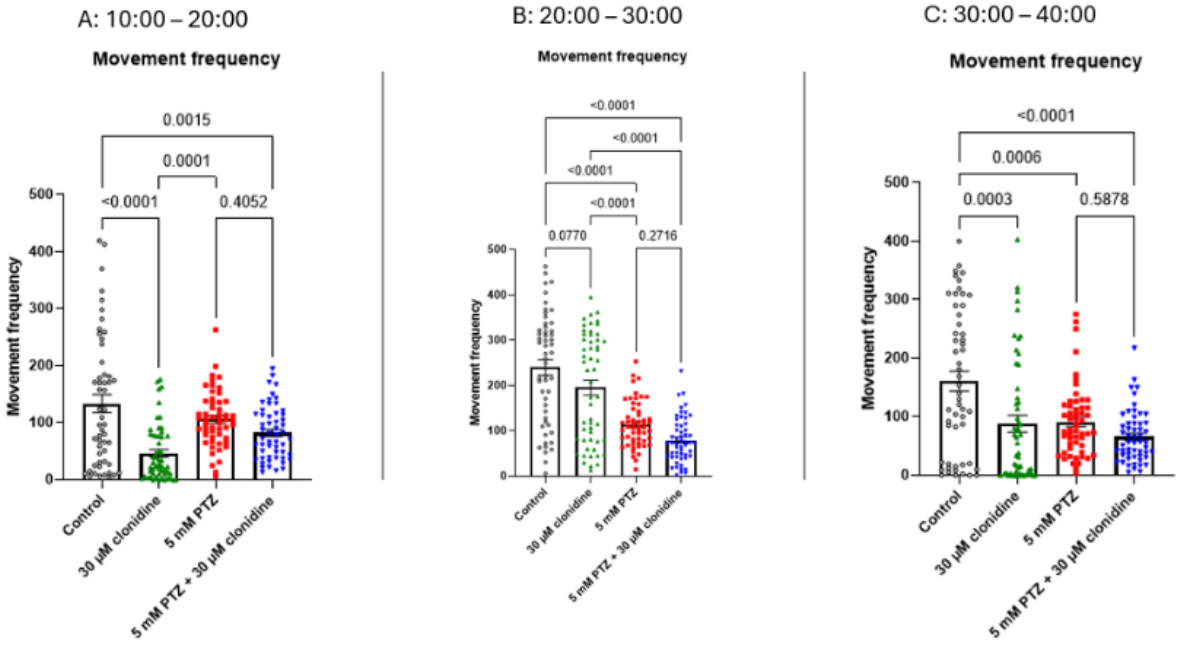

Figure 24: Scatter plot of the movement frequency in the different conditions: control, 30 µM clonidine, 5 mM PTZ and 5 mM PTZ + 30 µM clonidine. Control (white), 30 µM clonidine (green), 5 mM PTZ (red) and 5 mM PTZ + 30 µM clonidine (blue) are plotted on the x-axis; the parameter movement frequency in a time bin of 10 minutes ((A) min. 10:00-20:00 with F-value = 14.47 and p-value < 0.0001, (B) min. 20:00-30:00 with F-value = 34.33 and p-value < 0.0001 and (C) min. 30:00-40:00 with F-value = 11.06 and p-value < 0.0001) is plotted on the y-axis. All the three PTZ+clonidine tests

are plotted together (n = 54 zebrafish/condition, except for the control condition: 53 zebrafish/condition (excluded: well A6 in trial 3 in test 1) (3 tests, 3 trials/test (9 trials in total))). Data are plotted as mean ± SEM, a one-way ANOVA test with Šidák correction for multiple comparisons as post-hoc test is chosen, and p-values are shown above the graph.

Here it can be concluded that this project can prove that 5 dpf zebrafish can be a great model to see differences in behavior due to the adrenergic system by using an α_2-agonist. Due to the selected parameters, the results show no effect on the PTZ-induced behavior. Further and more advanced models with various concentrations of the compound are needed to exactly highlight the effect of the agonist on the behavior during an induced seizure.

7.1.1.4 Effect of the α_2-antagonist atipamezole in PTZ-induced seizures

Due to the limited availability of pharmacokinetic data in 5 dpf zebrafish epilepsy models, the drug concentrations for atipamezole are based on existing literature [43,44,45] and own preliminary experiments conducted at various, gradually increasing drug concentrations: 0 nM, 5 nM, 10 nM, 20 nM, 50 nM, 100 nM, 1 µM, 10 µM, 30 µM, 50 µM, 100 µM and 200 µM atipamezole (Figure 25). A concentration of 30 µM atipamezole is selected for further behavior analyses, since 5 dpf zebrafish treated with higher concentrations of atipamezole are not following the normal light-dark pattern of the control zebrafish anymore (≥50 µM) or are not moving at all, possibly due to toxicity effects (≥100 µM).

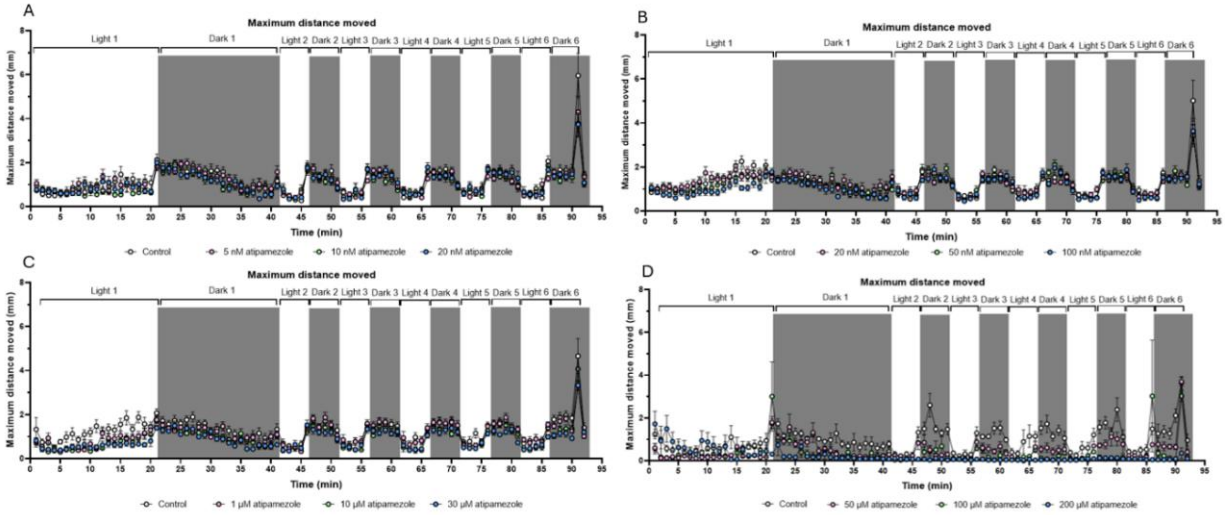

Figure 25: Maximum distance moved (mm) for different atipamezole concentrations. The parameter maximum distance moved (mm) (mean ± SEM) is plotted on the y-axis for the different conditions, whereas different time points (minutes) are plotted on the x-axis. White and grey squares indicate light and dark periods, respectively. (A) Control (white), 5 nM atipamezole (pink), 10 nM atipamezole (light green), 20 nM atipamezole (light blue) (n = 18 zebrafish/condition (3 trials)), (B) Control (white), 20 nM atipamezole (pink), 50 nM atipamezole (light green), 100 nM atipamezole (light blue) (n = 18 zebrafish/condition (3 trials)), (C) Control (white), 1 µM atipamezole (pink), 10 µM atipamezole (light green), 30 µM atipamezole (light blue) (n = 18 zebrafish/condition, except for the 1 µM atipamezole concentration: 17 zebrafish/condition (excluded: well B4 in trial 3) (3 trials)), (D) Control (white), 50 µM atipamezole (pink), 100 µM atipamezole (light green), 200 µM atipamezole (light blue) (n = 6 zebrafish/condition (1 trial)).

In the overview graphs (Figure 26), only small differences are seen between the control group and atipamezole-treated group on the one hand, and the PTZ-treated group and the PTZ-atipamezole co-treated group on the other hand. However, between the two first mentioned groups (control and atipamezole) and the two last mentioned groups (PTZ and PTZ+atipamezole), differences in maximum distance moved can be noticed. These findings are further explored in the analyses below.

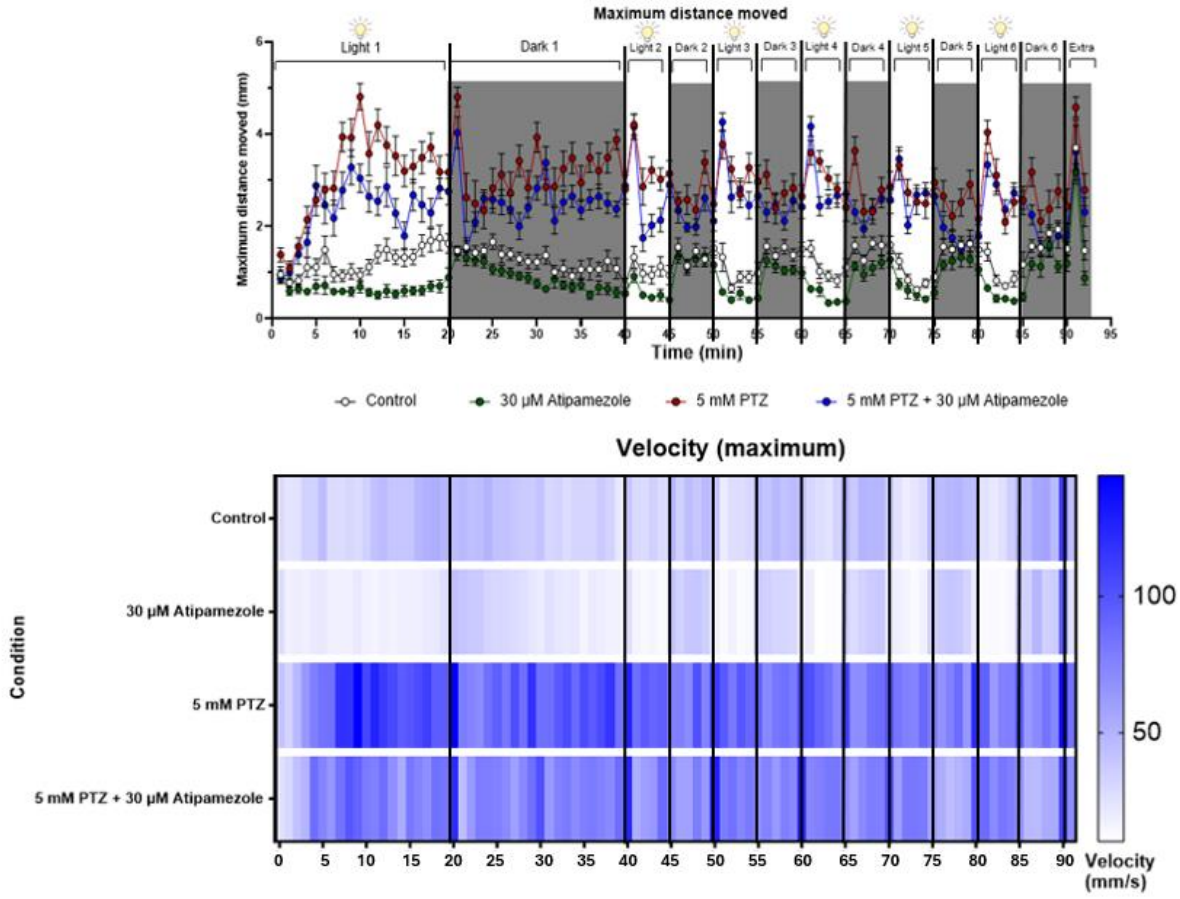

Figure 26: Overview of the maximum distance moved in mm (upper graph) and heatmap of the maximum velocity in mm/s (lower graph) in the following conditions: control (white), 30 µM atipamezole (green), 5 mM PTZ (red) and 5 mM PTZ + 30 µM atipamezole (blue). On the upper graph, the parameter maximum distance moved (mm) (mean ± SEM) is plotted on the y-axis, whereas different time points (minutes) are plotted on the x-axis. White and grey squares indicate light and dark periods, respectively. On the lower graph, the parameter maximum velocity (mm/s) is plotted. On the x-axis, the time in minutes (min) can be seen; on the y-axis, the different conditions can be seen. The more intense the color blue is, the higher the maximum velocity. (n = 18 zebrafish/condition (3 trials))

For both parameters, maximum distance moved and maximum velocity, the scatter plots indicate a significant decrease in the atipamezole-treated group compared to the control group, except in the time bin of min. 30:00-40:00, where for both parameters there is no significant difference (Figure 27C and Figure 28C). Additionally, for this compound, there is a significant reduction of seizure behavior in the PTZ+atipamezole co-treated group compared to the PTZ-group, which is not seen in the clonidine results. This suggests that there is an effect induced by treatment with 30 µM atipamezole on the seizure behavior, however, there is also a decrease in activity in the control group compared to the atipamezole-treated group. For all the other comparisons, significant p-values are seen which can be found in the graphs (Figures 27 and 28).

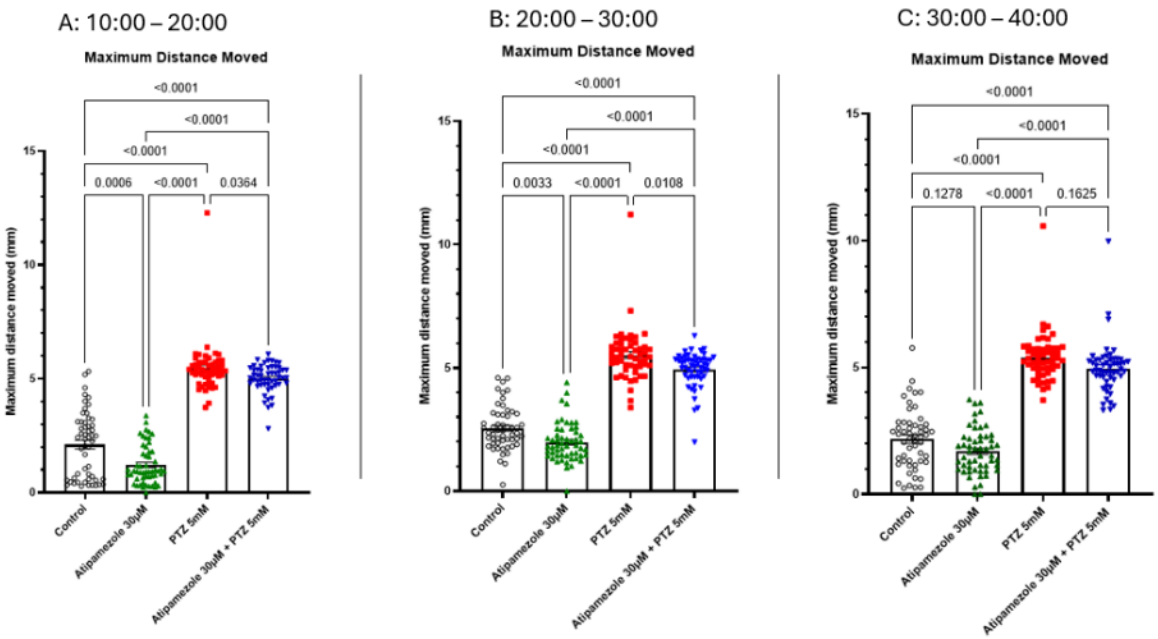

Figure 27: Scatter plot of the maximum distance moved (mm) in the different conditions: control, 30 µM atipamezole, 5 mM PTZ and 5 mM PTZ + 30 µM atipamezole. Control (white), 30 µM atipamezole (green), 5 mM PTZ (red) and 5 mM PTZ + 30 µM atipamezole (blue) are plotted on the x-axis; the parameter maximum distance moved (mm) in a time bin of 10 minutes ((A) min. 10:00-20:00 with F-value = 220.9 and p-value < 0.0001, (B) min. 20:00-30:00 with F-value = 232.5 and p-value < 0.0001 and (C) min. 30:00-40:00 with F-value = 189.8 and p-value < 0.0001) is plotted on the y-axis. All the three PTZ+atipamezole tests are plotted together (n = 54 zebrafish/condition (3 tests, 3 trials/test (9 trials in total))). Data are plotted as mean ± SEM, a one-way ANOVA test with Šidák correction for multiple comparisons as post-hoc test is chosen, and p-values are shown above the graph.

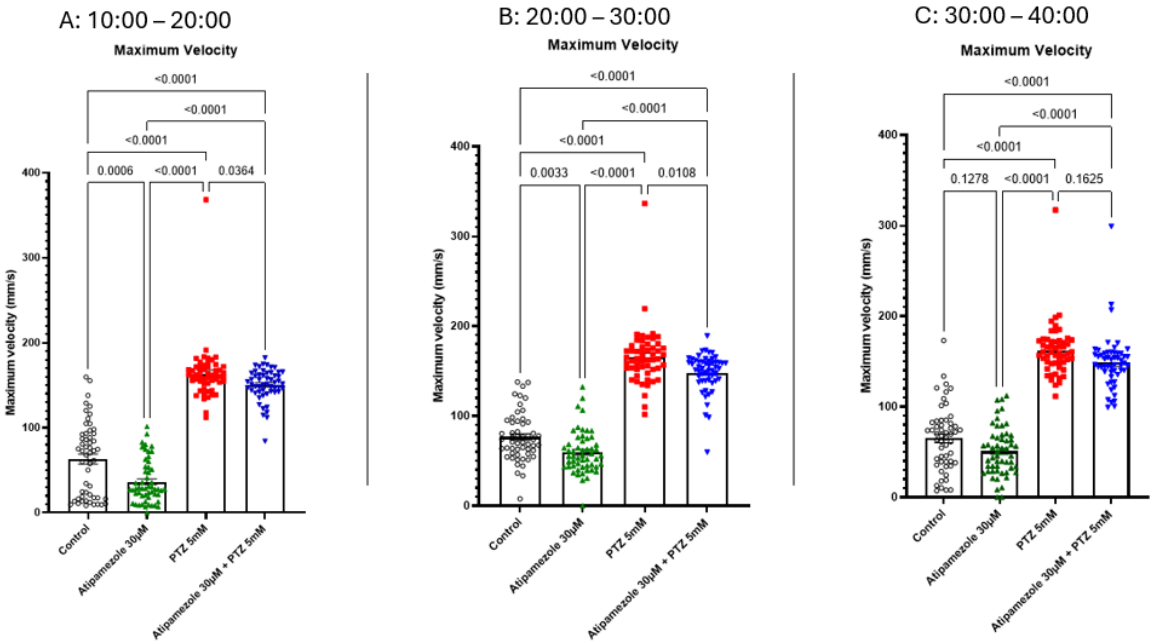

Figure 28: Scatter plot of the maximum velocity (mm/s) in the different conditions: control, 30 µM atipamezole, 5 mM PTZ and 5 mM PTZ + 30 µM atipamezole. Control (white), 30 µM atipamezole (green), 5 mM PTZ (red) and 5 mM PTZ + 30 µM atipamezole (blue) are plotted on the x-axis; the parameter maximum velocity (mm/s) in a time bin of 10 minutes (((A) min. 10:00-20:00 with F-value = 220.9 and p-value < 0.0001, (B) min. 20:00-30:00 with F-value = 232.5 and p-value < 0.0001 and (C) min. 30:00-40:00 with F-value = 189.8 and p-value < 0.0001) is plotted on the y-axis. All the three PTZ+atipamezole tests are plotted together (n = 54 zebrafish/condition (3 tests, 3 trials/test (9 trials in

total))). Data are plotted as mean ± SEM, a one-way ANOVA test with Šidák correction for multiple comparisons as post-hoc test is chosen, and p-values are shown above the graph.

Lastly, there is a highly significant increase in movement frequency in the PTZ+atipamezole co-treated group compared to the PTZ-treated group. This finding implies that the PTZ+atipamezole co-treated group exhibits behavior more closely resembling that of the control group, however, only for this parameter.

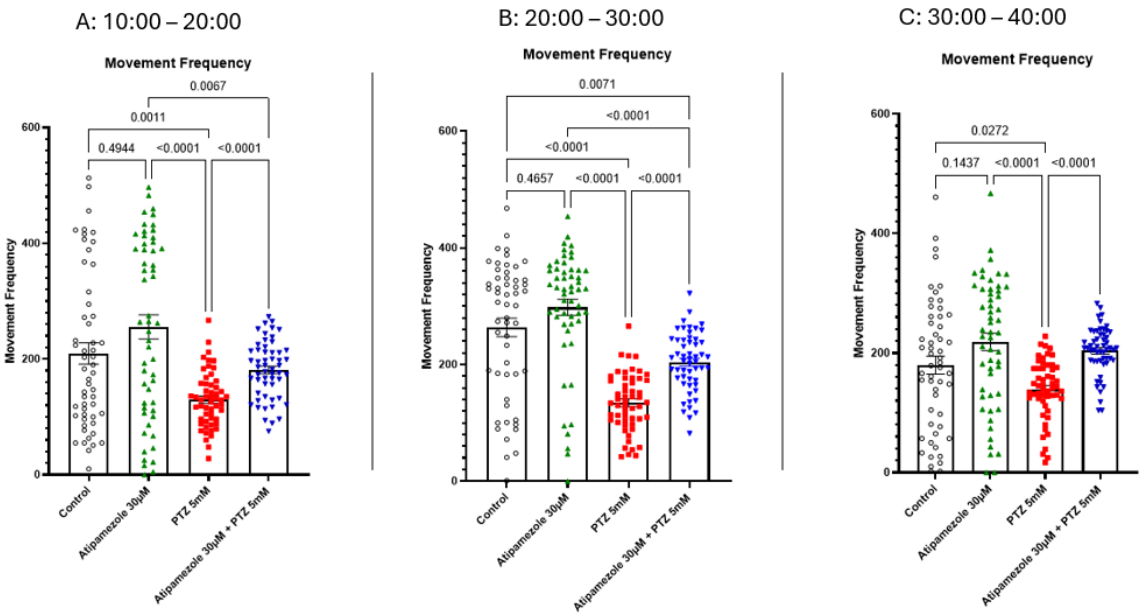

Figure 29: Scatter plot of the movement frequency in the different conditions: control, 30 µM atipamezole, 5 mM PTZ and 5 mM PTZ + 30 µM atipamezole. Control (white), 30 µM atipamezole (green), 5 mM PTZ (red) and 5 mM PTZ + 30 µM atipamezole (blue) are plotted on the x-axis; the parameter movement frequency in a time bin of 10 minutes ((A) min. 10:00-20:00 with F-value = 12.53 and p-value < 0.0001, (B) min. 20:00-30:00 with F-value = 39.88 and p-value < 0.0001 and (C) min. 30:00-40:00 with F-value = 11.54 and p-value < 0.0001) is plotted on the y-axis. All the three PTZ+atipamezole tests are plotted together (n = 54 zebrafish/condition (3 tests, 3 trials/test (9 trials in total))). Data are plotted as mean ± SEM, a one-way ANOVA test with Šidák correction for multiple comparisons as post-hoc test is chosen, and p-values are shown above the graph.

It can be concluded from those results that 30 µM atipamezole exhibits an increasing effect on the movement frequency and decreases the seizure-induced behavior of the PTZ-group (seen in lower maximum distance moved and maximum velocity). However, the α_2-antagonist also exerts a decreasing effect of locomotor response on the atipamezole group compared to the control group.

7.1.2 Results of the alternating light-dark phases

7.1.2.1 Selection of the most informative parameter for the alternating phases

Next, the alternating light-dark phases (40:00-90:00) are examined. This can provide valuable information about how environmental factors (e.g., light exposure) may influence seizure-like behavior and if this can be affected using adrenergic agonists/antagonists and AEDs. Thus, in this section the effect of a light stimulus on the behavior of 5 dpf zebrafish treated with PTZ is investigated. The parameters maximum distance moved, maximum velocity and movement frequency are selected above (7.1.1.1) based on their ability to discriminate between the control zebrafish and the PTZ-phenotype in the stable light (10:00-20:00), switch light-dark (20:00-30:00) and stable dark (30:00-40:00) periods. The parameters maximum distance moved (Figure 30A), maximum velocity (Figure 30B) and movement frequency (Figure 30C) are also plotted for both the control condition and PTZ-treated condition in the alternating

phases (40:00-90:00). The parameter maximum distance moved is selected as the most informative parameter for analysis of the alternating light/dark phases.

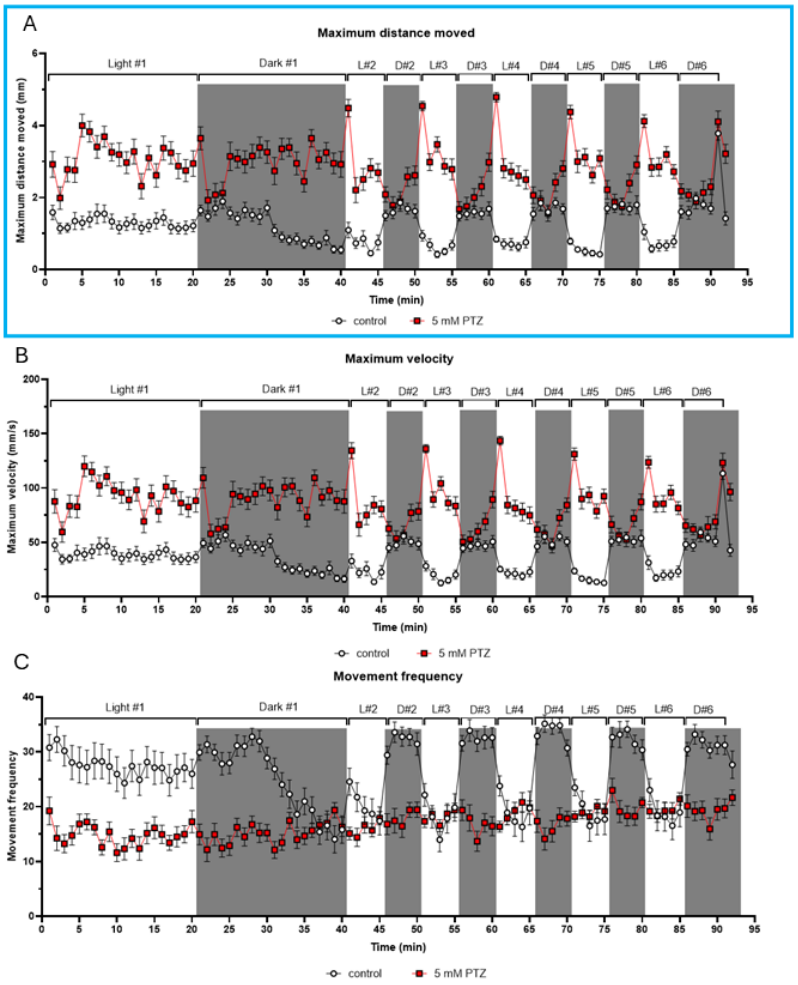

Figure 30: Different parameters (maximum distance moved, maximum velocity and movement frequency) are plotted for the control condition and the PTZ-condition. The parameters (A) maximum distance moved (mm), (B) maximum velocity (mm/s) and (C) movement frequency (mean ± SEM) are plotted on their respective y-axis, whereas the different time points (minutes) are plotted on the x-axis. White and grey squares indicate light and dark periods, respectively. The selected parameter (maximum distance moved) is indicated with a blue square. (n = 66 zebrafish/condition (3 tests, 3-4 trials/test (11 trials in total)))

Under normal, control conditions, 5 dpf zebrafish exhibit increased locomotor activity, characterized by greater maximum distance moved and velocity during the dark phases, while showing decreased maximum distance movement and velocity during the light phases. This pattern is reserved by PTZ treatment, where the animals demonstrate increased maximum distance moved and maximum velocity during the light conditions and decreased maximum distance moved and maximum velocity during the dark phases. Conversely, regarding the number of times a 5 dpf zebrafish initiates a locomotor response (the movement frequency), it can be said that in normal control conditions a higher movement frequency is seen in the stable phases, whereas PTZ treatment results in a lower movement frequency. However, in the alternating phases, the PTZ-group does not follow a specific pattern for the movement frequency. Differences in maximum distance moved are observed between the light and dark phase transitions, with the biggest variability occurring within the first minute (min. 41, min. 51, min. 61, min. 71 and min. 81) immediately following a change in light. To investigate this important finding, the value of every last minute of every dark period is subtracted from the value of every first minute of every light period (Δlight-dark). Then the average of those five different dark-light transitions is plotted. The vice versa is done for the light-dark transitions (Δdark-light). These differences are visualized per treatment condition using scatter plots below.

7.1.2.2 Delta maximum distance moved

This project shows that the noradrenergic compounds clonidine and atipamezole reverse significantly the PTZ-induced seizure behavior in the light-dark conditions, and even diverging more from the baseline (control group), while the PTZ+VA co-treated group exhibits behavior more closely resembling to that of the control group. This is not seen in the dark-light conditions.

7.1.2.2.1 Behavioral differences during dark-light transitions

There are no significant differences seen between any treated group (VA, clonidine, atipamezole) compared to the control group in the dark-light results. A significant decrease is observed in the VA+PTZ co-treated group compared to the PTZ-treated group, but no other significant difference is seen in a co-treated group compared to a PTZ-group. Further, all other comparisons result in a significant difference (Figure 31).

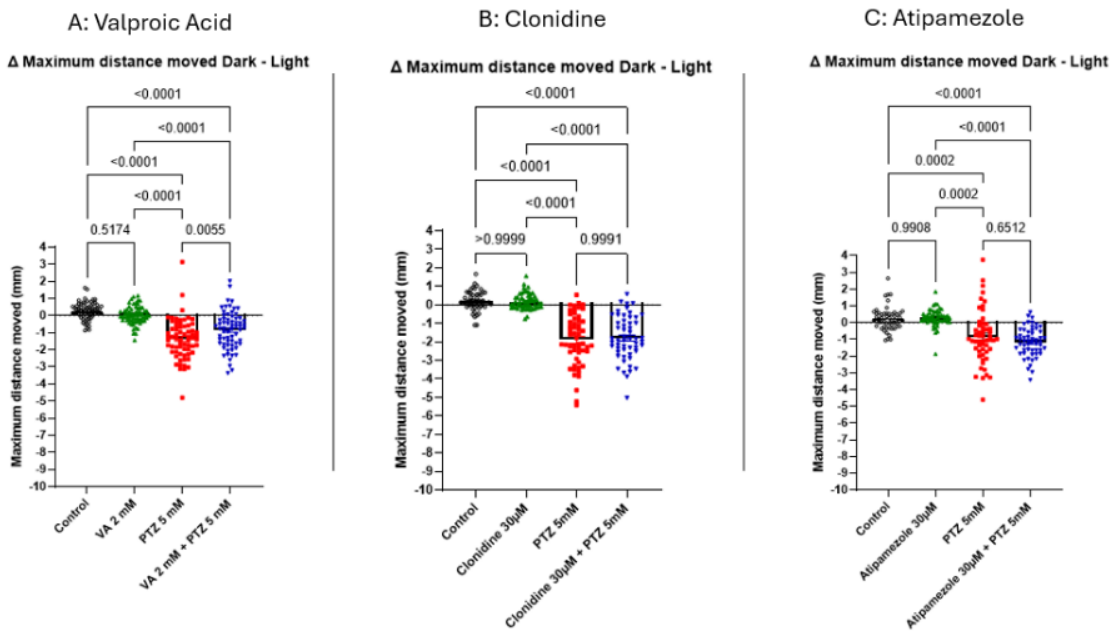

Figure 31: Scatter plot of the average of the difference (Δ) in maximum distance moved per minute between the dark-light phases in the different conditions: (1) control (white), (2) 2 mM VA/30 µM clonidine/30 µM atipamezole (green), (3) 5 mM PTZ (red), (4) 5 mM PTZ + 2 mM VA/30 µM clonidine/30 µM atipamezole (blue). The different conditions are plotted on the x-axis, the maximum distance moved (mm) is plotted on the y-axis. All the three tests per condition are plotted together. (A) 3 tests of 5 mM PTZ + 2 mM VA (n = 66 zebrafish/condition (3 tests, 3-4 trials/test (11 trials in total))) with F-value = 49.56 and p-value < 0.0001, (B) 3 tests of 5 mM PTZ + 30 µM clonidine (n = 53 zebrafish/condition (3 tests, 3 trials/test (9 trials in total))) with F-value = 77.45 and p-value < 0.0001 and (C) 3 tests of 5 mM PTZ + 30 µM atipamezole (n = 54 zebrafish/condition (3 tests, 3 trials/test (9 trials in total))) with F-value = 30.00 and p-value < 0.0001. Data are plotted as mean ± SEM, a one-way ANOVA test with Šidák correction for multiple comparisons as post-hoc test is chosen, and p-values are shown above the graph.

7.1.2.2.2 Behavioral differences during light-dark transitions

In the comparison between the treated groups and the control group for the light-dark results, there is a significant difference between the VA-group and the control, but no other treated group (clonidine and atipamezole) has a significant difference compared to the control. In these observations, the noradrenergic compound atipamezole reverse significantly the PTZ-induced seizure behavior by even diverging more from the baseline (control group), while the PTZ+VA co-treated group exhibits behavior more closely resembling to that of the control group.

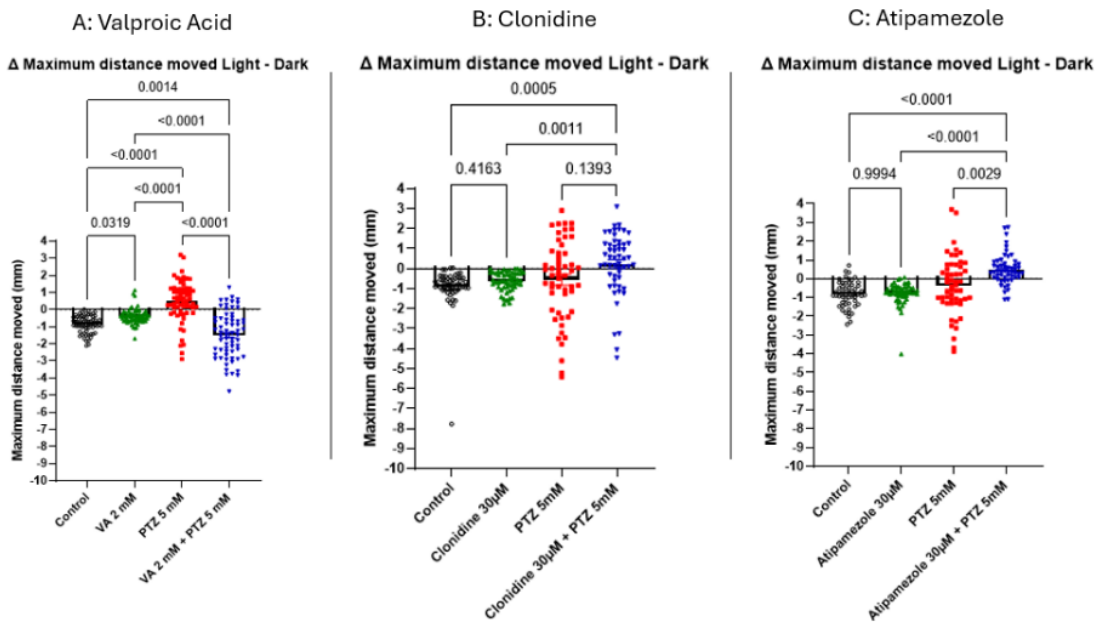

Figure 32: Scatter plot of the average of the difference (Δ) in maximum distance moved (mm) per minute between the light-dark phases in the different conditions: (1) control (white), (2) 2 mM VA/30 µM clonidine/30 µM atipamezole (green), (3) 5 mM PTZ (red), (4) 5 mM PTZ + 2 mM VA/30 µM clonidine/30 µM atipamezole (blue) (GraphPad Prism (version 9.0.0)). The different conditions are plotted on the x-axis, the maximum distance moved (mm) is plotted on the y-axis. All the three tests per condition are plotted together. (A) 3 tests of 5 mM PTZ + 2 mM VA (n = 66 zebrafish/condition) with F-value = 50.33 and p-value < 0.0001, (B) 3 tests of 5 mM PTZ + 30 µM clonidine (n = 53 zebrafish/condition) with F-value = 6.673 and p-value < 0.0001 and (C) 3 tests of 5 mM PTZ + 30 µM atipamezole (n = 54 zebrafish/condition) with F-value = 19.63 and p-value < 0.0001. Data are plotted as mean ± SEM, a one-way ANOVA test with Šidák correction for multiple comparisons as post-hoc test is chosen, and p-values are shown above the graph.

7.2 Expression analysis

In the second part of this thesis, the expression of different noradrenaline receptor genes in 5 dpf zebrafish is assessed. Therefore, primers for different reference genes and noradrenaline receptor genes are designed and tested on their efficiency (7.2.1). Afterwards, expression levels of reference genes are evaluated on their stability in 5 dpf zebrafish tissues of 10 heads and 10 bodies (7.2.2). Stable reference genes and noradrenaline receptor genes are tested for their expression levels in pools of 1, 2, 3, 6 and 12 zebrafish heads and full bodies (containing both heads and bodies) (7.2.3).

7.2.1 Primer design and primer efficiency testing

The designs of the forward and reverse primer sequences for the different noradrenaline receptor genes (*adra1aa*, *adra1ab*, *adra1ba*, *adra1bb*, *adra2a*, *adra2b*, *adrb1*, *adrb2a* and *adrb2b)* and for the reference genes (*b2m*, *cat*, *cyp19a1b*, *eef1a1a*, *eif2s2*, *gapdh*, *hprt1*, *lsm12b*, *mobk13*, *rnf7*, *rpl7*, *rpl13a*, *rplp2*, *rps18*, *sdha*, *slc25a5*, *tbp*, *tuba1a*, *ube2a* and *ywhaz*) can be found in Table 3. For each of these genes, primer efficiency is assessed with an initial optimalisation experiment by performing an RT-qPCR analysis on a cDNA dilution series as template. Table 3 shows the sequences for the primer pairs that are used in further experiments. An overview of all the designed primer pairs can be found in Addendum (Supplementary Tables 8 and 9). In Table 3 and Supplementary Tables 8 and 9, primer efficiencies are colored in green or red, respectively indicating whether the primer pair efficiency is or isn't meeting the pre-requirement of falling into the range of 0.8-1.2, since a deviation up to 20% from the ideal 100% primer efficiency is tolerated. New primer pairs are designed when a primer pair doesn't meet these requirements, hence the number of designs after the gene name.

Table 3. Primer design for the (a) noradrenaline receptor genes and (b) reference genes. Table 3 shows the sequences of the forward primer (5'-3') and the reverse primer (5'-3'), and the primer efficiencies (tested with RT-qPCR with a cDNA dilution series as template) for the specific (a) noradrenaline receptor genes and (b) reference genes.

(a) Noradrenaline receptor genes			
Gene	**Forward primer (5' – 3')**	**Reverse primer (5' – 3')**	**Primer efficiency**
*adra1aa*_3	TACTCTGTTGGCTTCCGTTTT	AAGACTGTGTCCGAGGGTC	1.162
*adra1ab*_3	GCTCCATCTTCCCATCCCA	GTTCAGGCAGCTGTTGAAGT	1.047
*adra1ba*_1	AGAAAGCTGCTAAAACGCTTG	GGAGGACGGAGACTGGTG	0.9921
*adra1bb*_3	GGCTGCCATTCTTCCTTACTT	CGAAGACTGGTGTTGAATGA	1.028
*adra2a*_1	ACACATTCACAGCGTTTTGTG	TTGCAGTAGCCGAACCAGAA	1.049
*adra2b*_4	CTGGCCACACTAATGGCAC	GTGGCTTCAGGAGAGTACG	1.192
*adrb1*_1	TGACTCTAAACGCGCCACG	ACCAGTATATTTCCCACTACAA	1.125
*adrb2a*_2	GGGAAACATAAGGTCCTCAAT	AGAATGGACATGAGTGTGCC	0.9489
*adrb2b*_1	GCGCTGGTCATCAGTGCC	CGAAGGGCACCACCATAAG	1.071
(b) Reference genes			
Gene	**Forward primer (5' – 3')**	**Reverse primer (5' – 3')**	**Primer efficiency**
*b2m*_1	TCTCCATTGAACTGCTGAAG	ACGCTGCAGGTATATTCATC	0.9584
*cat*_1	AGCCCAGCCCAGACAAGAT	GATGGCGATGTGTGTCTGG	1.032
*eef1a1a*_1	CGCAAGAAGCTGCCAATTTC	CTGATCTGCCCTGGGTGG	1.066
*eif2s2*_1	GGTGGTGAGGAGAGAGAGT	TTTAAGTCATCAAGGTCATCTG	1.067
*gapdh*_1	CGCTGGCATCTCCCTCAA	TCAGCAACACGATGGCTGTA	1.009
*lsm12b*_1	CTCTAGCATCCTTGAATATTAG	GCTTGGGACAACTTGTCTTC	1.024
*mobk13*_1	GTTTGGAGCTCAATGGCTTG	CATCTGGGTACATGTGTCTG	1.007
*rnf7*_1	ACAAACAAGAAGACTGCGTTG	GCAGTTGTGGAAGGAGTGG	1.016
*rpl7*_1	ACGTCTGAAGAAAGCGAAGG	ATGAGCTTCCTGGTGACTTTG	0.9996
*rplp2*_1	GGAGTGTCGGGATCGAGG	GTCTTTGCCATTCAGTTCACT	1.053
*rps18*_1	TTTGCCATCACCGCTATTAAG	CTTTCCTCAGAACCACATGG	1.150
*sdha*_1	CACTCGCTTCTGCACACTC	AGTAGCTGGTATCGTACCTC	0.9372
*tuba1a*_1	TCATCTTCTCCTTCCACACT	GTACGTGGGTGAGGGTAT	1.052
*ywhaz*_1	GAGCTGAAGGCCATCTGCA	TGCGGATCAGAAACTTGTCC	0.9339
*hprt1*_2	GAACGTCTGGCCAGAGATAT	AGCAAAAAACTTGTAGCCTCC	1.074
*rpl13a*_3	GCCAAGCAAGTGCTGTTGG	CACCACCACAATTTTGTGGC	1.050

As an illustration, the calculations and results for the *adra1ab*_2 primer pair (F: 5' GCTGCCGTTTTTTCTTGTGC 3', R: 5' GGTCTGTGGGATGGGAAGA 3') can be seen in Figure 33. This figure displays on the left a table with the Cq-values obtained from the LightCycler480, reflecting at which cycle a signal was picked up with the designed primers. In the middle figure, a graph plots the mean Cq-values in function of the logarithm of the concentration of the cDNA template dilution series (ng/µl).

On the right side of Figure 33 the melting curve generated by the software of the LightCycler480 can be seen. This melting curve gives a first impression about the specificity of the primers. When only one (big) peak is seen, which is the case for the primer pair for *adra1ab*_2, it can be concluded that the primers are binding with specificity to the gene, which

was also tested *in silico* beforehand. On the left bottom of Figure 33, the formula to calculate the primer efficiency is shown, which is based on the coefficient of the slope (rc: 'richtingscoëfficiënt') of the equation shown in the middle of the figure, leading to a final primer efficiency for *adra1ab*_2 of 1.214. This result is not in the range of 0.8 to 1.2 and therefore, a new primer pair is designed for the *adra1ab*_2 gene. It can be noted that for some primer pairs, a required primer efficiency between 0.8 and 1.2 is achieved, but that the primers are not binding with specificity to the gene (non-specific binding/amplification), which is then reflected is more than one (big) peak on the melting curve. In these cases, new primer pairs are designed.

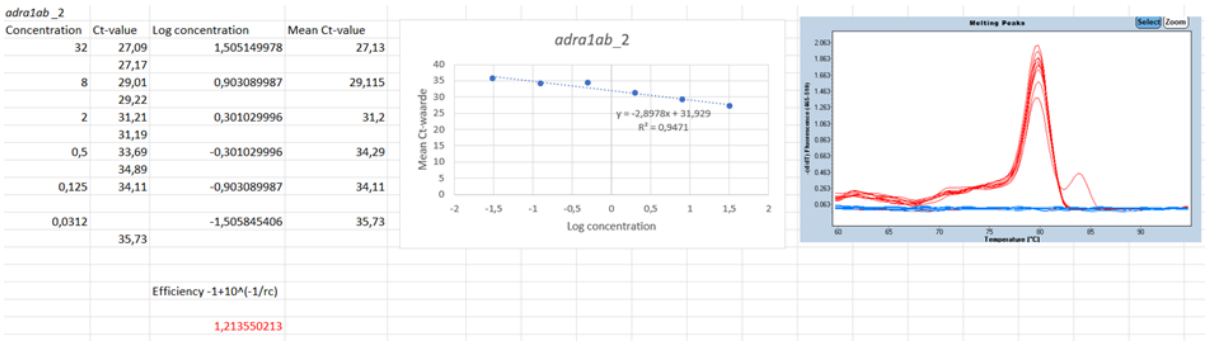

adra1ab_2

Concentration	Ct-value	Log concentration	Mean Ct-value
32	27,09	1,505149978	27,13
	27,17		
8	29,01	0,903089987	29,115
	29,22		
2	31,21	0,301029996	31,2
	31,19		
0,5	33,69	-0,301029996	34,29
	34,89		
0,125	34,11	-0,903089987	34,11
0,0312		-1,505845406	35,73
	35,73		
		Efficiency -1+10^(-1/rc)	
		1,213550213	

Figure 33. Example of the results of the primer efficiency testing and calculations for *adra1ab*_2. On the left side of this figure, a table with the logarithm of the concentrations of the cDNA template dilution series (ng/µl) and the mean Cq-values (Ct-values), generated by the LightCycler480 can be seen. In the middle panel, a graph is plotted displaying this mean Cq-value in function of the logarithm of the concentration. An equation and a value for R^2 is given. The right panel shows the melting curves generated by the LightCycler 480. On the bottom left side of the figure, the formula for calculating the primer efficiency is given, making use of the slope coefficient ('rc') of the equation from the middle panel.

An elaborate version of this primer efficiency testing and calculations for the remaining noradrenaline receptor genes and the reference genes can be found in the Addendum (12.2.1.1).

7.2.2 Optimization and selection of stable reference genes in 5 dpf zebrafish

RT-qPCR can be used to investigate changes in expression levels in genes of interest relative to reference genes. These reference genes (*b2m*, *cat*, *cyp19a1b*, *eef1a1a*, *eif2s2*, *gapdh*, *hprt1*, *lsm12b*, *mobk13*, *rnf7*, *rpl7*, *rpl13a*, *rplp2*, *rps18*, *sdha*, *slc25a5*, *tbp*, *tuba1a*, *ube2a* and *ywhaz)* are first tested to investigate expression stability in different zebrafish samples. For evaluating and making a selection of reference genes that are stable expressed in 5 dpf zebrafish heads (H) and bodies (B), an RT-qPCR experiment is performed on 8 series of 10 5 dpf zebrafish heads or bodies. A separate evaluation of the samples of 10 heads and the samples of 10 bodies is performed. geNorm analysis for zebrafish heads and bodies is both initiated on 24 samples for heads and 24 samples for bodies, and on 16 reference targets for both heads and bodies. For the head samples, 1 value is excluded, and for the body samples, also 1 value is excluded, due to the exclusion criteria of having a Cq-value difference between both duplicates of more than 0.5.

The optimal number of reference targets in this experimental situation is 2 (geNorm V < 0.15 when comparing a normalization factor based on the 2 or 3 most stable targets). With an average geNorm M-value (average expression stability value) of less than 0.5, this experiment shows a high reference target stability. Figure 34A shows the average expression stability of the reference targets in samples of 10 bodies, of which can be concluded that *rps18*, *rnf7* and *mobk13* show the most stable expression in these samples (M<0.35). For the samples of 10 heads, Figure 34B shows *gapdh*, *rpl13a_3* and *rnf7* as the most stable expressed reference genes in these samples of 10 heads (M<0.35). Working with three reference genes is chosen to provide a safety margin for further experiments: in case there is an issue with one of the

three reference genes in tissues of 1, 2, 3, 6 and 12 zebrafish heads/bodies, the other two reference genes can still be used. These reference genes for the zebrafish body (*rps18*, *rnf7* and *mobk13*) and head (*gapdh*, *rpl13a_3* and *rnf7*) samples are used in further experiments to evaluate the expression levels of noradrenaline receptors in 5 dpf zebrafish relative to these chosen reference genes.

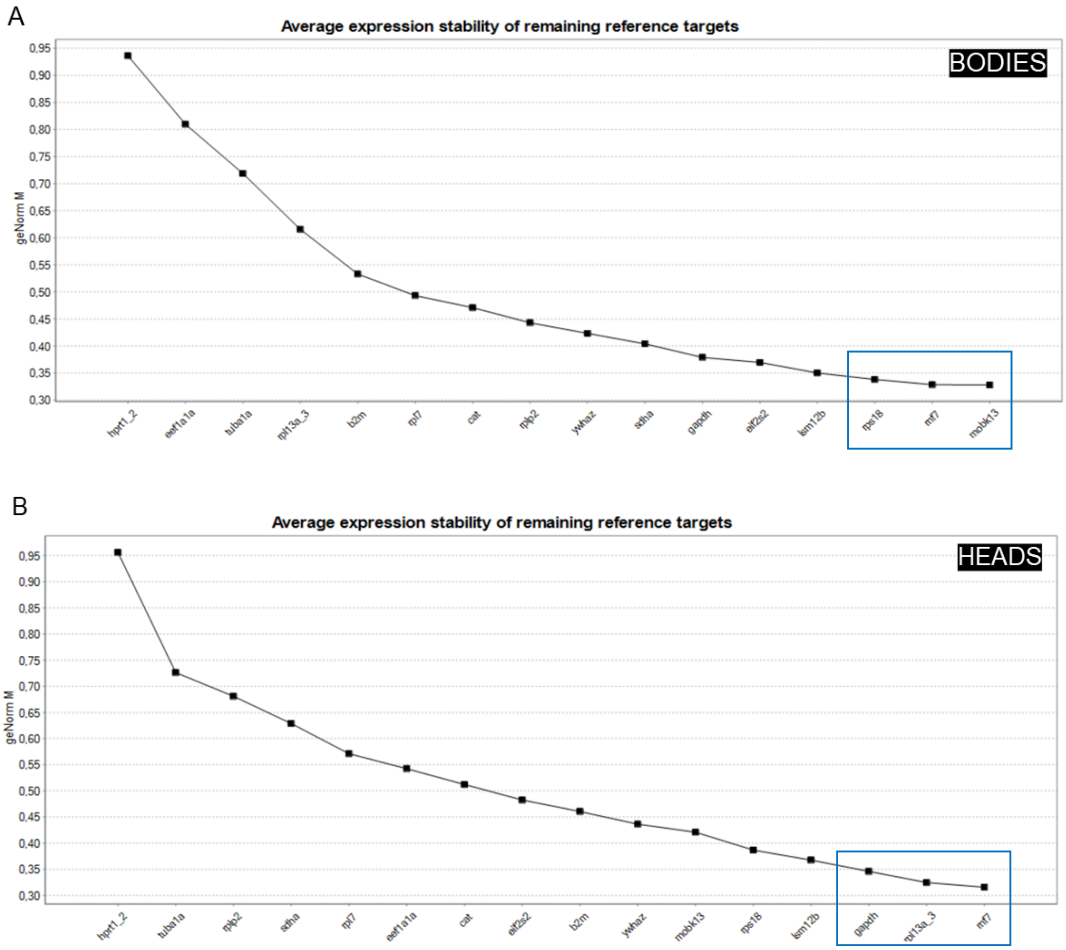

Figure 34: Output of the geNorm analysis performed with qbase+ (CellCarta). Evaluation of the stability of the expression levels of the different reference genes listed in Table 3. On the x-axis, the different reference genes can be seen; on the y-axis, the average expression stability value (geNorm M) is shown. The least stable reference genes are on the left side of the graph; the most stable reference genes are on the right side of the graph. (A) For the 10 bodies samples, the most stable reference genes are *rps18*, *rnf7* and *mobk13*. (B) For the 10 heads samples, the most stable reference genes are *gapdh*, *rpl13a_3* and *rnf7.*

7.2.3 Evaluating the noradrenaline receptor expression in 5 dpf zebrafish

The stability and expression of these six reference genes (body: *rps18*, *rnf7* and *mobk13,* head: *gapdh*, *rpl13a* and *rnf7)* is also tested in multiple samples of 1, 2, 3, 6 and 12 zebrafish heads and bodies. Both the 5 dpf zebrafish heads and bodies are analysed separately. *Gapdh* and *rnf7* are chosen based on their stable expression in 1, 2, 3, 6 and 12 zebrafish heads, and *rps18* and *rnf7* are chosen for the 1, 2, 3, 6 and 12 zebrafish body samples, as can be seen in Table 4.

Table 4. Expression analysis performed with qbase+ (CellCarta) on (a) the samples of 1, 2, 3, 6 and 12 zebrafish (5 dpf) heads and (b) the samples of 1, 2, 3, 6 and 12 zebrafish (5 dpf) bodies. The M-values (average expression stability values) and CV-values (coefficient of variation) are shown for the reference genes *gapdh* and *rnf7* (heads) and *rps18* and *rnf7* (bodies). M-values and CV-values that are below the threshold of 0.5 and 0.2, respectively, are colored in green.

(a) Samples: 1, 2, 3, 6 and 12 heads		
Reference target	**M**	**CV**
gapdh	0.366	0.115
rnf7	0.366	0.141
(b) Samples: 1, 2, 3, 6 and 12 bodies		
Reference target	**M**	**CV**
rps18	0.335	0.110
rnf7	0.335	0.122

To evaluate the noradrenaline receptor expression in 5 dpf zebrafish head and body samples, the expression level of different noradrenergic receptors (*adra1aa*, *adra1ab*, *adra1ba*, *adra1bb*, *adra2a*, *adra2b*, *adrb1*, *adrb2a* and *adrb2b*) are compared relative to the expression levels of above-mentioned reference genes (*gapdh* (head), *rps18* (body) and *rnf7* (head and body)). Figures 35 and 36 show the analysis of the expression levels of different noradrenaline receptors in multiple samples, namely in 1, 2, 3, 6 and 12 heads and 1, 2, 3, 6 and 12 bodies, respectively. Relative quantities (± SEM) are shown on the y-axis; the samples (head or body) are shown on the x-axis. Normally, every sample on the x-axis has 3 biological replicates, since 3 different clutches of zebrafish are used. However, datapoints with a Cq-value > 35 or with an unknown Cq-value are excluded from the analysis and are therefore not shown on these graphs. From these graphs, it can be seen that pools of lower numbers of zebrafish heads and bodies (1, 2 and 3 heads/bodies) show a large variability in relative quantity between the datapoints, or even lack datapoints. In the lower pools of zebrafish heads and bodies, it can be seen that the head samples lack even more datapoints in comparison to the body samples. The body samples mostly have 2-3 datapoints in the 1, 2 and 3 body samples, whereas the head samples mostly have 0-2 datapoints in the 1, 2 and 3 head samples.

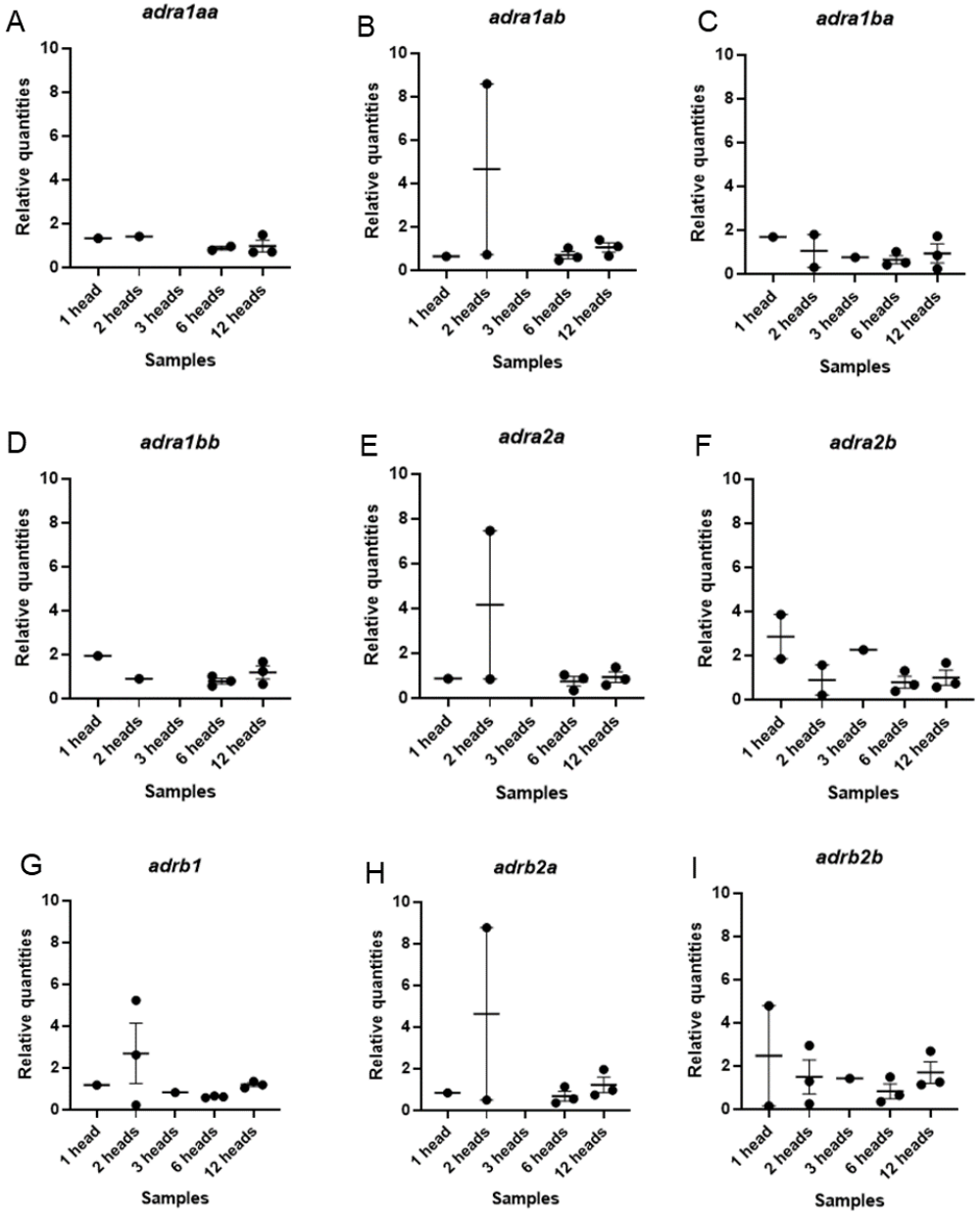

Figure 35. Expression analysis of (A) *adra1aa*, (B) *adra1ab*, (C) *adra1ba*, (D) *adra1bb*, (E) *adra2a*, (F) *adra2b*, (G) *adrb1*, (H) *adrb2a* and (I) *adrb2b* genes in 5 dpf zebrafish heads. Different numbers of zebrafish heads (1, 2, 3, 6 and 12 heads) are analysed, with 3 replicates each time (excluded replicates (Cq-value > 35 or Cq-value unknown) are not shown on these graphs). The number of zebrafish heads per sample is shown on the x-axis, whereas the relative quantities (± SEM) are shown on the y-axis.

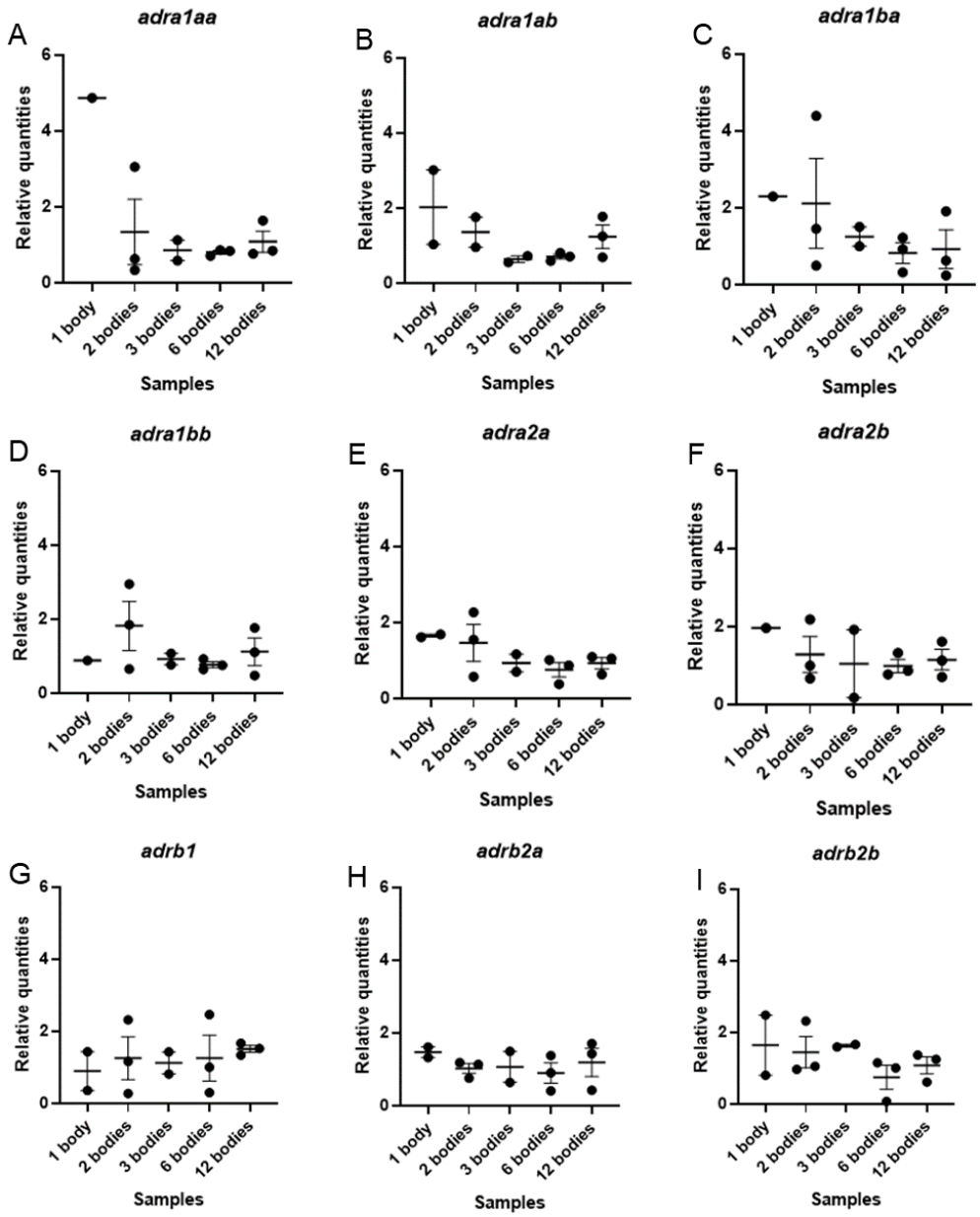

Figure 36. Expression analysis of (A) *adra1aa*, (B) *adra1ab*, (C) *adra1ba*, (D) *adra1bb*, (E) *adra2a*, (F) *adra2b*, (G) *adrb1*, (H) *adrb2a* and (I) *adrb2b* genes in 5 dpf zebrafish bodies. Different numbers of zebrafish bodies (1, 2, 3, 6 and 12 bodies) are analysed, with 3 replicates each time (excluded replicates (Cq-value > 35 or Cq-value unknown) are not shown on these graphs). The number of zebrafish bodies per sample is shown on the x-axis, whereas the relative quantities (± SEM) are shown on the y-axis.

In Figures 35 and 36, the expression of noradrenaline receptor genes can be seen in head and body samples. To further evaluate the expression of these adrenoceptor genes in these tissues, the average Cq-values of the RT-qPCR analyses are listed in Table 5. In general, a trend can be seen stating that the higher the number of pooled zebrafish heads or bodies (6-12), the lower the mean Cq-values are compared to lower amounts of pooled zebrafish heads or bodies (1-2-3). Overall, the mean Cq-values for the noradrenaline receptor genes expression in zebrafish heads and bodies range from 27.86 (*adrb2* in sample of 12 heads) and 27.05 (*adrb2b* in sample of 12 bodies) till 38.36 (*adra1ba* in sample of 3 heads) and 37.04 (adra1ba in sample of 1 body). *Adrb2b* seems to have the lowest mean Cq-value for the sample of 12 zebrafish heads (27.86), as well as for the sample of 12 zebrafish bodies (27.05), whereas *adra1bb* has the highest mean Cq-value in 12 zebrafish heads (34.36) and *adra1ba*

in 12 zebrafish bodies (32.91). From these observations, it can be concluded that there are no major differences between the lowest Cq-value of 12 zebrafish heads and the one of 12 zebrafish bodies, and between the highest Cq-value of 12 zebrafish heads and the one of 12 zebrafish bodies. It is therefore suspected that the expression of the noradrenaline receptors seen in the body samples comes from the head samples.

Table 5: Average Cq-values for the different noradrenaline receptor genes (*adra1aa*, *adra1ab*, *adra1ba*, *adra1bb*, *adra2a*, *adra2b*, *adrb1*, *adrb2a* and *adrb2b*) per sample of 1, 2, 3, 6 or 12 zebrafish heads (a) or bodies (b). For every sample, the Cq-value is the average Cq-value over the 3 zebrafish clutches (biological replicates), with every sample per clutch run in duplicate (technical replicates). Missing average Cq-values are indicated with a slash (/).

Cq-values		(a) Samples: 1, 2, 3, 6 and 12 heads				
		1 head	2 heads	3 heads	6 heads	12 heads
Genes	***adra1aa***	35.19	34.65	/	34.24	33.29
	adra1ab	34.48	34.85	35.7	33.13	32.04
	adra1ba	36.03	36.82	38.36	34.44	33.77
	adra1bb	35.62	36.29	/	35.10	34.36
	adra2a	34.56	35.06	35.81	33.57	32.47
	adra2b	33.73	35.96	35.28	32.13	31.30
	adrb1	33.81	34.21	34.73	31.05	29.62
	adrb2a	33.54	33.66	33.72	31.80	30.44
	adrb2b	33.06	33.43	34.59	29.52	27.86
Cq-values		**(b) Samples: 1, 2, 3, 6 and 12 bodies**				
		1 body	**2 bodies**	**3 bodies**	**6 bodies**	**12 bodies**
Genes	***adra1aa***	35.58	35.12	34.71	34.10	32.38
	adra1ab	34.90	32.09	33.52	32.39	30.66
	adra1ba	37.04	34.28	33.99	34.16	32.91
	adra1bb	36.72	34.35	34.93	33.20	32.58
	adra2a	35.03	33.36	32.95	33.12	31.20
	adra2b	33.16	32.06	32.95	31.65	30.02
	adrb1	32.23	31.96	32.91	30.60	28.58
	adrb2a	33.89	32.08	31.47	31.14	29.43
	adrb2b	31.93	29.25	30.75	29.60	27.05

8. Discussion

For this thesis, the parameters maximum distance moved, maximum velocity and movement frequency are chosen based on their ability to discriminate between the control zebrafish and the phenotype introduced by PTZ. Based on those parameters, it is shown that there are sporadic, very fast movements that are examined in electrophysiological studies of the Yaksi lab and are proven to be seizures [46]. To investigate the effect of the compounds and effect of a light stimulus on seizures, the choice is made to divide the behavioral experiments into two different sections. Firstly, a stable light period (10:00-20:00), followed by the switch from light to dark (20:00-30:00) and a stable dark period (30:00-40:00) are studied. Lastly, the alternating phases (40:00-90:00) are studied for the investigation of the effect of a light stimulus on zebrafish swimming behavior.

8.1 Behavior analysis

In the first part of this thesis, the effects of VA, clonidine and atipamezole on swimming behavior are assessed in both control zebrafish and PTZ-induced seizure zebrafish. Based on the analysis of the stable light (10:00-20:00), switch light to dark (20:00-30:00) and stable dark (30:00-40:00) period, it can be said that 2 mM VA and 30 µM atipamezole both exert an anticonvulsant effect. In contrast, 30 µM clonidine has no influence on the seizure-like behavior, but it influences the baseline behavior compared to the control group. Moreover, the results of the alternating light-dark phases show that both noradrenergic compounds clonidine (a trend is seen) and atipamezole are able to reverse the PTZ-induced behavior which suggests that the noradrenergic system may have an important role in PTZ-induced seizures.

8.1.1 Investigating the effect of valproic acid on induced seizure behavior

The mechanism of action of valproic acid, a first-line treatment option for epilepsy, is still not well understood. Due to the fact that only two-thirds of patients can reach seizure freedom with AEDs, it is still important to investigate existing medication and to try and understand how they work in the body. Prior research, primarily with rodents, has proven that these AEDs can influence the excitation/inhibition-balance in the brain, thereby exerting an anticonvulsant effect. Given this information, a zebrafish model with PTZ-induced seizures was used to examine the anticonvulsant effect of the AED [47].

5 dpf zebrafish have a very specific behavior pattern when exposed to light-dark conditions: they namely move more in dark phases compared to light phases. The convulsant agent PTZ induces a reversal in this locomotor activity in the 5 dpf zebrafish, characterized by an increased behavioral locomotor activity in the light and a decreased behavioral locomotor activity in the dark. This effect is then quantified in the alternating phases. VA shows an anticonvulsant effect, decreasing the locomotor behavior in both light and dark conditions. Thus, it can be concluded from these results that this drug is able to reverse the PTZ-induced behavior in the light condition [17].

Firstly, the results of the overview graph of the parameter maximum distance moved as well as the heatmap of maximum velocity prove that VA indeed exerts anticonvulsant effects and reverses the PTZ-induced locomotor activity of the 5 dpf zebrafish larvae in the light-induced seizures. Additionally, the results of the stable light and stable dark period show that VA has a significant decreasing effect on both the maximum distance moved and maximum velocity, however, it does not exert a significant increasing effect on the movement frequency. It appears from these results that VA has antiepileptic effects, but based on this study, this effect cannot pinpoint one single system, for example the noradrenergic system. It has to be taken into account that that several other systems in the brain, such as the GABAergic system and glutamatergic system, can also be influenced by VA and PTZ and thus, also exert effects. Since PTZ also influences the GABAergic system, it is unclear from this type of experiment to conclude what the exact mechanism-of-action of VA is [47]. However, the results do prove a reduction in the seizure behavior of the PTZ-VA co-treated zebrafish.

Furthermore, prior literature [17] shows that the movement pattern of 5 dpf zebrafish depends on the light-dark or dark-light transition. In the 5 dpf zebrafish model, the light-to-dark transition increases locomotion whereas the dark-to-light transition decreases that behavior. Our results show that when the conditions shift from dark to light, it is once again shown that VA is able to reverse the effect of PTZ, again illustrating an antiepileptic effect. However, the exact mechanism-of-action cannot be unraveled through this type of experiment and further investigation with larval and adult zebrafish where the exact stages of epilepsy can be seen and investigated is needed [17].

8.1.2 Investigating the role of clonidine and noradrenaline receptors on seizures

The pharmacology of α_2-receptor agonists and antagonists remains poorly understood in zebrafish. The role of the noradrenergic system during PTZ-induced seizures is further assessed using clonidine, a partial α_2-receptor agonist. It is hypothesized that the

noradrenergic agonist has a proconvulsant effect on the 5 dpf zebrafish (5.4.3.3). Based on this, this project tries to assess the importance of the noradrenergic system in a seizure and if a seizure can be nullified after treatment with an α_2-receptor agonist [17].

No decrease in PTZ-induced seizure activity is seen upon treatment with clonidine. However, an adverse effect is seen when the control group is compared to the clonidine-treated group, namely that clonidine exerts a sedation effect on the clonidine-treated group in comparison to the control group. The results of the alternating phases visualize the difference between the dark-light and light-dark transmission. No significant difference in locomotion is seen in any group for the Δ maximum distance moved during the dark-light transition. Conversely, there is a significant increase in Δ maximum distance moved when the results of the PTZ+clonidine co-treated group are compared to the PTZ-treated group. This implies that the effect of clonidine may be environmentally (light/dark) triggered, because a trend can be seen when the PTZ-group is compared to the PTZ+clonidine co-treated group. This observation is not seen in the stable phases.

Prior literature [48] has shown that activation of the α_2-receptor tends to cause sedation in zebrafish larvae. This sedation can be nullified with PTZ [48]. This is also proven by our results, since there is no significant difference between the PTZ-treated and PTZ+clonidine co-treated group, but there is a significant decrease in activity in the clonidine-group compared to the control group. This is analogous to previous results [48]. However, this type of experiment cannot fully prove that clonidine has an anticonvulsant effect. Studies with higher doses of the compound are needed to explore the effects of the noradrenergic agonist in an induced seizure model. Some rodent studies propose that the α_2-receptor agonist clonidine has a proconvulsant effect when administered in a high dose but has no effect at all when given in low doses. This suggests that the 30 µM concentration clonidine used in this project may be too low and further investigation is needed with higher doses and/or monitoring brain activity during a seizure to see the involvement of the noradrenaline system [49].

8.1.3 Exploring the effect of atipamezole and noradrenaline receptors on seizures

Atipamezole is a selective α_2-receptor antagonist which is used in various studies for epilepsy. This agent increases the release of noradrenaline in the brain. This project hypothesized that atipamezole will have an anticonvulsant effect. The majority of the studies are conducted in rodent models. Therefore, this project aims to assess the effect of atipamezole in a PTZ-induced seizure model in 5 dpf zebrafish and thereby tries to investigate the influence of the noradrenaline system in seizures [50].

The results of this project show a significant reduction in the seizure-like behavior of the 5 dpf zebrafish. Treatment with atipamezole results in a lower maximum distance moved and maximum velocity. Additionally, for the parameter movement frequency, there is a significant increase which is an important finding as it suggests that the PTZ+atipamezole co-treated group exhibits behavior more closely resembling that of the control group. It is also important to notice that in this project, the 30 µM concentration of atipamezole also decreases the locomotor activity of the atipamezole-treated group compared to the control group, which is analogous to the findings seen in the clonidine experiments.

Lastly, upon analysing and visualizing the results of the alternating phases, there is a distinction observed between the dark-light and light-dark transmissions. Those findings are similar to those seen in the clonidine experiment. There is only a significant increase in Δ maximum distance moved when the results of the PTZ+atipamezole co-treated group are compared to the PTZ-treated group. Those findings suggest that atipamezole may have an anticonvulsant effect and that the noradrenaline system may act as a starting point for the development of novel medication for epilepsy.

This thesis shows an anticonvulsant effect of atipamezole on PTZ behavior. Further studies need to examine the anticonvulsant α_2-receptor blockade with various concentrations of this antagonists and/or other incubation periods to further investigate the exact mechanism-of-

action. Other epilepsy models such as rats have shown a facilitation in seizure formation [35] which is contradictory to our findings.

8.2 Expression analysis

A second step is to investigate the involvement of the noradrenergic system in seizures, starting with exploring the expression levels of different noradrenergic receptors in 5 dpf zebrafish. It is of utmost importance to prove the expression and involvement of noradrenergic receptors in 5 dpf zebrafish, since also behavior analyses are performed on 5 dpf zebrafish with compounds targeting this noradrenergic neurotransmission system. However, studies related to expression levels of β-, α_2- and α_1-adrenergic receptors subtypes have not been extensively described, especially not in 5 dpf zebrafish, since most research is focused on adult zebrafish [45]. Moreover, only a few studies have focused on the regional expression and distribution of some noradrenergic receptors in adult zebrafish [51]. Therefore, in this research project, different noradrenaline receptor genes (*adra1aa*, *adra1ab*, *adra1ba*, *adra1bb*, *adra2a*, *adra2b*, *adrb1*, *adrb2a* and *adrb2b)* are studied for their expression levels in 5 dpf zebrafish body or head tissues. This will deliver us novel information, especially in relation to the study of seizures and epilepsy.

To investigate changes in expression levels in genes of interest (noradrenaline receptor genes) relative to reference genes, stable expressed reference genes are identified specifically for 5 dpf zebrafish 10 heads (*gapdh*, *rpl13a* and *rnf7*) and 10 bodies (*rps18*, *rnf7* and *mobk13*). The finding that *rpl13a* and *rnf7* are stable reference genes expressed in zebrafish is confirmed by an earlier literature study [52] that mentions *rpl13a* and *rnf7* as stable expressed reference genes in adult zebrafish. However, our experiments also prove stable expression of *rpl13a* in larval (5 dpf) zebrafish heads and stable expression of *rnf7* in larval (5 dpf) zebrafish heads and bodies.

These reference genes (heads: *gapdh*, *rpl13a* and *rnf7*, bodies: *rps18*, *rnf7* and *mobk13*) are used in further expression experiments to normalize the expression levels of the noradrenaline receptor genes (*adra1aa*, *adra1ab*, *adra1ba*, *adra1bb*, *adra2a*, *adra2b*, *adrb1*, *adrb2a* and *adrb2b*) in tissues of 1, 2, 3, 6 or 12 5 dpf zebrafish heads or bodies. Those pools of ascending numbers of 5 dpf zebrafish heads or bodies are used to determine the number of 5 dpf zebrafish heads and bodies that are needed to detect adrenoceptor expression levels.

The graphs for the expression analyses show that the datapoints (biological replicates) per sample are less spread when pools of 6-12 zebrafish heads or bodies are used. Additionally, a large variability in relative quantity is mainly seen in samples where lower numbers of zebrafish heads or bodies are pooled (1, 2 and 3 heads/bodies). From the mean Cq-values of the RT-qPCR analyses, it can be said that there is a trend towards a lower mean Cq-value the more zebrafish heads or bodies are pooled. In conclusion, at least 6 to 12 zebrafish heads or bodies need to be pooled to deliver reliable results in relation to expression of the noradrenaline receptors. When pooling higher numbers (ranging from 6 to 12) of 5 dpf zebrafish bodies and heads, expression of different noradrenergic receptor subtypes can be proven with less missing datapoints and with less variability in the samples, besides the fact that higher pools of zebrafish heads or bodies have lower mean Cq-values. Furthermore, there is no major difference between the mean Cq-values of the zebrafish heads and bodies samples, so it is suspected that the expression of the noradrenaline receptors seen in the body samples comes from the head samples.

The noradrenergic agonist (clonidine) and antagonist (atipamezole) both target the α_2-adrenoceptors: *adra2a* and *adra2b*. From the mean Cq-values for *adra2a* (12H: 32.47, 12B: 31.20) and *adra2b* (12H: 31.30, 12B: 30.02), it can be stated that these noradrenaline receptor genes are expressed in 5 dpf zebrafish heads and bodies. On the other hand, *adrb2b* seems to have the lowest mean Cq-value (12H: 27.86, 12B: 27.05). The relative high expression of *adrb2b* in 5 dpf zebrafish tissues is also confirmed by earlier studies, however, mainly muscle tissue, pancreas and liver are mentioned as tissues that show high *adrb2b* expression levels

[53]. Moreover, this study demonstrates expression of *adrb1* and *adrb2a*, both mainly in the zebrafish brain. This thesis confirms that *adrb1* and *adrb2a* are expressed in zebrafish tissue of 12 heads with mean Cq-values of 29.62 and 30.44, respectively. For the first time, the expression levels of different noradrenaline receptor genes separately in heads of 5 dpf zebrafish is demonstrated.

8.3 Limitations of the study and future perspectives

For the behavior experiments of this project, data from only three tests per testing condition (e.g., PTZ+VA test) are used, where every test consists of 3-4 trials with 24 zebrafish per trial (6 zebrafish/condition/trial). This leads, for the PTZ+VA experiments, to a total number of 66 zebrafish per condition (control/PTZ/VA/PTZ+VA). Although three different zebrafish clutches are used to yield reproducible results and to cover for the large variability seen in zebrafish clutches, one could opt for an even higher sample size with more clutches in future experiments.

Moreover, only one α_2-adrenergic agonist (clonidine) and antagonist (atipamezole) are tested on their effects on 5 dpf zebrafish swimming behavior. It would be interesting for further experiments to test adrenergic compounds targeting the α_1-adrenoceptors (e.g., methoxamine (α_1-adrenoceptor agonist), prazosin (α_1-adrenoceptor antagonist)) and targeting the β_2-adrenoceptors (e.g., salbutamol (β_2-adrenoceptor agonist), propranolol (β_2-adrenoceptor antagonist)) in this PTZ-induced seizure zebrafish model, since these two receptor types were mentioned above (5.4.3.2) as important key regulators of seizure suppression upon activation.

Furthermore, genetic zebrafish models could be constructed whereby specific adrenergic receptors are knocked down or knocked out. In this way, the role of noradrenaline in PTZ-induced seizures can further be confirmed and the different anticonvulsant or proconvulsant effects can be further assigned to the different subtypes of these noradrenaline receptors.

Additionally, by making use of $GRAB_{NE}$-sensors (GPCR activation-based noradrenaline sensors (genetically encoded fluorescent sensors)), noradrenaline releases and noradrenergic activity can be monitored *in vivo* with high temporal and spatial resolution, besides high ligand specificity. With this technique, changes in fluorescence levels will be picked up when noradrenaline binds to the noradrenergic receptors, which allows us to study noradrenaline concentration changes in the synaptic cleft (e.g., an increase in noradrenaline is expected upon treatment with an adrenergic antagonist (5.4.3.3)).

Further, noradrenaline is not only known for having effects on the brain, but also on the whole body, especially on cardiac output responses. DanioScope™ is a non-invasive video-based software tool (Noldus, The Netherlands) that could be used to analyze cardiovascular measurements (heart rate and inter-beat interval) of larval zebrafish.

In the behavior experiments, the effects of different proconvulsant (PTZ), antiepileptic (VA) and noradrenergic (clonidine, atipamezole) compounds on zebrafish swimming behavior are evaluated, and in the expression experiments, the expression levels of multiple noradrenaline receptor genes in 5 dpf zebrafish are identified, besides determination of the number of 5 dpf zebrafish heads or bodies needed to pick up noradrenaline receptor expression. In future studies, a combination of both approaches could be used to evaluate the noradrenaline receptor expression levels prior and after treatment with above-mentioned compounds in pools of 6-12 5 dpf zebrafish heads or bodies in both control and PTZ-treated zebrafish.

9. General conclusion

This project aimed to assess the involvement of the noradrenergic system in a PTZ-induced 5 dpf zebrafish model. This research aim was approached in two different ways. A first approach was to conduct behavior experiments using 5 dpf zebrafish, in order to assess the effects of VA (antiepileptic compound), clonidine (noradrenaline agonist) and atipamezole (noradrenaline antagonist) on the swimming behavior in both control zebrafish and PTZ-

induced seizure zebrafish. A second approach was to evaluate the expression levels of the noradrenaline receptor genes in 5 dpf zebrafish.

The results of both the stable light, switch from light to dark and stable dark period and the alternating light/dark-phases of the behavior experiments showed an anticonvulsant effect of the VA compound. This confirms that this medication is able to reverse the effect of PTZ and thereby exerts an antiepileptic effect, however, the exact mechanism-of-action remains unclear. One mechanism could be via working on the GABAergic system, because VA inhibits the function of the GABA-transaminase enzyme and thereby increases the GABA levels in the brain. However, this cannot be proven via this project and further research is needed to elucidate the possible pathways and working mechanisms. Treatment with 30 µM clonidine results in no significant decrease or increase of the seizure behavior in the stable light, switch light-dark and stable dark periods. However, our hypothesis stated that clonidine, a noradrenergic agonist, would have proconvulsant effects. A possible explanation could be the administration of a low concentration of clonidine (30 µM), since previous studies already proved that clonidine exerts proconvulsant effects at low doses and anticonvulsant effects at high doses. In contrast, the 30 µM clonidine-treated group showed a significant decrease of behavioral locomotion when compared to the control group. This suggests that clonidine does exert an effect on 5 dpf zebrafish, but further experiments with various concentrations of clonidine are needed. Further results of the alternating phases did show a reversed effect of the 30 µM PTZ+clonidine co-treated group in comparison to the PTZ-treated group. Thereby, it is also hypothesized that the effect of clonidine on the 5 dpf zebrafish seizure model may be environmentally triggered. Lastly, the atipamezole compound showed in both stable light, switch light-dark and stable dark periods and alternating phases a significant reduction in seizure behavior. This proves the hypothesis of our project stating that atipamezole would have an anticonvulsant effect. These results highlight the importance of the noradrenergic system in epilepsy, more specifically the role of the α_2-receptor.

For the expression experiments, we identified some novel stable expressed reference genes for RT-qPCR normalization with respect to the 5 dpf stage of zebrafish, and specifically for samples of zebrafish heads (*gapdh*, *rpl13a* and *rnf7*) and bodies (*rps18*, *rnf7* and *mobk13*). Additionally, this project proposed that at least 6 or 12 zebrafish heads or bodies need to be pooled to obtain reliable results for the expression of the noradrenergic receptors in 5 dpf zebrafish. To study the LC-NE circuit specifically in the zebrafish brain, tissues of 6-12 zebrafish heads need to be pooled for further analyses. Furthermore, our experiments show, for the first time, that the studied noradrenaline receptors are expressed in both 5 dpf zebrafish heads and bodies, however, due to relatively high mean Cq-values, we cannot prove that they are highly expressed.

To conclude, the behavior experiments prove that the noradrenergic system does have an important role during seizures. Moreover, expression levels of noradrenergic receptors could be demonstrated with the expression experiments. However, studying the involvement of noradrenaline in seizures is a complex topic, and therefore, we strongly believe that further investigation of the noradrenergic system in seizures and epilepsy is needed, to benefit the epilepsy patient population in the future. Therefore, some recommendations for future preclinical epilepsy studies were given above.

10. References

1. Thijs, R. D., Surges, R., O'Brien, T. J. & Sander, J. W. Epilepsy in adults. *Lancet* **393**, 689–701 (2019).
2. Gawel, K. *et al.* Seizing the moment: Zebrafish epilepsy models. *Neurosci. Biobehav. Rev. Biobehav. Rev.* **116**, 1–20 (2020).
3. Ioannou, P. *et al.* The burden of epilepsy and unmet need in people with focal seizures. *Brain Behav.* **12**, (2022).
4. Leibetseder, A., Eisermann, M., LaFrance, W. C., Nobili, L. & Von Oertzen, T. J. How to distinguish seizures from non-epileptic manifestations. *Epileptic. Disord.* **22**, 716–738 (2020).
5. Seidenberg, M., Pulsipher, D. T. & Hermann, B. Association of epilepsy and comorbid conditions. *Future Neurol.* **4**, 663–668 (2009).
6. Mesraoua, B. *et al.* Dramatic outcomes in epilepsy: depression, suicide, injuries, and mortality. *Curr. Med. Res. Opin.* **36**, 1473–1480 (2020).
7. Mesraoua, B. *et al.* Drug-resistant epilepsy: Definition, pathophysiology, and management. *J. Neurol. Sci.* **452**, 120766 (2023).
8. Rahman, M., Awosika, A. O. & Nguyen, H. Valproic acid. (2024).
9. Grone, B. P. & Baraban, S. C. Animal models in epilepsy research: legacies and new directions. *Nat. Neurosci.* **18**, 339–343 (2015).
10. De Calbiac, H., Dabacan, A., Muresan, R., Kabashi, E. & Ciura, S. Behavioral and physiological analysis in a zebrafish model of epilepsy. *J. Vis. Exp.* (2021) doi:10.3791/58837.
11. Bauer, B., Mally, A. & Liedtke, D. Zebrafish embryos and larvae as alternative animal models for toxicity testing. *Int. J. Mol. Sci.* **22**, 13417 (2021).
12. Kalueff, A. V., Stewart, A. M. & Gerlai, R. Zebrafish as an emerging model for studying complex brain disorders. *Trends Pharmacol. Sci.* **35**, 63–75 (2014).
13. Howe, K. *et al.* The zebrafish reference genome sequence and its relationship to the human genome. *Nature* **496**, 498–503 (2013).
14. Hason, M. & Bartůněk, P. Zebrafish Models of Cancer—New insights on modeling human cancer in a Non-Mammalian vertebrate. *Genes* **10**, 935 (2019).
15. Cleal, M. *et al.* The Free-movement pattern Y-maze: A cross-species measure of working memory and executive function. *Behav. Res. Methods* **53**, 536–557 (2020).
16. Blaser, R. E. & Peñalosa, Y. M. Stimuli affecting zebrafish (Danio rerio) behavior in the light/dark preference test. *Physiol. Behav.* **104**, 831–837 (2011).
17. Basnet, R. M., Zizioli, D., Taweedet, S., Finazzi, D. & Memo, M. Zebrafish Larvae as a behavioral model in Neuropharmacology. *Biomedicines* **7**, 23 (2019).
18. Bennun, A. The noradrenaline-adrenaline-axis of the fight-or-flight exhibits oxytocin and serotonin adaptive responses - ProQuest. *Int. J. Med. Biol. Front.* **Vol. 21**, 387–408 (2015).
19. Lin, H. & Vartanian, O. A neuroeconomic framework for creative cognition. *Perspect. Psychol. Sci.* **13**, 655–677 (2018).
20. Farrar, M. J., Kolkman, K. E. & Fetcho, J. R. Features of the structure, development, and activity of the zebrafish noradrenergic system explored in new CRISPR transgenic lines. *J. Comp. Neurol.* **526**, 2493–2508 (2018).
21. 系统管理员, Suwen, Z. & Guisheng, Z. New findings on adrenergic receptors shed light on partial agonism and biased signalling. (2020).
22. Wang, S., Wang, Z. & Mu, Y. Locus coeruleus in Non-Mammalian vertebrates. *Brain Sci.* **12**, 134 (2022).
23. Fontana, B. D. *et al.* Zebrafish models for attention deficit hyperactivity disorder (ADHD). *Neurosci. Biobehav. Rev. Biobehav. Rev.* **100**, 9–18 (2019).
24. Singh, C., Oikonomou, G. & Prober, D. A. Norepinephrine is required to promote wakefulness and for hypocretin-induced arousal in zebrafish. *eLife* **4**, (2015).
25. Demin, K. A. *et al.* Acute effects of amitriptyline on adult zebrafish: Potential relevance to antidepressant drug screening and modeling human toxidromes. *Neurotoxicol. Teratol.* **62**, 27–33 (2017).
26. Okanari, K. *et al.* Behavioral and neurotransmitter changes on antiepileptic drugs treatment in the zebrafish pentylenetetrazol-induced seizure model. *Behav. Brain Res.* **464**, 114920 (2024).
27. Hillman, K. L., Lei, S., Doze, V. A. & Porter, J. E. Alpha-1A adrenergic receptor activation increases inhibitory tone in CA1 hippocampus. *Epilepsy Res.* **84**, 97–109 (2009).
28. Giorgi, F. S., Pizzanelli, C., Biagioni, F., Murri, L. & Fornai, F. The role of norepinephrine in epilepsy: from the bench to the bedside. *Neurosci. Biobehav. Rev. Biobehav. Rev.* **28**, 507–524 (2004).

29. Dailey, J. W., Mishra, P. K., Ko, K. H., Penny, J. E. & Jobe, P. C. Noradrenergic abnormalities in the central nervous system of Seizure-Naive genetically Epilepsy-Prone rats. *Epilepsia* **32**, 168–173 (1991).
30. Berger, A. *et al.* How is the norepinephrine system involved in the antiepileptic effects of vagus nerve stimulation? *Front. Neurosci.* **15**, (2021).
31. Raedt, R. *et al.* Increased hippocampal noradrenaline is a biomarker for efficacy of vagus nerve stimulation in a limbic seizure model. *J. Neurochem.* **117**, 461–469 (2011).
32. Atzori, M. *et al.* Locus ceruleus norepinephrine release: a central regulator of CNS Spatio-Temporal activation? *Front. Synaptic Neurosci.* **8**, (2016).
33. Jurgens, C. W., Knudson, C. A., Carr, P. A., Perez, D. M. & Doze, V. A. α1 Adrenergic receptor regulation of interneuron function. ˜ œ*FASEB J.* **23**, (2009).
34. Zuscik, M. J. *et al.* Overexpression of the α1B-adrenergic receptor causes apoptotic neurodegeneration: Multiple system atrophy. *Nat. Med.* **6**, 1388–1394 (2000).
35. Ciltas, A. C. *et al.* The anticonvulsant effects of alpha-2 adrenoceptor agonist dexmedetomidine on Pentylenetetrazole-Induced seizures in rats. *Neurochem. Res.* **47**, 305–314 (2021).
36. Fitzgerald, P. J. Is elevated norepinephrine an etiological factor in some cases of epilepsy? *Seizure* **19**, 311–318 (2010).
37. Wu, H.-Q., Tullii, M., Samanin, R. & Vezzani, A. Norepinephrine modulates seizures induced by quinolinic acid in rats: selective and distinct roles of α-adrenoceptor subtypes. *Eur. J. Pharmacol.* **138**, 309–318 (1987).
38. Ozdemir, E. Adrenergic receptor system as a pharmacological target in the treatment of epilepsy (Review). *Med. Int.* **4**, (2024).
39. Rassier, G. T. *et al.* Evaluation of qPCR reference genes in GH-overexpressing transgenic zebrafish (Danio rerio). *Sci. Rep.* **10**, (2020).
40. Hu, Y., Xie, S. & Yao, J. Identification of Novel Reference Genes Suitable for qRT-PCR Normalization with Respect to the Zebrafish Developmental Stage. *PloS One* **11**, e0149277 (2016).
41. Vanhauwaert, S. *et al.* Expressed Repeat Elements Improve RT-qPCR Normalization across a Wide Range of Zebrafish Gene Expression Studies. *PloS One* **9**, e109091 (2014).
42. Sveinsdóttir, H. S. *et al.* Novel non-stimulants rescue hyperactive phenotype in an adgrl3.1 mutant zebrafish model of ADHD. *Neuropsychopharmacology* **48**, 1155–1163 (2022).
43. Yang, X. *et al.* High-throughput screening in larval zebrafish identifies novel potent sedative-hypnotics. *Anesthesiology* **129**, 459–476 (2018).
44. Ruuskanen, J. O. *et al.* Conserved structural, pharmacological and functional properties among the three human and five zebrafish α2-adrenoceptors. *Br. J. Pharmacol.* **144**, 165–177 (2005).
45. Ruuskanen, J. O., Peitsaro, N., Kaslin, J. V. M., Panula, P. & Scheinin, M. Expression and function of α2-adrenoceptors in zebrafish: drug effects, mRNA and receptor distributions. *J. Neurochem.* **94**, 1559–1569 (2005).
46. Myren-Svelstad, S. *et al.* Elevated photic response is followed by a rapid decay and depressed state in ictogenic networks. *Epilepsia* **63**, 2543–2560 (2022).
47. Effect of various antiepileptic drugs in zebrafish PTZ-Seizure model. (2014).
48. Benoit, E., Lyons, D. G. & Rihel, J. Noradrenergic tone is not required for neuronal activity-induced rebound sleep in zebrafish. *J. Comp. Physiol. [B]* (2023) doi:10.1007/s00360-023-01504-6.
49. Fletcher, A. & Forster, E. A. A proconvulsant action of selective α2-adrenoceptor antagonists. *Eur. J. Pharmacol.* **151**, 27–34 (1988).
50. Nissinen, J. *et al.* Disease-modifying effect of atipamezole in a model of post-traumatic epilepsy. *Epilepsy Res.* **136**, 18–34 (2017).
51. Ampatzis, K. & Dermon, C. R. Regional distribution and cellular localization of β2-adrenoceptors in the adult zebrafish brain (Danio rerio). *J. Comp. Neurol.* **518**, 1418–1441 (2010).
52. Xu, H. *et al.* Genome-wide identification of suitable zebrafish Danio rerio reference genes for normalization of gene expression data by RT-qPCR. *J. Fish Biol.* **88**, 2095–2110 (2016).
53. Wang, Z. *et al.* Zebrafish β-adrenergic receptor mRNA expression and control of pigmentation. *Gene* **446**, 18–27 (2009).

11. Poster

GHENT UNIVERSITY · FACULTY OF MEDICINE AND HEALTH SCIENCES · UZ GENT · CENTER FOR MEDICAL GENETICS GHENT · 4BRAIN

TARGETING THE NORADRENALINE RECEPTORS IN A SEIZURE-INDUCED ZEBRAFISH MODEL

Markella Gryllionaki[1,2], Maïté Verstraeten[1,2], Zoë Malfait[1], Delfien Syx[1], Robrecht Raedt[2]

[1]Center for Medical Genetics, Department of Biomolecular Medicine, Ghent University Hospital, 9000 Ghent, Belgium.
[2]4BRAIN, Department of Head and Skin, Ghent University, 9000 Ghent, Belgium.

I. INTRODUCTION

EPILEPSY

- **65 million** epilepsy patients worldwide
- **Disbalance** in inhibitory and excitatory signaling
- **1 in 3 patients** do not gain seizure control using antiepileptic drugs
- **Novel treatment** options are needed: ↓ side effects & ↑ efficacy

In order to develop better antiepileptic drugs, a deeper understanding of the **underlying molecular mechanisms of epilepsy** is needed. Recently, a growing interest has arisen for the role of the **noradrenergic neurotransmission** system in regulating brain hyperexcitability and seizure susceptibility.

ZEBRAFISH MODEL

Advantages: high-throughput drug screening, permeable and transparant, high fecundity, easy to house

II. MATERIAL AND METHODS

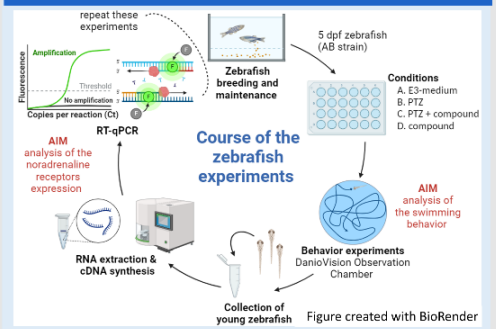

Fig. 1. Graphical abstract of the course of the zebrafish experiments. To study the effects of a noradrenaline agonist (e.g., clonidine) and antagonist (e.g., atipamezole) on seizures, the swimming behavior (total distance moved) is assessed of 5dpf wild-type (AB) zebrafish divided into 4 different conditions: control (E3-medium), PTZ (pentylenetetrazole), compound (e.g., valproic acid, clonidine, atipamezole) and PTZ in combination with the compound. To evaluate the expression of noradrenaline receptors in larval untreated and treated zebrafish, RNA will be extracted from 5dpf zebrafish for cDNA synthesis using the iScript Advanced cDNA synthesis kit (Bio-Rad) and RT-qPCR analysis using the SsoAdvancedTM SYBR Green Supermix and the LightCycler 480. This will allow to study possible expression changes of noradrenaline receptors concomitant to experimental seizure induction and its treatment.

III. RESULTS AND DISCUSSION

BEHAVIOR ANALYSIS

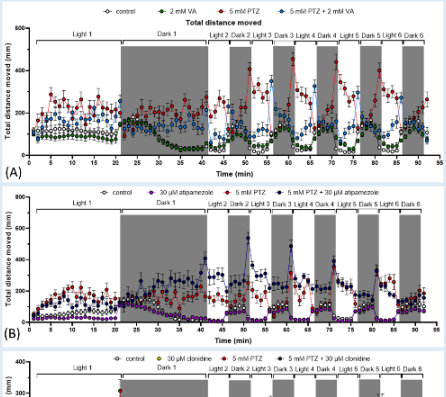

Fig. 2. Total distance moved measured during behavior analysis with 5dpf zebrafish. To study the effects of 2 mM valproic acid (VA) (antiepileptic drug), 30 µM clonidine (alpha-2 adrenergic agonist) and 30 µM atipamezole (alpha-2 adrenergic antagonist) on seizures, the swimming behavior (total distance moved) is assessed of 5dpf zebrafish divided into 4 different conditions: control, compound (VA, atipamezole, clonidine), PTZ and PTZ in combination with the compound. Time (min) and total distance moved (mm) are represented on the x- and y-axis, respectively. **(A)** Untreated controls (white) and VA (green) induce a higher total distance moved during dark phases and a lower total distance moved during light phases, whereas this pattern is reversed after PTZ (red) administration, resulting in light-induced seizures. VA rescues the phenotype induced by PTZ (light blue), leading to a lower total distance moved in the light phases. (n = 24, data expressed as mean ± SD) **(B)** Both the control (white), the PTZ (red) and the atipamezole (purple) conditions are following a light-dark movement pattern, whereas it can be concluded that 30 µM atipamezole does not exert an effect on seizures (dark blue). (n = 18, data expressed as mean ± SD) **(C)** As expected, the alpha-2 adrenergic agonist clonidine (30 µM) has a suppressant effect on the swimming behavior, resulting in a lower total distance moved in the clonidine condition (yellow). Clonidine rescues the PTZ-induced seizure phenotype in most dark phases, however, in the light phases an increase in total distance moved can be seen for the PTZ + clonidine condition (black), thus showing no rescue of the PTZ-phenotype in light phases. (n = 18, data expressed as mean ± SD)

EXPRESSION ANALYSIS

Reference gene	Primer efficiency (%)
rpl13a	105
rnf7	102
rps18	115
cat	103
sdha	94
ywhaz	93
mobk13	100
lsm12b	102
b2m	96
gapdh	100
eef1a1a	107
eif2s2	107
rplp2	105
rpl7	100

Noradrenaline receptor gene	Primer efficiency (%)
adra1aa	116
adra1ab	105
adra1ba	99
adra1bb	103
adra2a	105
adra2b	119
adrb1	112
adrb2a	95
adrb2b	107

Table 1. Primer efficiencies for the noradrenaline receptor genes and reference genes. Table 1 shows the primer efficiencies (in %) tested with RT-qPCR (using a cDNA dilution series as template) for in-house designed primers specifically targeting the zebrafish orthologs of the noradrenaline receptor genes and reference genes. Primers are designed using Ensembl, UCSC Genome Browser and NCBI primer-blast. Primer efficiencies are ideally 100%, but a deviation up to 20% is tolerated before including them in future experiments.

IV. CONCLUSION AND FUTURE PERSPECTIVES

- **Behavior analysis**: The swimming behavior (total distance moved) is assessed in 5dpf zebrafish, which are divided into 4 conditions: control (E3-medium), 5 mM PTZ, compound (2 mM VA, 30 µM atipamezole or 30 µM clonidine) and PTZ in combination with the compound. 2 mM VA exerts an anti-seizure effect reflected in a lower total distance moved in the light phases compared to the 5 mM PTZ group. Both the alpha-2 noradrenergic agonist (30 µM clonidine) and antagonist (30 µM atipamezole) have shown no effect on rescuing the seizure phenotype. However, clonidine (30 µM) exerts a suppressive effect on the swimming behavior in comparison with a control group. In the upcoming experiments, other swimming behavior parameters, such as velocity, movement frequency and total distance moved, will be analyzed and compared between the different conditions.
- **Expression analysis**: As a first step, primers are designed and tested for their efficiency, specifically targeting the noradrenaline receptor genes and reference genes in 5dpf zebrafish. After these preliminary steps, future experiments consist out of collections of untreated and treated 5dpf zebrafish for RNA extraction, cDNA synthesis and RT-qPCR analysis for noradrenaline receptor genes and reference genes. This will allow to study possible expression changes of noradrenaline receptors concomitant to experimental seizure induction and its treatment.
- In conclusion, 5dpf wild-type **zebrafish** will be used to deepen the study of **seizures** by investigating which noradrenaline receptors are expressed in larval zebrafish and by comparing a noradrenergic agonist (clonidine) and antagonist (atipamezole) with a known antiepileptic drug (valproic acid) via a behavior analysis in seizure-induced zebrafish, as well as via expression analysis of the noradrenaline receptors.

V. REFERENCES

Akyuz, E. et al. Revisiting the role of neurotransmitters in epilepsy: An updated review. *Life Sciences* 265, 118826, doi:10.1016/j.lfs.2020.118826 (2021).
Gupta, P., Khobragade, S. B. & Shingatgeri, V. M. Effect of Various Antiepileptic Drugs in Zebrafish PTZ-Seizure Model. *Indian Journal of Pharmaceutical Sciences* 76, 157-163 (2014).
Thijs, R. D., Surges, R., O'Brien, T. J. & Sander, J. W. Epilepsy in adults. *The Lancet* 393, 689 701, doi:10.1016/s0140-6736(18)32596-0 (2019).
Yaksi, E., Jamali, A., Diaz Verdugo, C. & Jurisch-Yaksi, N. Past, present and future of zebrafish in epilepsy research. *The Febs journal* 288, 7243-7255, doi:10.1111/febs.15694 (2021).

Contact
Markella.Gryllionaki@ugent.be
Maite.Verstraeten@ugent.be
Universiteit Gent
@ugent
Ghent University

Figure 37. Poster of this thesis.

12. Addendum

12.1 Material & methods

12.1.1 Behavior analysis

12.1.1.1 Setting up a zebrafish breeding and maintaining young (5 dpf) zebrafish

Material and chemicals:

- Breeding tank: inner tank, outer tank and divider
- System water
- Adult female (2) and male (2) zebrafish (AB strain)

Protocol:

1. Assemble the breeding tank (Figure 38 Step A) by putting an inner tank into an outer tank and putting a divider in the middle of the inner tank.
2. Fill the tank with system water (Figure 38 Step B).
3. Put 2 female zebrafish on one side of the divider and 2 male zebrafish on the other side of the divider (Figure 38 Step C). Male zebrafish are recognized by their slender, torpedo shaped body with a yellowish belly, whereas female zebrafish have a more rounded figure with a whitish belly.
4. Put the tank in the breeding area overnight (Figure 38 Step D).

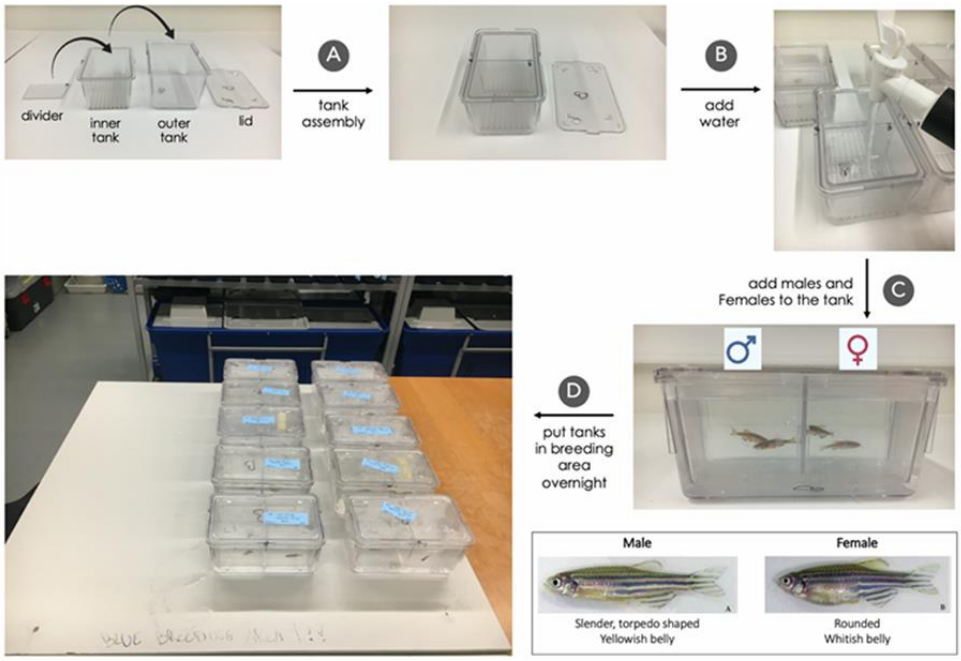

Figure 38. Setting up the breeding of zebrafish. The tank is first assembled by placing a divider and an inner tank into an outer tank (step A). Afterwards, system water is used to fill up the tanks (step B). Male and female zebrafish are selected from an original tank and placed on separate sides of the assembled tank (step C). The differences between male and female zebrafish are shown on the figure below right. In a last step, the tanks are put overnight in the breeding area in the zebrafish core facility (step D).

5. In the morning, when the lights in the facility come on, remove the divider, and tilt the inner tank diagonally to create a ‘naturally’ shore feeling for the zebrafish (Figure 39 Step A).
6. Allow the animals to breed for about 1 hour and check whether there are eggs (Figure 39 Step B).

7. Collect the eggs with a sieve and rinse with system water to eliminate dirt particles (Figure 39 Step C).
8. Transfer the eggs with E3 medium in a Petri dish (Figure 39 Step D).
9. Check under the stereoscope if the eggs are fertilized and start to divide. Remove non-fertilized eggs.
10. Put the Petri dish with the fertilized eggs in an incubator at 28°C (Figure 39 Step E).

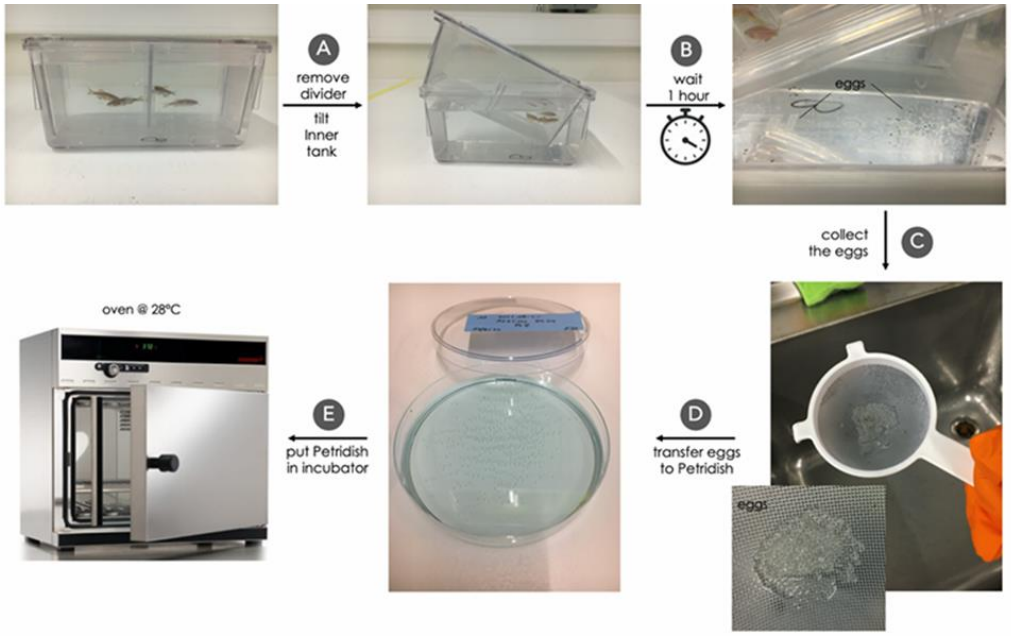

Figure 39. Zebrafish breeding and collection of eggs. The divider is removed from the inner tank and the inner tank is tilled diagonally in the outer tank (step A). Approximately an hour is waited for the zebrafish to have bred (step B). Afterwards, the eggs are collected with a sieve and rinsed with system water (step C). The eggs can then be transferred to a Petri dish filled with E3 medium (step E), before being placed into the incubator/oven (step E).

12.1.1.2 Generating randomized plate layouts with PlateDesigner

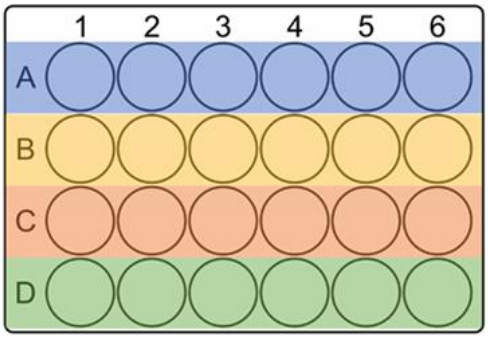

Figure 40. Standard plate layout used for the behavior experiments. Each color (rows A-D) in this plate layout displays another condition applied to the 5 dpf zebrafish in the behavior experiments.

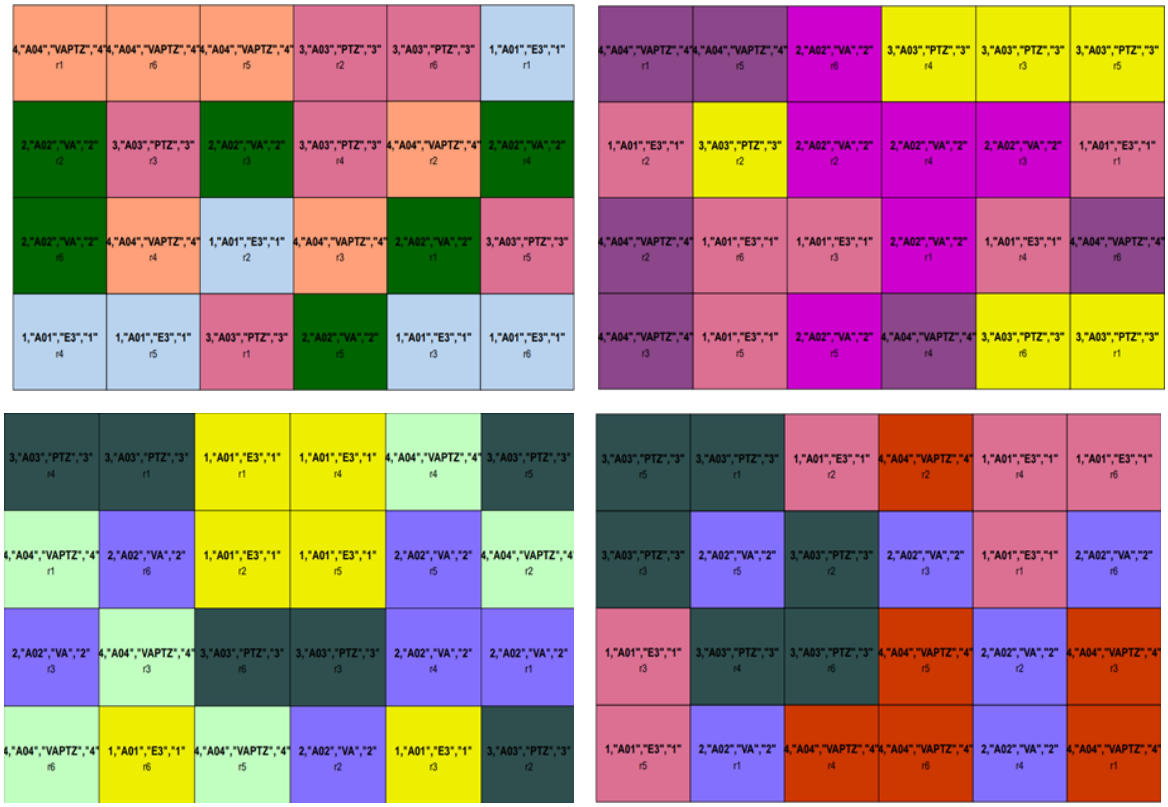

Figure 41. Different plate layouts for the behavior experiments (generated with PlateDesigner). Each plate displays 4 different conditions, in this case: control ('E3'), PTZ ('PTZ'), VA ('VA') and PTZ in combination with VA ('VAPTZ'). Different colors are used to visualize these 4 different conditions per plate.

12.1.1.3 Protocol: Behavior analysis

Material and chemicals:

- 24-well plate
- Printed layouts of the randomized well plate designs
- Zebrafish, 5 days post fertilization (5 dpf)
- E3 medium
- 4 mM valproic acid (sodium salt) (VA) = stock solution
- 20 mM pentylenetetrazole (PTZ) = stock solution

Protocol (for the behavior experiments with (1) E3 medium, (2) 2 mM VA, (3) 5 mM PTZ and (4) 5 mM PTZ + 2 mM VA):

1. Take the Petri dish with the zebrafish out of the incubator and check under the microscope.
2. Turn on the Observation Chamber (temperature control unit: 28°C) and put new distillated water in.
3. Turn on the software: EthoVision XT15 > New from template > Custom template > This pc > DATA (D:) > Noldus > EthoVision > Experiments > Give the experiment a new name.
4. Make the working solutions for valproic acid (VA) and pentylenetetrazole (PTZ).
5. Shake the working solutions.
6. Add 1 ml E3 medium or 1 ml VA (2 mM) with a P1000 pipet as indicated in the randomized plate layouts.

7. Carefully add one 5 dpf zebrafish to each well using a plastic pipet. Be careful not to transfer too much of the E3 medium from the Petri dish where the zebrafish are housed. Start with the VA wells since an incubation period of 15 minutes is used for VA. Start the timer for 15 minutes when you pipetted zebrafish in all the VA wells. Then add one 5 dpf zebrafish in the other wells.
8. Incubate the plate for 15 minutes.
9. Add 1 ml (with a P1000 pipet) of the solutions as indicated in the plate layouts.
10. Place the 24-well plate in the DanioVision Observation Chamber.
    - Tilt the 24-well plate and put the part closest to you in the water reservoir. (Figure 42 Step A)
    - To avoid air bubbles, slowly lower the upper part of the 24-well plate.
    - Lower the lens to prevent angular distortion. (Figure 42 Step B)

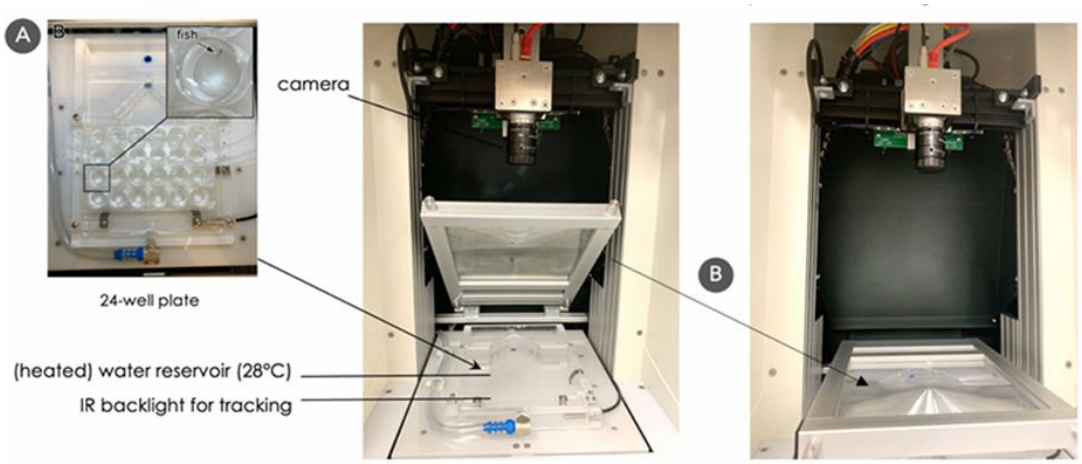

Figure 42. DanioVision Observation Chamber (Noldus, The Netherlands). After the 24-well plate is filled up according to the right conditions and with 1 zebrafish in each well, the well plate is placed into the heated water reservoir of the DanioVision Observation Chamber (step A). Afterwards, the well plate is appropriately enclosed in the machine by lowering the lens (step B).

11. Open the EthoVision XT15 software and check the SETUP tab:
    - Arena Settings:
        - Make sure that all the wells are enclosed in the appropriate arena. (number of arenas: 24)
        - Arena settings > Grab background Image > Grab Image from camera > Yes
        - Arena settings > shape size and position > width: 17 mm, height: 17 mm > A1 > right click > duplicate complete arena > OK
        - Arena settings > select shape and arena > check them one for one, make sure that also the labels are moving by drawing a square with the computer mouse around the selected well.
        - Arena settings > calibrator: make sure that this distance is 11,4 cm (from outside of well A1 to outside of well A6).
    - Trial Control Settings:
        - The protocol that we will use consists of a 20-minute light phase (5%), followed by a 20-minute dark phase, followed by 5 cycles of alternating light and dark phases of 5 minutes each (total duration: 1h32min).
    - Detection Settings:
        - Make sure every zebrafish in every well is detected by the software: the center point is indicated in red, surrounded by yellow to indicate the rest of the zebrafish.

- Trial List:
    - Check for your Trial if the settings are correct and if the correct treatment is indicated.
    - Set up > Trial list > Trial 1-4 (for 4 well plates) > Arena (in the well plate) has to match with the right condition (control = E3 medium/PTZ/VA/PTZ+VA), which you can adjust in the last column (user-defined).

12. Go to the ACQUISITION tab:
    - Check again if all zebrafish are detected (red center point and yellow surroundings).
    - Close the DanioVision Observation Chamber.
    - Start the acquisition of the trial by clicking on the button 'Ready for start'.
13. Cleanup
    - Zebrafish will be collected in a separate Petri dish with tricaine to euthanize them. Carefully transfer only the zebrafish to the Tricaine solution and avoid transferring the solutions. The euthanized zebrafish are collected in the dedicated waste container.
    - PTZ and VA are collected in a dedicated waste container.

12.1.2 Expression analysis

12.1.2.1 Protocol: RNA extraction

RNA extraction initial preparation:

Please read the handbook supplied in the Qiagen kit to familiarize yourself with the reagents before you begin. If working with a new Qiagen kit, add 44 ml of 100% Rnase-free ethanol to the Buffer RPE concentrate.

1. Clean work surface and pipettes with RNase Away and wipe with 70% ethanol.
2. Thaw and keep DNase1, DNase buffer, and RNase-free 70% ethanol on ice. The number of samples to be processed at a time depends on the user (between 6 to 12 samples at a time). Prepare 1.5 ml tubes and the spin columns, collection tubes and elution tubes from the Qiagen kit as needed, depending on the number of samples. You need extra 1.5 ml tubes for collecting the clear phase of the sample after step 3 and for dry spinning of the spin columns at step 13.
3. Step 1-4 must be performed in a fume hood. Collect tips, tubes etc. contaminated with Trizol or chloroform as hazardous waste.

RNA extraction protocol:

1. Remove the samples from -80°C freezer and add 100µl of Trizol to the tube.
2. Homogenize the samples in the tube using the Eppendorf micro-tube sample pestle (this step allows for dissociation of the nucleoprotein complexes) and using the automatic crusher. Add another 400 µl of Trizol to the tube (total 500 µl per tube). Vortex briefly and incubate the sample for 5 minutes at room temperature (shake it from time or place tubes on a rocker). At this point, the sample can be frozen at -80°C for performing RNA extraction later, or proceed to next step.
3. Add 0.2 ml chloroform to the sample. Cap the tube and shake vigorously for about 15 seconds, then incubate it for 5 minutes at room temperature (20°C to 30°C). After 5 minutes, there will be a clear aqueous phase (nucleic acid phase) on top of the pink Trizol phase (protein phase).
4. Remove the colorless upper aqueous phase by pipetting it out carefully into a new 1.5 ml centrifuge tube. Place the tubes on ice. You must be careful not to include any of the Trizol phase as this will induce protein contamination in your RNA. Discard the Trizol (pink) phase into a hazardous waste container. After this step, all subsequent steps can be performed outside the fume hood.
5. Add one volume of Rnase-free 70% ethanol to the aqueous phase and mix thoroughly by pipetting.

6. Add upto 700 µl of this sample to a RNeasy MINI column placed in a 2 ml collection tube and centrifuge for 30 seconds at 13000 rpm. Discard the flowthrough.

Note: If the volume exceeds 700 µl, load aliquots successively onto the RNeasy column and centrifuge as above. Discard the flowthrough after each centrifugation step.

7. Add 350 µl Buffer RW1 (from the RNeasy kit) to the RNeasy column. Centrifuge for 30 seconds at 13000 rpm to wash the column. Discard the flowthrough.
8. Dnase digestion – Prepare Dnase digestion enzyme by mixing 10 µl Dnase I stock solution with 70 µl Buffer RDD (from Qiagen Rnase-free Dnase set) for each sample. Mix gently (do not vortex). Mix a stock solution depending on the number of samples being processed. Make enough for X samples + 10% extra. Avoid multiple freeze-thaw cycles of the Dnase1 enzyme. Once reconstituted, aliquot in 100 µl volume in tubes and freeze at -20°C.
9. Pipet the Dnase I incubation mix (80 µl) directly onto the RNeasy silica-gel membrane, and incubate at room temperature for exactly 15 minutes.
10. Pipet 350 µl Buffer RWA1 into the RNeasy mini column and centrifuge for 30 seconds at 13000 rpm. Discard flowthrough and collection tubes.
11. (Transfer the RNeasy mini column to a new 2 ml collection tube (supplied in the RNeasy Mini kit)). Pipet 500 µl Buffer RPE onto the RNeasy column. Centrifuge for 30 seconds at 13000 rpm to wash the column. Discard the flowthrough.
12. Add another 500 µl Buffer RPE onto the RNeasy column. Centrifuge for 2 minutes at 13000 rpm to dry the RNeasy silica gel membrane. Discard the flowthrough and collection tube.
13. Place the RNeasy column in a new 1.5 ml centrifuge tube (not supplied in kit), and centrifuge at full speed (13000 rpm) for 1 minute (this eliminates any chance of possible Buffer RPE carryover).
14. To elute the RNA, transfer the RNeasy column to a new 1.5 m collection tube (supplied with kit). Pipet 25 µl RNase-free water directly onto the RNeasy silica-gel membrane. Close the tube and centrifuge for at least 1 minute at 13000 rpm to elute. At this point, RNA can be quantified using Nanodrop right away if desired.
15. Store RNA at -20°C for short-term or -80°C for long-term storage. Avoid repeated freeze-thaw of the RNA. If thawing RNA for quantification, be prepared to make cDNA before freezing rest of RNA again.

12.1.2.2 Protocol: cDNA synthesis

Principle

RNA is transcribed into complementary DNA (cDNA) by reverse transcriptase from total RNA.

Reagents

- nuclease free water (Sigma #W-4502) (aliquot in 1 ml, and dispose after use)
- iScript Advanced cDNA synthesis kit (Bio-Rad #172-5038)

Procedure

1. Add 500 ng of total RNA to an RNase free 0.2 ml tube. Work on ice.
2. Add 4 µl iScript reaction mix to each tube.
3. Add 1 µl of iScript reverse transcriptase (keep enzyme on ice before use, do not vortex, just spin down).
4. Add nuclease-free water up to an end volume of 20 µl.
5. Incubate the reaction mix in a thermal cycler to perform the reverse transcription and inactivation.
   - 5 minutes at 25°C
   - 30 minutes at 42°C
   - 5 minutes at 85°C
   - ∞ minutes at 4°C
6. Prepare a 5 ng/µl dilution of your samples in nuclease-free water.

12.1.2.3 Protocol: cDNA dilution series

Reagents

- Template: Zebrafish qPCR Reference Total RNA (25 µg, 1µg/µl)
- Carrier nucleic acids: tRNA from brewer's yeast (Roche #10 106 517 001, 100 mg, lyophilised)
- Nuclease-free water (Sigma #W-4502)

Method

1. Prepare 50x and 1x carrier (tRNA) solutions:
   - Dilute 9 µg carrier in nuclease-free water to obtain a final volume of 36 µl 50x carrier solution (250 ng/µl) and vortex thoroughly.
   - Dilute 29 µl 50x solution with 1421 µl nuclease-free water to obtain a 1x carrier solution (5 ng/µl) and vortex thoroughly.
2. Follow the 'cDNA synthesis for real-time RT-PCR using iScript' protocol (*Addendum: 12.1.2.2*) to synthesize cDNA from 10 µg of QPCR Reference Total RNA in a volume of 100 µl.
3. Dilute the 100 µl of cDNA with 6.25 µl 50x carrier and 206.25 µl H_2O (point 1: 32 ng/µl cDNA and 5 ng/µl carrier), vortex thoroughly.
4. Dilute 78 µl of the point one solution with 234 µl 1x carrier (point 2: 8 ng/µl RNA and 5 ng/µl carrier), vortex thoroughly.
5. Repeat the previous step four times to obtain the dilution points 3 to 6 (see Table 6).
6. Add 240 µl of 1x carrier to a tube marked as negative control.
7. Aliquot all solutions in 6 equal parts (approximately 40 µl each) and store at -20°C.

Table 6: cDNA dilution series

	Starting volume	Diluted with
Point 1: 32 ng/µl	100 µl cDNA	6.25 µl 50x carrier + 206.25 µl nuclease-free water
Point 2: 8 ng/µl	78 µl point 1	234 µl 1x carrier
Point 3: 2 ng/µl	78 µl point 2	234 µl 1x carrier
Point 4: 0.5 ng/µl	78 µl point 3	234 µl 1x carrier
Point 5: 0.125 ng/µl	78 µl point 4	234 µl 1x carrier
Point 6: 0.0312 ng/µl	78 µl point 5	234 µl 1x carrier
Negative control	240 µl 1x carrier	

qPCR analysis

1. Follow the 'SYBR Green I qPCR' protocol (*Addendum: 12.1.2.4*).
2. Use 2 µl of template for each reaction and perform all reactions in duplicate (6 x 2 reactions).
3. Perform 2 negative control reactions with 2 µl of 1x carrier to check for the absence of nonspecific amplification of carrier sequences.
4. Perform 2 negative no template control reactions to check for contamination.
5. Perform linear regression, calculate the correlation coefficient, the amplification efficiency and its corresponding error (using the Excel-sheet).

Notes

Version October 18, 2006 issued by Filip Pattyn
Center for Medical Genetics, Ghent University Hospital, Belgium

12.1.2.4 Protocol: RT-qPCR analysis

Reagents

- Custom 2x SsoAdvanced™ SYBR Green Supermix (Bio-Rad, 172-5264) (dNTPs, Sso7d fusion polymerase, $MgCl_2$, SYBR® Green I, Enhancers, Stabilizers)
- Nuclease-free water (Sigma-Aldrich, W4502)
- Custom primers IDT (forward and reverse, see Table 3)
- Template (gDNA, cDNA or standard series)

Materials

- Hard-Shell® 384-well 480 qPCR plates, CLR/WHT (Bio-Rad, HSR-4805)
- Microseal® 'C' optical seals (Bio-Rad, MSC-1001)
- LightCycler 480 (Roche, model LC480)
- CFX 384 (Bio-Rad)
- Pipettes, tips, tubes

Method

When performing an RT-qPCR, work in a dedicated UV cabinet (no flow, UV decontamination bulbs). Always work with filtertips.

1. Thaw all components at room temperature.
2. Make sure that the SsoAdvanced SYBR Green Supermix is protected from light.
3. Prepare a mastermix for each assay:
   2.5 µl SsoAdvanced Mastermix
   0.25 µl Forward primer (5 µM)
   0.25 µl Reverse primer (5 µM)
   = 3 µl total volume per reaction

Note: prepare a mastermix for more samples than needed.

4. Vortex the mastermix and spin down.
5. Distribute the mastermix in the 384-well plate (3 µl for each reaction).
6. Add 2 µl cDNA sample (2.5 ng/µl), or water (no template control) to the correct wells. Run all samples in duplicate.
7. Seal the plate with the sealing foil. Wrap in aluminium foil if not used immediately.
8. Spin down the plate: 1 min, 2500 rpm.
9. Insert the plate in the LightCycler 480 and run the SsoAdvanced program:
   - Make sure the LC480 is powered on
   - Start LightCycler 480 SW 1.5 (on desktop)
   - Log in to: T2011
   - Choose NEW EXPERIMENT
   - Choose APPLY TEMPLATE (bottom left)
   - Navigator opens, choose Template - CMGG operator - Templates - Run Templates - Sso Advanced FZK
   - Insert plate in loading unit. Close loading unit.
   - The system will ask where to save the run.
   - After saving, the run will start automatically.

Table 7: PCR program

	Cycle(s)	Temperature	Time
Enzyme activation	1	95°C	2 min.
PCR	44	95°C 60°C 72°C	5 sec. 30 sec. 1 sec.
Dissociation curve		Default setting	

12.2 Results

12.2.1 Expression analysis

12.2.1.1 Primer design and primer efficiency testing

Supplementary Table 8. Primer design for the noradrenaline receptor genes. Table 8 shows the sequences of the forward primer (5'-3') and the reverse primer (5'-3'), and the primer efficiencies (tested with RT-qPCR with a cDNA dilution series as template) for the specific noradrenaline receptor genes. Ideally the primer efficiency is 100% (1), but a deviation up to 20% is tolerated (0.8-1.2). The colors green and red are indicating whether the primer pair efficiency is or is not between this range, respectively. New primer pairs are designed when a primer pair does not meet these requirements, hence the number of designs after the gene name.

Noradrenaline receptor genes			
Gene	**Forward primer (5' – 3')**	**Reverse primer (5' – 3')**	**Primer efficiency**
First design			
*adra1aa*_1	GTATCGTGGTGGGATGCTTC	GTGATCTTGAAGACTGTGTC	/
*adra1ab*_1	CTCTTGGGATTGTGGTGGG	TCTGTGGGATGGGAAGATG	/
*adra1ba*_1	AGAAAGCTGCTAAAACGCTTG	GGAGGACGGAGACTGGTG	0.9921
*adra1bb*_1	GGAAAAGAAAGCAGCAAAGAC	CCGAAGACTGGTGTTGAATG	/
*adra2a*_1	ACACATTCACAGCGTTTTGTG	TTGCAGTAGCCGAACCAGAA	1.049
*adra2b*_1	ACAGAGACATGATCGCCACCGC	TTTCTCTCGGTTCACCATCG	1.272
*adrb1*_1	TGACTCTAAACGCGCCACG	ACCAGTATATTTCCCACTACAA	1.125
*adrb2a*_1	CCGCCACTGATGTTCTGTG	CAGTAAGGACTGGTAGCGG	1.323
*adrb2b*_1	GCGCTGGTCATCAGTGCC	CGAAGGGCACCACCATAAG	1.071
Second design			
*adra1aa*_2	GGCTTCCGTTTTTCCTGGTT	TGAAGACTGTGTCCGAGGG	2.246
*adra1ab*_2	GCTGCCGTTTTTTCTTGTGC	GGTCTGTGGGATGGGAAGA	1.214
*adra1bb*_2	CTGCCATTCTTCCTTACTTTG	CAAGCCAGAAGATGATGGAG	0.8395
*adra2b*_2	ACAGAGACATGATCGCCACCGC	TGGTGTTCTTGCAGAGGATC	-0.9984
*adrb2a*_2	GGGAAACATAAGGTCCTCAAT	AGAATGGACATGAGTGTGCC	0.9489
Third design			
*adra1aa*_3	TACTCTGTTGGCTTCCGTTTT	AAGACTGTGTCCGAGGGTC	1.162
*adra1ab*_3	GCTCCATCTTCCCATCCCA	GTTCAGGCAGCTGTTGAAGT	1.047
*adra1bb*_3	GGCTGCCATTCTTCCTTACTT	CGAAGACTGGTGTTGAATGAA	1.028
*adra2b*_3	CTGCCTGGCCACACTAATG	TGGCTGTTGCAAAGGCTGC	/
Fourth design			
*adra2b*_4	CTGGCCACACTAATGGCAC	GTGGCTTCAGGAGAGTACG	1.192

Supplementary Table 9. Primer design for the reference genes. Table 9 shows the sequences of the forward primer (5'-3') and the reverse primer (5'-3'), and the primer efficiencies (tested with RT-qPCR with a cDNA dilution series as template) for specific reference genes. Ideally the primer efficiency is 100% (1), but a deviation up to 20% is tolerated (0.8-1.2). The colors green and red indicate whether the primer pair efficiency is or is not between this range, respectively. New primer pairs are designed when a primer pair does not meet these requirements, hence the number of design after the gene name.

Reference genes			
Gene	**Forward primer (5' – 3')**	**Reverse primer (5' – 3')**	**Primer efficiency**
First design			
*b2m*_1	TCTCCATTGAACTGCTGAAG	ACGCTGCAGGTATATTCATC	0.9584
*cat*_1	AGCCCAGCCCAGACAAGAT	GATGGCGATGTGTGTCTGG	1.032
*cyp19a1b*_1	AAGGCCATCCTAGTAACCAT	GGTTGTTGGTCTGTCTGATG	1.553
*eef1a1a*_1	CGCAAGAAGCTGCCAATTTC	CTGATCTGCCCTGGGTGG	1.066
*eif2s2*_1	GGTGGTGAGGAGAGAGAGT	TTTAAGTCATCAAGGTCATCTG	1.067
*gapdh*_1	CGCTGGCATCTCCCTCAA	TCAGCAACACGATGGCTGTA	1.009
*hprt1*_1	GAGGAGCGTTGGATACAGA	CTCGTTGTAGTCAAGTGCAT	-0.5763
*lsm12b*_1	CTCTAGCATCCTTGAATATTAG	GCTTGGGACAACTTGTCTTC	1.024
*mobk13*_1	GTTTGGAGCTCAATGGCTTG	CATCTGGGTACATGTGTCTG	1.007
*rnf7*_1	ACAAACAAGAAGACTGCGTTG	GCAGTTGTGGAAGGAGTGG	1.016
*rpl7*_1	ACGTCTGAAGAAAGCGAAGG	ATGAGCTTCCTGGTGACTTTG	0.9996
*rpl13a*_1	AGGCTGAAGGTGTTTGATG	TTTCAGACGCACAATCTTGA	1.387
*rplp2*_1	GGAGTGTCGGGATCGAGG	GTCTTTGCCATTCAGTTCACT	1.053
*rps18*_1	TTTGCCATCACCGCTATTAAG	CTTTCCTCAGAACCACATGG	1.150
*sdha*_1	CACTCGCTTCTGCACACTC	AGTAGCTGGTATCGTACCTC	0.9372
*slc25a5*_1	GTCGTCGTATGATGATGCAG	AGCAGTCAATTGTGCCACTG	-0.9545
*tbp*_1	AAGTTTACGGTGGACACAAT	CAGGCAACACACCACTTTAT	2.695
*tuba1a*_1	TCATCTTCTCCTTCCACACT	GTACGTGGGTGAGGGTAT	1.052
*ube2a*_1	GCCTGAAGGAACACCTTTTG	TTGTTAGGATATTCTTCTG	/
*ywhaz*_1	GAGCTGAAGGCCATCTGCA	TGCGGATCAGAAACTTGTCC	0.9339
Second design			
*hprt1*_2	GAACGTCTGGCCAGAGATAT	AGCAAAAAACTTGTAGCCTCC	1.074
*rpl13a*_2	ACGCCTGGCTTTTCACATTCA	AGTCTGCGTAGATAGTCACC	0.9675
Third design			
*rpl13a*_3	GCCAAGCAAGTGCTGTTGG	CACCACCACAATTTTGTGGC	1.050

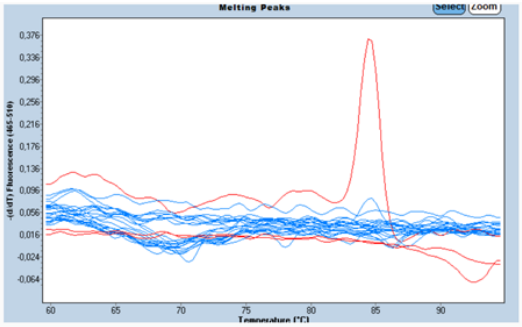

adra1aa _2

Concentration	Ct-value	Mean Ct-value	Log concentration	Mean Ct-value
32	30,45	30,365	1,505149978	30,365
	30,28			
8	31,57	31,63	0,903089987	31,63
	31,68			
2	33,31	32,72	0,301029996	32,72
	32,13			
0,5			-0,301029996	
0,125			-0,903089987	
0,0312			-1,505845406	
		Efficiency -1+10^(-1/rc)		
		2,245635343		

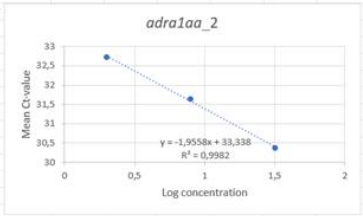

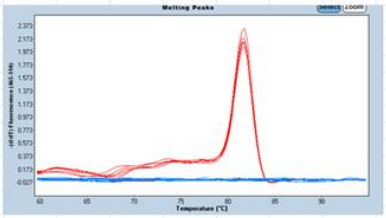

adra1aa _3

Concentration	Ct-value	Log concentration	Mean Ct-value
32	29,74	1,505149978	29,95
	30,16		
8	31,86	0,903089987	31,575
	31,29		
2		0,301029996	33,63
	33,63		
0,5	35,26	-0,301029996	35,26
0,125		-0,903089987	
0,0312	35,12	-1,505845406	
NTC			
		Efficiency -1+10^(-1/rc)	
		1,161531902	

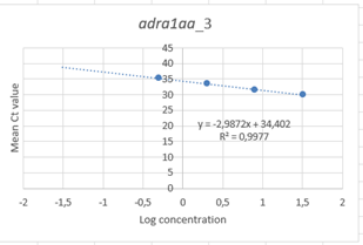

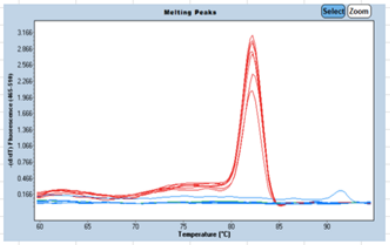

Figure 43. Results of the primer efficiency testing and calculations for *adra1aa*_1 (only the melting curve is shown here), *adra1aa*_2 and *adra1aa*_3.

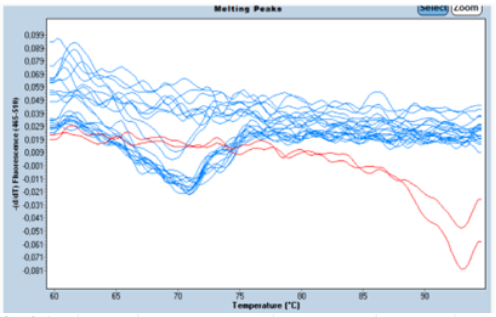

adra1ab _2

Concentration	Ct-value	Log concentration	Mean Ct-value
32	27,09	1,505149978	27,13
	27,17		
8	29,01	0,903089987	29,115
	29,22		
2	31,21	0,301029996	31,2
	31,19		
0,5	33,69	-0,301029996	34,29
	34,89		
0,125	34,11	-0,903089987	34,11
0,0312		-1,505845406	35,73
	35,73		
	Efficiency -1+10^(-1/rc)		
	1,213550213		

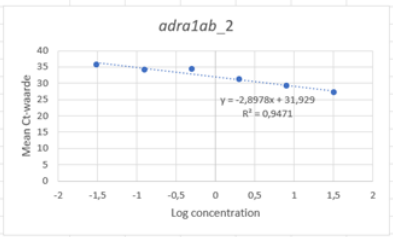

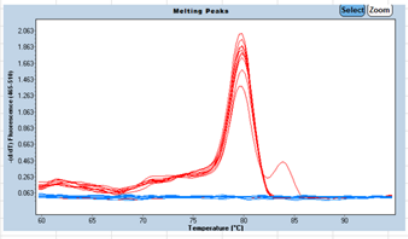

adra1ab _3

Concentration	Ct-value	Log concentration	Mean Ct-value
32	26,49	1,505149978	26,505
	26,52		
8	28,01	0,903089987	27,91
	27,81		
2	30,66	0,301029996	30,63
	30,6		
0,5	31,63	-0,301029996	31,87
	32,11		
0,125	35,04	-0,903089987	34,17
	33,3		
0,0312		-1,505845406	36,05
	36,05		
NTC			

Efficiency -1+10^(-1/rc)

1,046916137

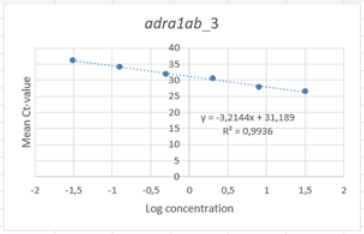

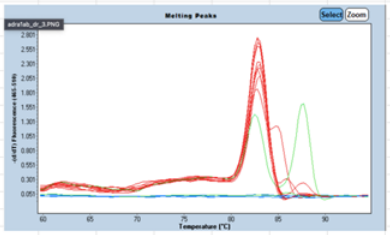

Figure 44. Results of the primer efficiency testing and calculations for *adra1ab*_1 (only the melting curve is shown here), *adra1ab*_2 and *adra1ab*_3.

adra1ba _1

Concentration	Ct-value	Mean Ct-value	Log concentration
32	30,21	30,43	1,505149978
	30,65		
8	31,34	31,56	0,903089987
	31,77		
2	34,8	34,52	0,301029996
	34,24		
0,5		34,53	-0,301029996
	34,53		
0,125		39,00	-0,903089987
	39		
0,0312			-1,505845406

Efficiency -1+10^(-1/rc)

0,992102054

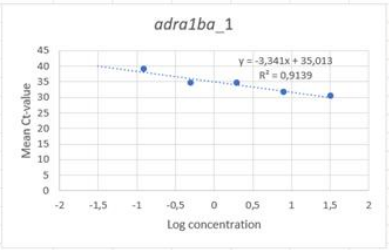

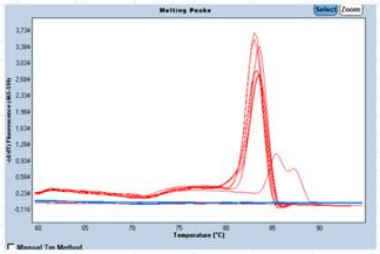

Figure 45. Results of the primer efficiency testing and calculations for *adra1ba*_1.

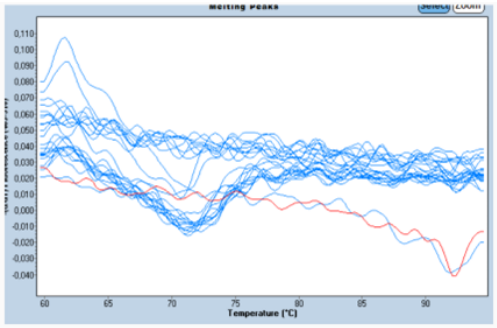

adra1bb _2

Concentration	Ct-value	Mean Ct-value	Log concentration	Mean Ct-value
32	27,12	27,395	1,505149978	27,395
	27,67			
8	29,93	29,88	0,903089987	29,88
	29,83			
2	32,58	32,36	0,301029996	32,36
	32,13			
0,5	33,35	34,15	-0,301029996	34,15
	34,94			
0,125			-0,903089987	
0,0312			-1,505845406	

Efficiency: -1+10^(-1/rc)

0,839489523

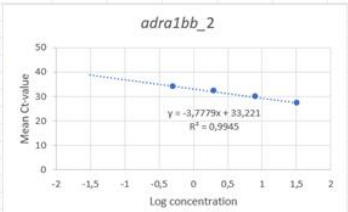

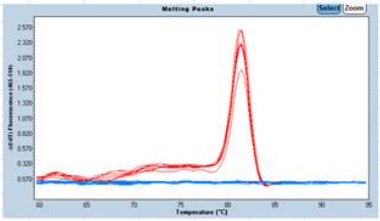

adra1bb _3

Concentration	Ct-value	Log concentration	Mean Ct-value
32	28,31	1,505149978	28,195
	28,08		
8	29,82	0,903089987	29,92
	30,02		
2	32,32	0,301029996	32,165
	32,01		
0,5	34,49	-0,301029996	35,05
	35,61		
0,125	35,46	-0,903089987	35,435
	35,41		
0,0312		-1,505845406	
NTC			
		Efficiency -1+10^(-1/rc)	
		1,027739483	

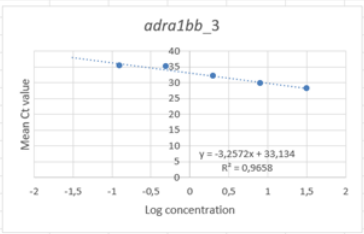

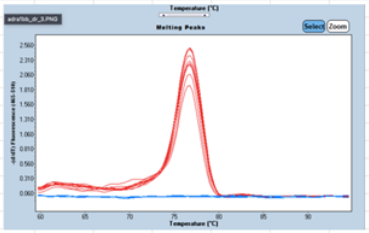

Figure 46. Results of the primer efficiency testing and calculations for *adra1bb*_1 (only the melting curve is shown here), *adra1bb*_2 and *adra1bb*_3.

adra2a _1

Concentration	Ct-value	Log concentration	Mean Ct-value
32	26,19	1,505149978	26,19
	26,19		
8	27,73	0,903089987	27,75
	27,77		
2	30,49	0,301029996	30,365
	30,24		
0,5	32,52	-0,301029996	32,825
	33,13		
0,125	33,63	-0,903089987	33,315
	33		
0,0312	35,22	-1,505845406	
NTC			
		Efficiency -1+10^(-1/rc)	
		1,049018553	

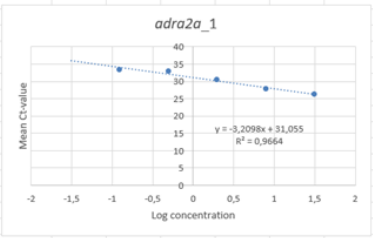

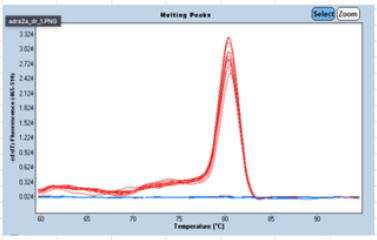

Figure 47. Results of the primer efficiency testing and calculations for *adra2a*_1.

adra2b _1

Concentration	Ct-value	Log concentration	Mean Ct-value
32	25,48	1,505149978	25,455
	25,43		
8	26,75	0,903089987	26,69
	26,63		
2	29,43	0,301029996	29,29
	29,15		
0,5	31,19	-0,301029996	31,225
	31,26		
0,125	33,55	-0,903089987	32,805
	32,06		
0,0312	32,47	-1,505845406	33,225
	33,98		
NTC	37,45		
	35,54		
		Efficiency -1+10^(-1/rc)	
		1,272179838	

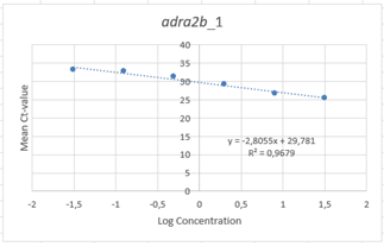

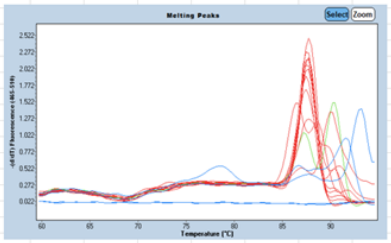

adra2b_2

Concentration	Ct-value	Log concentration	Mean Ct-value
32	37,56	1,505149978	37,56
8	30,3	0,903089987	29,205
	28,11		
2	29,57	0,301029996	29,24
	28,91		
0,5	31,57	-0,301029996	31,185
	30,8		
0,125	32,7	-0,903089987	32,565
	32,43		
0,0312	33,72	-1,505845406	33,645
	33,57		
		Efficiency -1+10^(-1/rc)	
		rc = 0,358	
		-0,998390452	

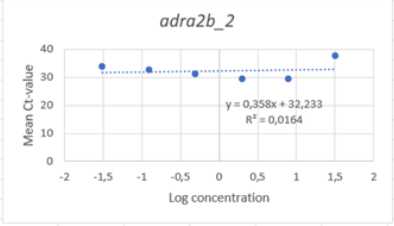

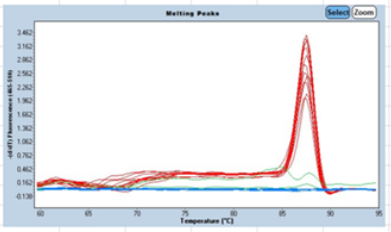

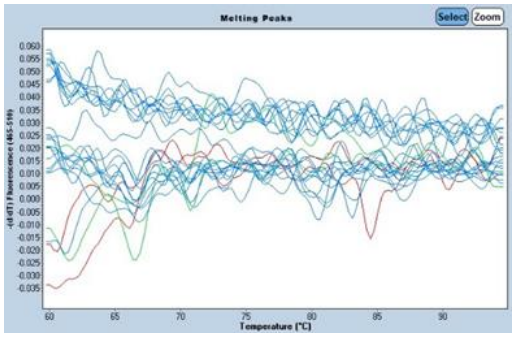

*adra2b*_4

Concentration	Ct-value	Log concentration	Mean Ct-value
32		1,505149978	27,6
	27,6		
8		0,903089987	
2	31,08	0,301029996	31,17
	31,26		
0,5	34,77	-0,301029996	34,315
	33,86		
0,125		-0,903089987	35,8
	35,8		
0,0312		-1,505845406	35,7
	35,7		
NTC			
		Efficiency -1+10^(-1/rc)	rc = - 2,9338
		1,192072249	

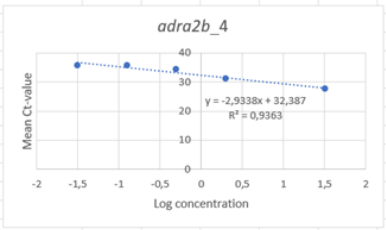

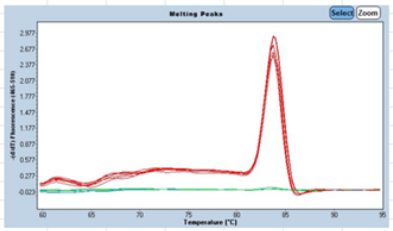

Figure 48. Results of the primer efficiency testing and calculations for *adra2b*_1, *adra2b*_2, *adra2b*_3 (only the melting curve is shown here) and *adra2b*_4.

*adrb1*_1

Concentration	Ct-value	Mean Ct-value	Log concentration
32	27,65		1,51
	28,29		
8	27,12	27,13	0,9
	27,14		
2	28,92	28,855	0,3
	28,79		
0,5	32,59	32,14	-0,3
	31,69		
0,125	32,27	33,095	-0,9
	33,92		
0,0312	34,21	34,21	-1,51
		Efficiency -1+10^(-1/rc)	
		1,124659743	

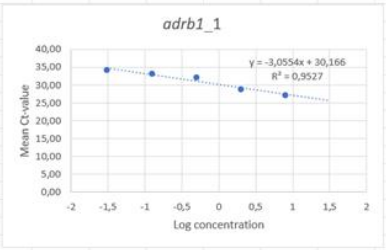

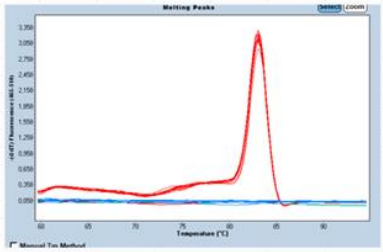

Figure 49. Results of the primer efficiency testing and calculations for *adrb1*_1.

*adrb2a*_1

Concentration	Ct-value	Mean Ct-value	Log concentration
32	26,64	26,83	1,51
	27,02		
8	27,57	27,65	0,9
	27,73		
2	29,72	29,59	0,3
	29,46		
0,5	31,45	31,355	-0,3
	31,26		
0,125	32,77	33,625	-0,9
	34,48		
0,0312	34,41	34,41	-1,51
		Efficiency -1+10^(-1/rc)	
		1,322550861	

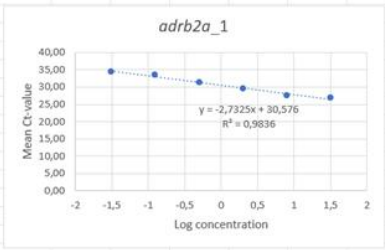

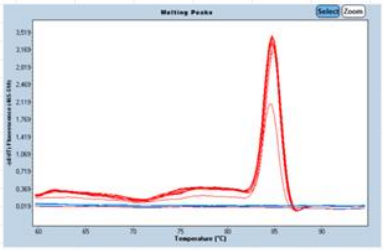

adrb2a _2

Concentration	Ct-value	Log concentration	Mean Ct-value
32	26,43	1,505149978	26,58
	26,73		
8	28,1	0,903089987	28,27
	28,44		
2	30,61	0,301029996	30,63
	30,65		
0,5	31,67	-0,301029996	32,72
	33,77		
0,125	34,71	-0,903089987	34,7
	34,69		
0,0312	39	-1,505845406	36,85
	34,7		
	39		
		Efficiency -1+10^(-1/rc)	
		0,948854776	

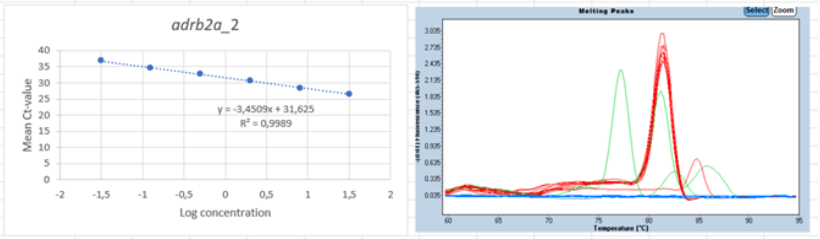

Figure 50. Results of the primer efficiency testing and calculations for *adrb2a*_1 and *adrb2a*_2.

adrb2b _1

Concentration	Ct-waarde	Mean Ct-value	Log concentration
32	29,6	29,92	1,505149978
	30,24		
8	31,1	31,30	0,903089987
	31,5		
2	33,61	33,82	0,301029996
	34,02		
0,5	35,16	35,43	-0,301029996
	35,7		
0,125			-0,903089987
0,0312			-1,505845406
		Efficiency -1+10^(-1/rc)	
		1,070739963	

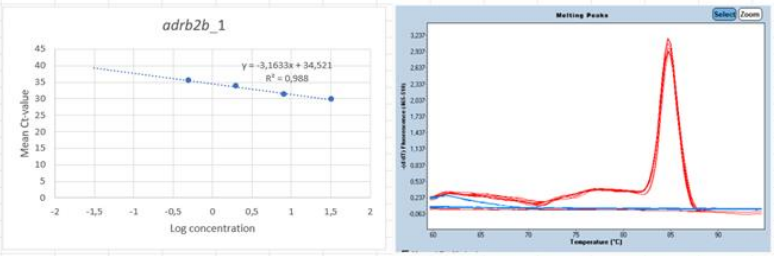

Figure 51. Results of the primer efficiency testing and calculations for *adrb2b*_1.

b2m _1

Concentration	Ct-value	Log concentration	Mean Ct-value
32		1,505149978	
8	25,93	0,903089987	25,74
	25,55		
2	27,55	0,301029996	27,555
	27,56		
0,5	29,88	-0,301029996	29,865
	29,85		
0,125	31,75	-0,903089987	31,845
	31,94		
0,0312	32,51	-1,505845406	
	31,76		
NTC			
		Efficiency -1+10^(-1/rc)	
		0,95844393	

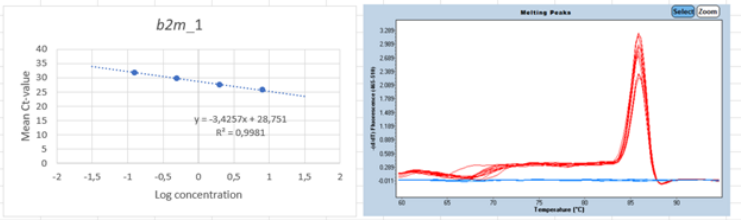

Figure 52. Results of the primer efficiency testing and calculations for *b2m*_1.

cat _1

Concentration	Ct-value	Log concentration	Mean Ct-value
32	21,05	1,505149978	21,215
	21,38		
8	23,12	0,903089987	23,51
	23,9		
2	25,28	0,301029996	25,38
	25,48		
0,5	27,11	-0,301029996	27,115
	27,12		
0,125	28,89	-0,903089987	28,99
	29,09		
0,0312	31,44	-1,505845406	31,265
	31,09		
NTC	39		36,805
	34,61		34,61
		Efficiency -1+10^(-1/rc)	
		1,032380649	

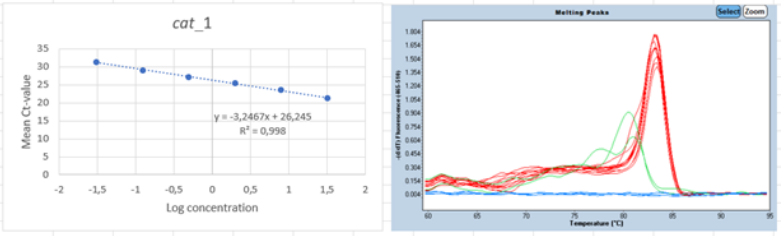

Figure 53. Results of the primer efficiency testing and calculations for *cat*_1.

cyp19a1b _1

Concentration	Ct-value	Log concentration	Mean Ct-value
32	28,86	1,505149978	30,57
	32,28		
8	32,58	0,903089987	31,92
	31,26		
2	33,52	0,301029996	33,6
	33,68		
0,5	39	-0,301029996	36,58
	34,16		
0,125	36,04	-0,903089987	35,635
	35,23		
0,0312		-1,505845406	
NTC			
		Efficiency -1+10^(-1/rc)	
		1,553093251	

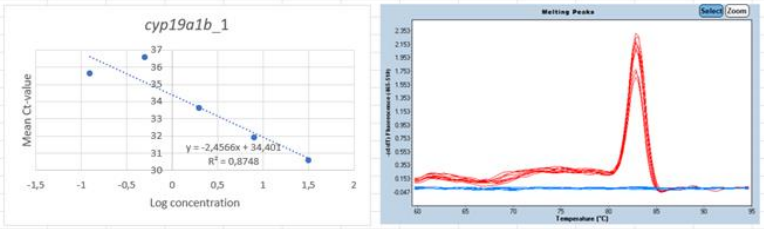

Figure 54. Results of the primer efficiency testing and calculations for *cyp19a1b*_1.

eef1a1a _1

Concentration	Ct-value	Log concentration	Mean Ct-value
32	21,92	1,505149978	21,895
	21,87		
8	23,2	0,903089987	23,16
	23,12		
2	25,93	0,301029996	25,8
	25,67		
0,5	27,5	-0,301029996	27,53
	27,56		
0,125	29,56	-0,903089987	29,57
	29,58		
0,0312	31,09	-1,505845406	31,075
	31,06		
NTC	34,88		35,875
	36,87		
		Efficiency -1+10^(-1/rc)	
		1,066420786	

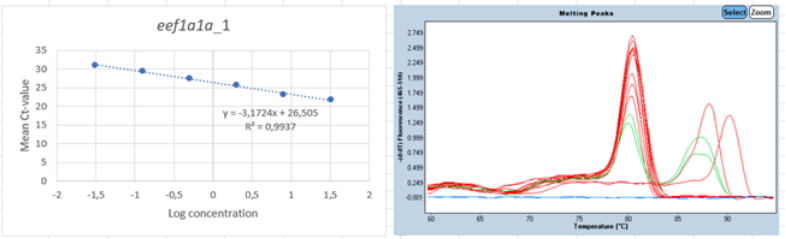

Figure 55. Results of the primer efficiency testing and calculations for *eef1a1a*_1.

eif2s2 _1

Concentration	Ct-value	Log concentration	Mean Ct-value
32	20,04	1,505149978	20,355
	20,67		
8	21,9	0,903089987	21,775
	21,65		
2	24,15	0,301029996	24,14
	24,13		
0,5	25,96	-0,301029996	25,955
	25,95		
0,125	27,79	-0,903089987	27,905
	28,02		
0,0312	29,73	-1,505845406	29,685
	29,64		
NTC			
		Efficiency -1+10^(-1/rc)	
		1,066562639	

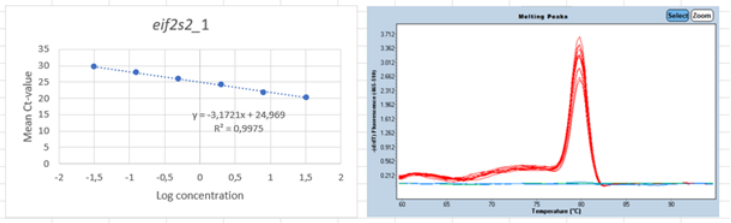

Figure 56. Results of the primer efficiency testing and calculations for *eif2s2*_1.

gapdh _1

Concentration	Ct-value	Log concentration	Mean Ct-value
32	17,25	1,505149978	17,23
	17,21		
8	18,93	0,903089987	18,87
	18,81		
2	21,04	0,301029996	21,685
	22,33		
0,5	23,5	-0,301029996	23,31
	23,12		
0,125	25,12	-0,903089987	25,17
	25,22		
0,0312	27,04	-1,505845406	27,04
NTC			
		Efficiency -1+10^(-1/rc)	
		1,008723453	

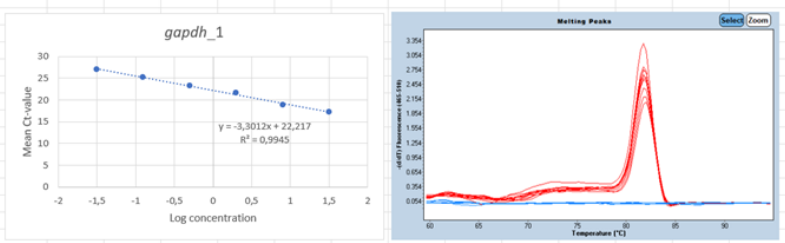

Figure 57. Results of the primer efficiency testing and calculations for *gapdh*_1.

*hprt1*_1

Concentration	Ct-value	Log concentration	Mean Ct-value
32		1,505149978	
8		0,903089987	
2	39	0,301029996	39
0,5	36,17	-0,301029996	36,17
0,125	36,28	-0,903089987	36,28
0,0312	33,58	-1,505845406	33,58
NTC			

Efficiency -1+10^(-1/rc)
-0,576270885

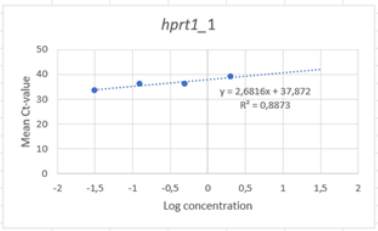

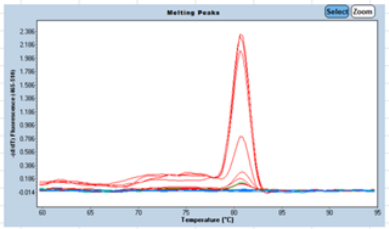

*hprt1*_2

Concentration	Ct-value	Log concentration	Mean Ct-value
32	21,51	1,505149978	21,61
	21,71		
8	22,97	0,903089987	22,995
	23,02		
2	25,51	0,301029996	25,36
	25,21		
0,5	27,05	-0,301029996	27,04
	27,03		
0,125	28,78	-0,903089987	28,655
	28,53		
0,0312	31,58	-1,505845406	31,18
	30,78		
NTC			

Efficiency -1+10^(-1/rc)
1,074325287

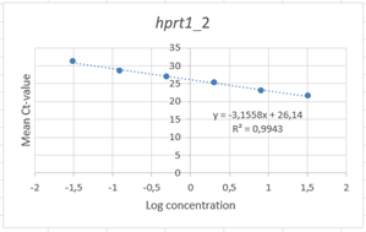

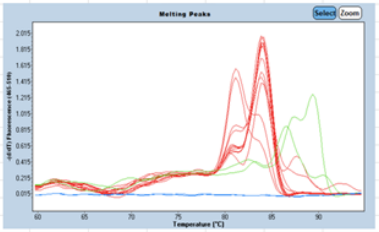

Figure 58. Results of the primer efficiency testing and calculations for *hprt1*_1 and *hprt1*_2.

*lsm12b*_1

Concentration	Ct-value	Log concentration	Mean Ct-value
32	21,61	1,505149978	21,56
	21,51		
8	22,93	0,903089987	23,005
	23,08		
2	24,94	0,301029996	24,94
	24,94		
0,5	27,59	-0,301029996	27,595
	27,6		
0,125	29,05	-0,903089987	29,265
	29,48		
0,0312	31	-1,505845406	31,035
	31,07		
NTC			

Efficiency -1+10^(-1/rc)
1,024361619

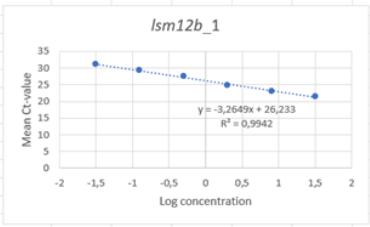

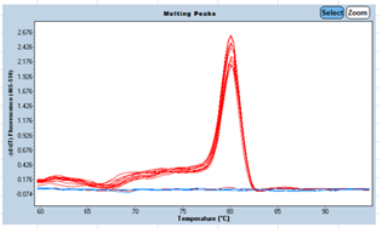

Figure 59. Results of the primer efficiency testing and calculations for *lsm12b*_1.

*mobk13*_1

Concentration	Ct-value	Log concentration	Mean Ct-value
32	20,83	1,505149978	20,835
	20,84		
8	22,66	0,903089987	22,68
	22,7		
2	24,69	0,301029996	24,735
	24,78		
0,5	27,28	-0,301029996	27,165
	27,05		
0,125	28,74	-0,903089987	28,795
	28,85		
0,0312	30,69	-1,505845406	30,615
	30,54		
NTC			

Efficiency -1+10^(-1/rc)
1,006732519

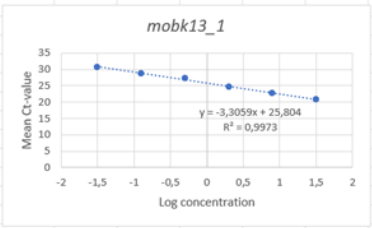

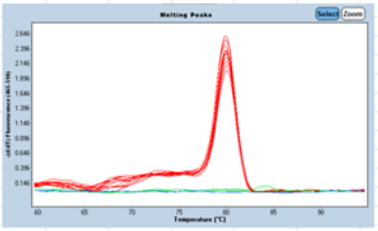

Figure 60. Results of the primer efficiency testing and calculations for *mobk13*_1.

rnf7_1

Concentration	Ct-value	Log concentration	Mean Ct-value
32	19,94	1,505149978	19,935
	19,93		
8	21,97	0,903089987	21,93
	21,89		
2	24,48	0,301029996	24,375
	24,27		
0,5	26,23	-0,301029996	26,17
	26,11		
0,125	28,06	-0,903089987	27,995
	27,93		
0,0312	29,91	-1,505845406	29,785
	29,66		
NTC	29		32,295
	35,59		

Efficiency -1+10^(-1/rc)
1,015515792

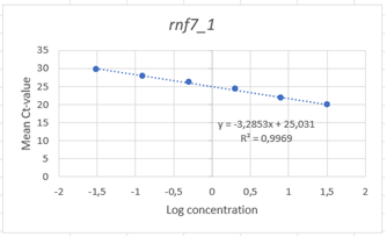

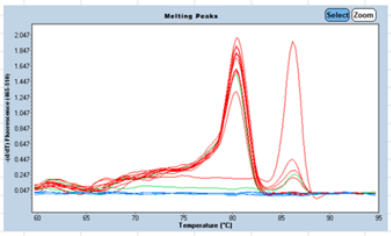

Figure 61. Results of the primer efficiency testing and calculations for *rnf7*_1.

rpl7_1

Concentration	Ct-value	Log concentration	Mean Ct-value
32	15,44	1,505149978	15,295
	15,15		
8	17,11	0,903089987	17,055
	17		
2	19,88	0,301029996	19,775
	19,67		
0,5	21,71	-0,301029996	21,705
	21,7		
0,125	23,66	-0,903089987	23,665
	23,67		
0,0312	25	-1,505845406	24,95
	24,9		
NTC			

Efficiency -1+10^(-1/rc)
0,999552871

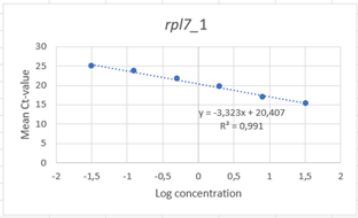

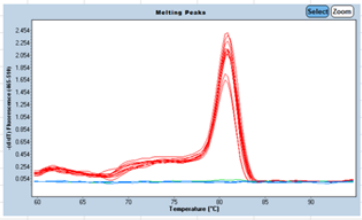

Figure 62. Results of the primer efficiency testing and calculations for *rpl7*_1.

rpl13a _1

Concentration	Ct-value	Log concentration	Mean Ct-value
32	14,92	1,505149978	15,465
	16,01		
8	20,67	0,903089987	19,28
	17,89		
2	19,59	0,301029996	19,3
	19,01		
0,5	20,76	-0,301029996	20,78
	20,8		
0,125	22,76	-0,903089987	22,68
	22,6		
0,0312	24,28	-1,505845406	24,285
	24,29		
NTC			

Efficiency -1+10^(-1/rc)
1,386871257

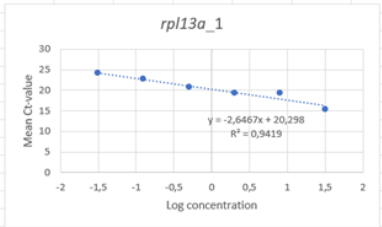

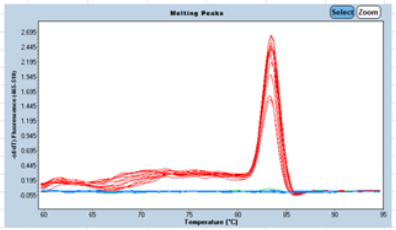

rpl13a _2

Concentration	Ct-value	Log concentration	Mean Ct-value
32	25,52	1,505149978	25,55
	25,58		
8	27,3	0,903089987	27,235
	27,17		
2	29,75	0,301029996	29,825
	29,9		
0,5	31,65	-0,301029996	31,605
	31,56		
0,125	32,82	-0,903089987	33,91
	35		
0,0312		-1,505845406	35,53
	35,53		
NTC			

Efficiency -1+10^(-1/rc)
0,967518477

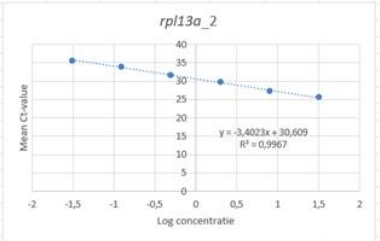

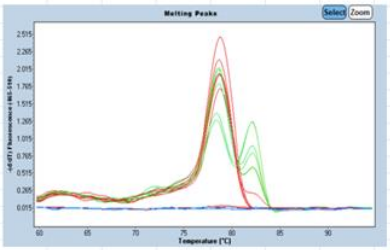

rpl13a_3

Concentration	Ct-value	Log concentration	Mean Ct-value
32	15,9	1,505149978	15,9
8			
	20,94		
2	20,18	0,301029996	19,94
	19,7		
0,5	22,34	-0,301029996	22,145
	21,95		
0,125	23,8	-0,903089987	23,75
	23,7		
0,0312	25,51	-1,505845406	25,51
	25,51		

Efficiency -1+10^(-1/rc)
rc = -2,7845
1,05039411

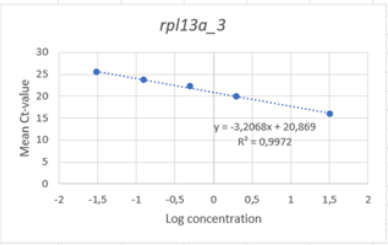

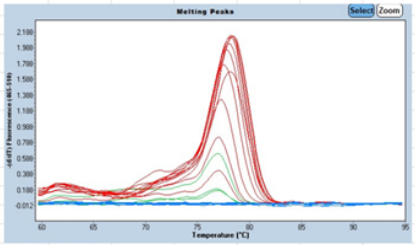

Figure 63. Results of the primer efficiency testing and calculations for *rpl13a*_1, *rpl13a*_2 and *rpl13a*_3.

rplp2 _1

Concentration	Ct-value	Log concentration	Mean Ct-value
32	15,33	1,505149978	15,215
	15,1		
8	16,91	0,903089987	16,78
	16,65		
2	19,15	0,301029996	19,19
	19,23		
0,5	21,12	-0,301029996	21,11
	21,1		
0,125	22,97	-0,903089987	23,025
	23,08		
0,0312	24,65	-1,505845406	24,58
	24,51		
NTC			

Efficiency -1+10^(-1/rc)
1,052694495

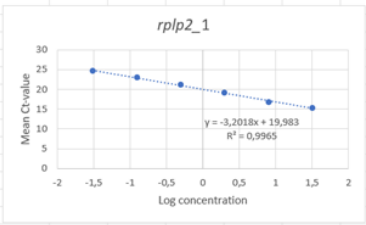

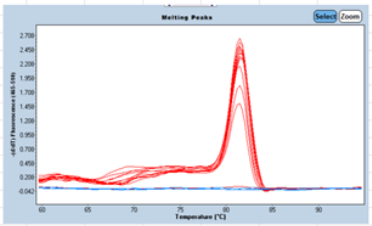

Figure 64. Results of the primer efficiency testing and calculations for *rplp2*_1.

rps18_ 1

Concentration	Ct-value	Log concentration	Mean Ct-value
32	15,53	1,505149978	16,125
	16,72		
8	18,66	0,903089987	18,07
	17,48		
2	19,69	0,301029996	19,72
	19,75		
0,5	21,58	-0,301029996	21,605
	21,63		
0,125	23,16	-0,903089987	23,22
	23,28		
0,0312	25,34	-1,505845406	25,34
	25,34		
NTC			

Efficiency -1+10^(-1/rc)
1,149658448

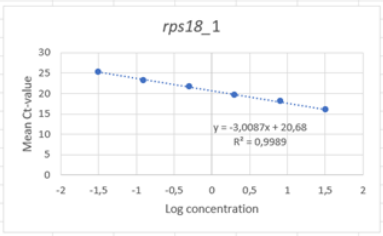

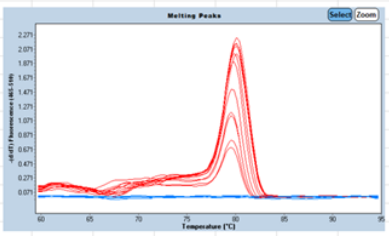

Figure 65. Results of the primer efficiency testing and calculations for *rps18*_1.

sdha _1

Concentration	Ct-value	Log concentration	Mean Ct-value
32	22,75	1,505149978	22,9
	23,05		
8	24,3	0,903089987	24,415
	24,53		
2	26,68	0,301029996	26,68
	26,68		
0,5	28,85	-0,301029996	28,685
	28,52		
0,125	30,31	-0,903089987	30,45
	30,59		
0,0312	32,65	-1,505845406	33,555
	34,46		
NTC			

Efficiency -1+10^(-1/rc)
0,937238189

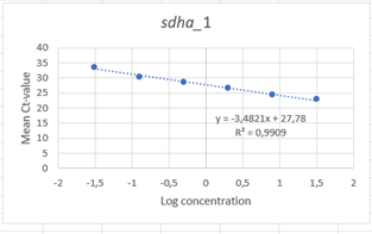

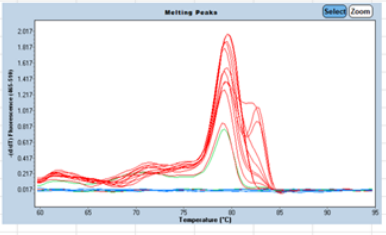

Figure 66. Results of the primer efficiency testing and calculations for *sdha*_1.

slc25a5_1

Concentration	Ct-value	Log concentration	Mean Ct-value
32	23,45	1,505149978	28,995
	34,54		
8	22,47	0,903089987	21,07
	19,67		
2	19,25	0,301029996	19,19
	19,13		
0,5	23,02	-0,301029996	21,72
	20,42		
0,125		-0,903089987	22,6
	22,6		
0,0312	24,32	-1,505845406	24,43
	24,54		
NTC			
		Efficiency -1+10^(-1/rc)	
		-0,954549578	

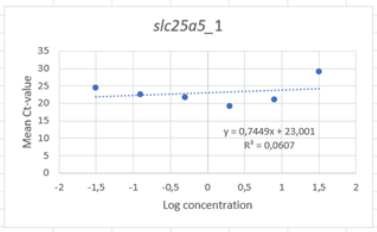

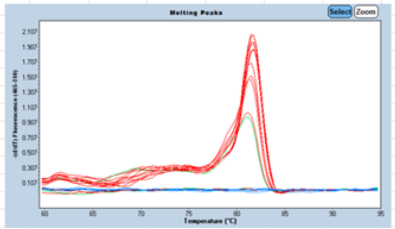

Figure 67. Results of the primer efficiency testing and calculations for *slc25a5*_1.

tbp_1

Concentration	Ct-value	Log concentration	Mean Ct-value
32	25,77	1,505149978	28,365
	30,96		
8	28,16	0,903089987	27,31
	26,46		
2	27,84	0,301029996	27,725
	27,61		
0,5	29,31	-0,301029996	29,325
	29,34		
0,125	31,56	-0,903089987	31,92
	32,28		
0,0312	31,98	-1,505845406	32,705
	33,43		
NTC			
		Efficiency -1+10^(-1/rc)	
		2,694888326	

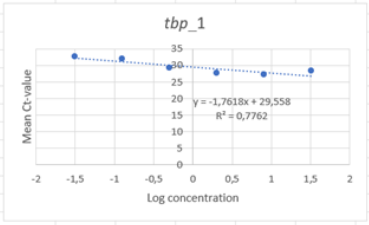

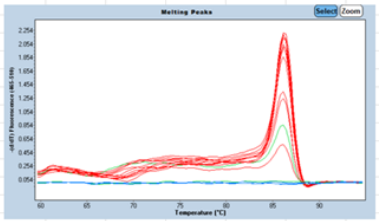

Figure 68. Results of the primer efficiency testing and calculations for *tbp*_1.

tuba1_1

Concentration	Ct-value	Log concentration	Mean Ct-value
32	22,67	1,505149978	22,685
	22,7		
8	24,15	0,903089987	24,19
	24,23		
2	26,65	0,301029996	26,565
	26,48		
0,5	28,72	-0,301029996	28,715
	28,71		
0,125	30,02	-0,903089987	30,27
	30,52		
0,0312	31,98	-1,505845406	32,11
	32,24		
NTC			
		Efficiency -1+10^(-1/rc)	
		1,051911269	

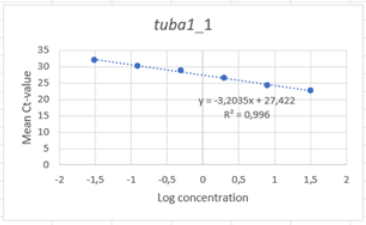

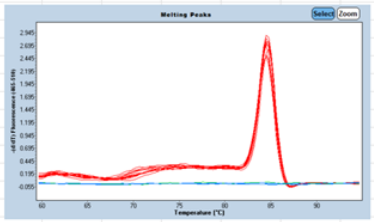

Figure 69. Results of the primer efficiency testing and calculations for *tuba1a*_1.

ube2a_1

Concentration	Ct-value	Log concentration	Mean Ct-value
32		1,505149978	
8		0,903089987	
2	39	0,301029996	39
	39		
0,5	39	-0,301029996	39
	39		
0,125	39	-0,903089987	39
	39		
0,0312	39	-1,505845406	39
	39		
NTC			
		Efficiency -1+10^(-1/rc)	
		/	

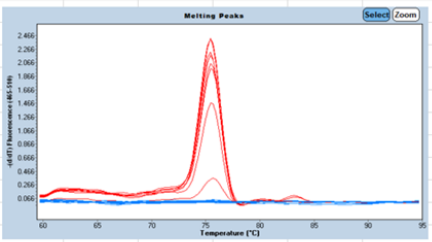

Figure 70. Results of the primer efficiency testing and calculations for *ube2a*_1.

ywhaz _1

Concentration	Ct-value	Log concentration	Mean Ct-value
32	23,67	1,505149978	23,44
	23,21		
8	25,05	0,903089987	25,015
	24,98		
2	27,26	0,301029996	27,305
	27,35		
0,5	29,46	-0,301029996	29,19
	28,92		
0,125	30,83	-0,903089987	30,87
	30,91		
0,0312	33,74	-1,505845406	34,265
	34,79		
NTC			
		Efficiency -1+10^(-1/rc)	
		0,933938541	

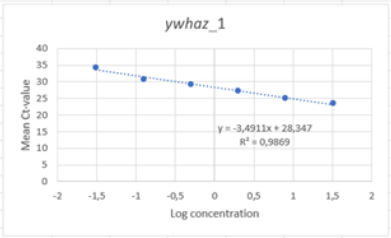

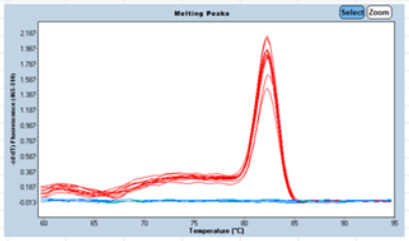

Figure 71. Results of the primer efficiency testing and calculations for *ywhaz*_1.